VERIFICATION OF SHRP (11) STUDY RESULTS FOR CONDITIONS OF PAKISTAN AND PERFORMANCE ENHANCEMENT OF AASHTO DESIGNED PAVEMENT SECTIONS

By

Ahmed Javed

A THESIS

Submitted to
Michigan State University
in partial fulfillment of the requirements
for the degree of

MASTER OF SCIENCE

Department of Civil and Environmental Engineering

1998

ABSTRACT

VERIFICATION OF SHRP(11) STUDY RESULTS FOR CONDITIONS OF PAKISTAN AND PERFORMANCE ENHANCEMENT OF AASHTO DESIGNED PAVEMENT SECTIONS

By

Ahmed Javed

A total of 243 artificial pavement sections were designed for the ranges of variables in Pakistan using AASHTO DNPS-86 Computer Program. The mechanistic responses were then analyzed to verify the accuracy and applicability of SHRP results to conditions in Pakistan.

The performance of 9 out of 243 pavement sections and 3 additional pavement sections were compared relative to the roughness, fatigue and rut. During the comparison, it was found that the fatigue and rut performance of these 12 pavement sections was very low as compared to their roughness performance.

It was concluded that Pakistan needs to treat/stabilize its pavement bases to achieve fatigue/rut performance which is equal to or greater than the roughness performance of the pavement sections considered in this study.

TABLE OF CONTENTS

CHAPTER 8

LIST OF TABLES

LIST OF TABLES (Continued)

LIST OF TABLES (Continued)

LIST OF TABLES (Continued)

LIST OF FIGURES

LIST OF FIGURES (Continued)

LIST OF FIGURES (Continued)

LIST OF FIGURES (Continued)

LIST OF FIGURES (Continued)

LIST OF FIGURES (Continued)

LIST OF FIGURES (Continued)

CHAPTER I

INTRODUCTION

1.1 GENERAL

One of the most vital elements in the **defence** and **socio-economic** development of any country is an effective transport system. Today's transport system includes road, rail, air and marine transportation. In Pakistan, road transportation overwhelmingly dominates the other three transportation modes. The share of **road freight** and **passenger traffic** is estimated at **80%** and **85%** respectively (1). The construction and maintenance of the country's road network consumes a large proportion of the national budget. In the Seventh Five-Year Plan (1988-93) an investment of Rupees 61.957 billion was made in the road infrastructure and the Eight Five-Year Plan (1993-98) envisages an investment of Rupees 74.687 billion. The budget allocations for road maintenance and new construction schemes for financial years 1992-93 and 1993-94 are Rupees 15.556 billion and Rupees 11.323 billion respectively.

Road projects, thus, represent one of the most costly of all public investments. In addition, road projects result in a stream of costs that goes on for as long as the roadway exists. This costs stream includes not only the initial construction cost but other costs such as:

- Rehabilitation: Restoration
Resurfacing
Reconstruction

- Maintenance: Routine minor repairs

- Road User: Fuel consumption
Oil consumption
Tire wear
Parts replacement
Vehicle depreciation
Travel time
Accident

The above-mentioned costs are greatly affected by the **rate and amount of deterioration** of the pavement structure. Various studies have shown that the **Asphalt Concrete** (AC) pavement deterioration is a function of:

- Pavement structural design
- Bituminous mixture design
- Traffic load and volume
- Construction practices and quality control
- Maintenance policy and procedures
- Environmental conditions

Pavement design, (**pavement structural design** and

bituminous mixture design) is the most influential factor affecting the life-cycle cost of the pavement. Figure 1.1 shows that the pavement structural design has the most impact on the life cycle cost of a pavement (2). Inadequate pavement structural design and/or deficient bituminous mixture design cause **premature fatigue cracking, rutting and/or shear failure of the pavement structure. These** distress types lead to **accelerated maintenance requirements** and **increased user costs**. The World bank study (3) has established that road user costs due to rough and unsafe driving conditions are 8 to 10 fold higher than the increased maintenance costs borne by the highway authorities. Moreover, due to the budgetary constraints, highway authorities may not be able to carry out timely preventive maintenance to arrest the premature pavement deterioration. Lack of or inadequate maintenance lead to premature failure of pavements. Thus, road networks, built at great expense are lost due to inadequate pavement structural and bituminous mixture designs.

1.2 PROBLEM STATEMENT

In recent years, premature manifestation of rutting and fatigue cracking and their rapid development to high-severity levels have been observed on many AC pavements in Pakistan. These prematurely deteriorated AC pavements represent a loss of precious infrastructure worth billions of Rupees. If this problem is continued to be neglected then new AC pavements will also crumble prematurely and the associated **avoidable**

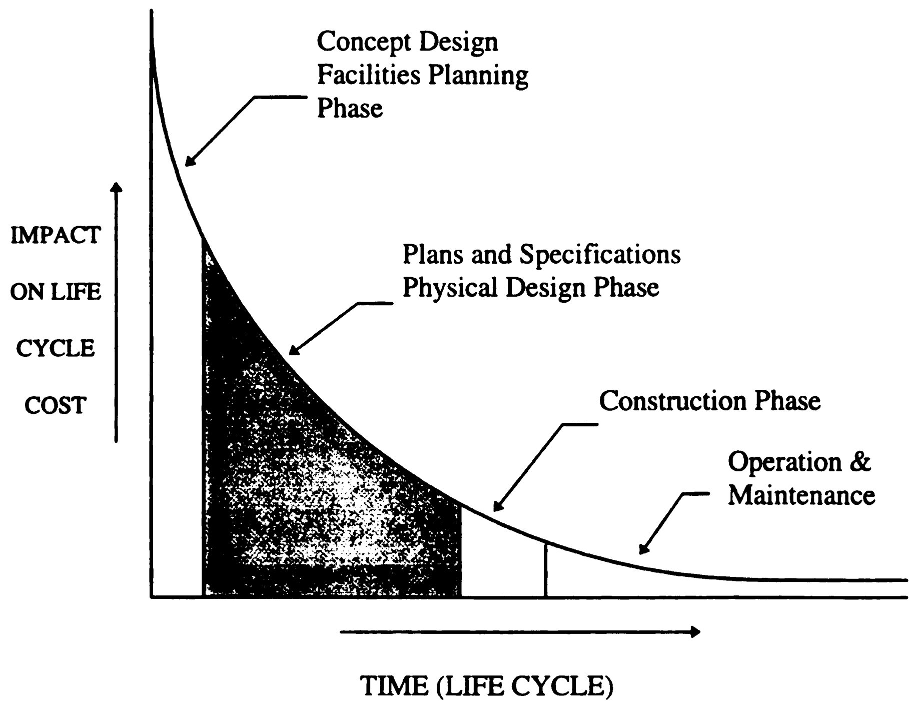

Figure 1.1 : Decision makers influence cost

costs will form a formidable obstacle to the socio-economic development of Pakistan.

1.3 CAUSES OF THE PROBLEM

In Pakistan, like in many other developing countries of the world, the economics of truck transportation have contributed to an increase in the average gross weight of trucks such that the majority of the trucks are operating well above the legal axle load limits. A recent axle load survey carried out by the Military College of Engineering (MACE) at Taxila, Rawat, Dina and Muridke on highway N-5 shows gross overloading of trucks (4). The degree of overloading in Pakistan may be assessed from the Truck Factors (pavement damage per pass in terms of 18,000 lbs single axle load) which are presented in Table 1.1. As it can be seen, the highest truck factor in U.S.A. is 1.59 compared to 15.82 in Pakistan. As axle loads have increased, the use of higher tire pressure has become more popular in the trucking industry to support the increased axle loads. Heavy axle loads and high tire pressures cause **higher levels of plastic strains** in AC pavements, which, in turn, result in accelerated fatigue damage and rutting failure.

The pavement structural and bituminous mixture design procedures being currently used in Pakistan, the **AASHTO** and the **MARSHALL** mix design are **empirical** and were developed for much **lighter loads** and **lower tire pressures**. **Hence, in Pakistan, where trucks are heavily overloaded the use of this**

Table 1.1: Truck Factors at Taxila on N-5 (Loaded Vehicles)

Truck Type	Axle Configuration	Truck Factor	Truck Factors Range in USA
2-axle	Both single	4.757	0.15 - 0.21
3-axle	One single & one tandem	11.850	0.29 - 1.59
4-axle	All single	6.996	0.43 - 1.32
4-axle	Two single & one tandem	4.380	0.43 - 1.32
5-axle	One single & two tandem	14.730	0.71 - 1.39
6-axle	One single, one tandem & one tridem	15.820	0.71 - 1.39

procedure for designing AC pavements requires an extensive extrapolation and thus, it is highly questionable. In addition, since the AASHTO procedure disregards the effects of traffic loads on pavement system behavior (i.e., stresses, strains and deflections), the procedure is not capable of providing adequate designs for traffic loading conditions existent in Pakistan.

1.4 STUDY OBJECTIVES

In view of the limitations of the AASHTO empirical model to conditions in Pakistan and its inherent inability to consider the effects of high traffic loads on pavement performance and recognizing that the development of a pavement design procedure for Pakistan is a time dependent process, the overall objective of this study is to work out the predicted rut and fatigue life/performance of the AASHTO designed pavement sections (using various rut and fatigue performance models) . The study consists of two parts, the first part addresses the sensitivity of the AASHTO design procedure to the traffic levels and range of material properties being used in Pakistan. The second part addresses the rut and fatigue life/performance of the AASHTO designed pavement sections. The two parts will be executed according to the following steps (for details see chapter 4):-

1. Establish a series of AC pavement structural design for traffic levels existent in Pakistan.

2. Compute the mechanistic responses of each pavement section and analyze sensitivity to the AASHTO determined layer thicknesses and subsequently verify SHRP study results (see section 4.10.2).

3. Select AASHTO designed pavement sections with constant variables and estimate the "critical pavement responses" for 23,000-lb and 28,000-lb single axle loads (120 psi tire pressure).

4. Calculate the "fatigue and rut life" for each pavement section using various fatigue and rut performance prediction models.

5. Re-compute the fatigue and rut life of the AASHTO designed pavement sections by using the alternative materials, and different combinations of layer thicknesses, and various existing fatigue/rut models.

CHAPTER 2

BACKGROUND

2.1 INTRODUCTION

In the early stages of development, the design and/or evaluation of a pavement structure consisted of rule-of-thumb procedures based on judgement and past experience. During the period 1920 to 1940, engineers made a concerted effort to evaluate the structural properties of soil. In the 1920's, the U.S. Bureau of Public Road (BPR) developed a soil classification system based upon the observed field performance of soils under highway pavements. This system, in conjunction with the accumulated data, helped the highway engineer to correlate performance with subgrade types. Beginning in the late 1940's highway engineers were faced with the need to predict the performance of pavement structures subjected to heavier wheel loads and more frequencies than they had ever experienced before. This need necessitated the design and execution of several road test experiments including the maryland Road Test, the WASHO Road Test in Idaho, and the AASHO Road Test in Illinois. Results of the road tests have led to the development of empirical design procedures that were limited to certain soil and material types for which they were developed. In order to extend the road test results to other materials and to be able to calculate the effects of various wheel loads and mixed traffic on the pavement performance; mechanistic design method were developed which provided the capability of estimating the stresses and strains induced in the pavement structure due to various axle load magnitudes and configurations. The mechanistic approaches were later augmented with pavement performance and distress prediction models which were developed using the results of the various road tests, field observations, and laboratory test results.

2.2 STRUCTURAL COMPONENTS OF A FLEXIBLE PAVEMENT

The load carrying capacity of a truly flexible pavement is brought about by the load-distributing characteristics of the layered system. Classical flexible pavements consist of a series of layers with the highest-quality materials placed at or near the surface. Hence, the strength of a typical flexible pavement is the result of building up thick layers and, thereby, distributing the load over the subgrade (5). The various layers which act as structural components in a flexible pavement are subbase, base, and asphalt concrete (2). The main objective of a flexible pavement structural design is to determine the thickness and vertical position of each paving material. The pavement is designed to provide a serviceable roadway for the predicted design traffic over the selected design life.

2.3 PAVEMENT DESIGN CONCEPTS

There are several basic design concepts that form the nucleus of any rational pavement design procedure. These include the limitation of roadbed stress, surface deflection, tensile strain at the bottom of the asphalt, and shear stress.

2.3.1 Subgrade Stress.

The subgrade stress can be decreased by increasing the thicknesses of the asphalt, base, and/or subbase layers. The literature (5) reveals that another efficient method of reducing the vertical compressive subgrade stress is to increase the rigidity (moduli) of the upper pavement layers. In a layered system, the major influence upon the stress is usually exerted by the stiffness of the layer directly above the subgrade. Hence in a three layer system, the subbase layer modulus E_3 has the more pronounced effect upon stress reduction, while the base layer modulus E_2 controls the subgrade stress for two layered systems. Therefore, in order to reduce the subgrade stress to some tolerable design value, one can either increase the layer thicknesses or use more rigid material.

2.3.2 Surface Deflection

Depending upon the type of layered pavement structure considered, the percentage of the total surface deflection contributed by the subgrade layer varies from about 70 to 95 percent. It can, therefore, be assumed that most of the deflection is caused by the elastic compression of the subgrade layer. Deflections are simply the mathematical integration of the vertical strain with depth. Since the strain magnitude, for a given material, the strain magnitude at a given point is a direct function of the stress state, it can be deduced that the same general factors that tend to decrease the subgrade vertical compressive stress also tend to decrease the pavement deflection. It should be noted that a greater reduction in stress can be accomplished by increasing the modulus or rigidity of the pavement layer than by increasing the layer thicknesses (5).

2.3.3 Tensile Stress

High tensile stress at the bottom of the asphalt layer causes shorter fatigue life. In general, increasing the modulus of the AC layer relative to that of the base (increasing modulus ratio) or decreasing the thickness of the AC relative to that of the base (decreasing thickness ratio) cause higher tensile strain. It should be pointed out that a maximum tensile stress value does occur at some low AC thickness value. Further decreases in this parameter causes bearing capacity failure (5).

2.3.4 Shear Stress

On any given horizontal plane in a layered structure, the maximum horizontal shear stress (τ_{rz}) occurs directly under the edge of the loaded area. The τ_{rz} value is zero directly under the center of the loaded area and it decreases as the radial distance from the edge of the loaded area increases. Increasing the modulus value of the AC layer causes an increase in the shear stress. It should be noted that the maximum τ_{rz} value within the pavement structure occurs about middepth (neutral axis) in the surface layer. The thickness of the surface layer also plays a significant role in the magnitude of shear stress development. For fixed modular ratio E_1 and E_2, as the thickness of the surface layer increases, the magnitude of the shear stress is decreases and the location of the maximum shear stress shifts upward from about middepth of the layer to approximately the third point.

2.4 DESIGN CRITERIA

A number of design criteria are used to describe the terminal or failure conditions (5,6,7,). These include ride quality, rut and alligator (fatigue) cracking. These terms are defined below:-

2.4.1 Ride Quality

The functional performance of a pavement concerns how well the pavement serves the user. In this context, riding comfort or ride quality is the dominant characteristics. In order to quantify riding comfort, the "serviceability-performance" concept was developed at the AASHO road test in 1957. The serviceability of a pavement is expressed in terms of the Present Serviceability Index (PSI). For flexible pavements, the PSI is obtained from measurements of roughness and distress(cracking, patching and rut depth).The PSI scale ranges from 0 (impassible pavement) to 5 (excellent pavement). The initial serviceability index (p_i) is an engineering estimate of the PSI value immediately after construction. Value of (p_i) established for AASHO road test conditions was 4.2 for flexible pavements. The terminal serviceability index (p_t) is the lowest acceptable PSI level before resurfacing or reconstruction becomes necessary for the particular class of highway. An index of 2.5 or 3.0 is often suggested for use in the design of major highways, and 2.0 for highways with a lower classification (6).

The original serviceability equation was developed at the AASHO Road Test (5) and is presented below.

$$PSI = 5.03 - 1.91 \log(1+SV) - 1.38(RD)^2 - 0.01(C + p)^{1/2}$$

Where

PSI = Present Serviceability Index

log = logarithm (base 10)

Sv = Slope variance

C = Linear Feet of major cracking per 1000 ft^2 area

P = Bituminous patching in ft^2 per 1000 ft^2 area

RD = Rut Depth in inches (both wheel tracks) measured with a 4-foot straight edge

Since, the effects of the terms C, P, and RD in the equation on PSI are minor relative to the effect of the slope variance (SV), many agencies rely only on SV to estimate ride quality (6).

2.4.2 Rutting

A rut is a surface depression in the wheel paths. Pavement uplift may occur along the sides of the rut; however, in many instances, ruts are noticeable only after a rainfall, when wheel paths are filled with water. Rutting stems from a permanent deformation in any of the pavement layers or subgrade, usually caused by consolidation or lateral movement of the materials due to traffic loads. Rutting may be caused by plastic movement in the mix in hot weather or inadequate compaction during construction. Significant rutting can lead to major structural failure of the pavement and hydroplaning potential. Wear of the surface in the wheel path from studded tires can also cause a type of "rutting" (6).

2.4.3 Alligator or Fatigue Cracking.

Alligator or fatigue cracking is a series of interconnecting cracks caused by fatigue failure of the asphalt concrete surface (or stabilized base) under repeated traffic loading. The cracking initiates at the bottom of the asphalt surface (or stabilized base) where tensile stress or strain is highest under a wheel load. The cracks propagate to the surface initially as one or more longitudinal parallel cracks. After repeated traffic loading, the cracks connect, forming many-sided sharp-angled pieces that develop a pattern resembling chicken wire or the skin of an alligator. The pieces are usually less than 1 foot on the longest side. Alligator cracking occurs only in areas that are subjected to repeated traffic loading. Therefore, it would not occur over an entire area unless the entire area was subjected to traffic loading. Alligator cracking is considered a major structural distress (6).

2.5 DESIGN APPROACHES

In order to calculate the layer thicknesses of various given materials to achieve a certain "life" of the pavement, two basic approaches are being followed, namely, "empirical" and "mechanistic-empirical".

2.5.1 Empirical Design Approach

Empirical design approach is derived from experience or observations alone. Empirically derived relationships define the interaction between performance, load and pavement thickness for a given geographic location and climatic conditions. They are easy and simple to use.

2.5.1.1 Empirical Design Concept

Empirical design approach relies largely on engineering experience and judgement, mathematical performance or distress models based on measurements of field performance or some combination thereof, often without consideration of structural theory. These models are generally used to determine the required pavement thickness for a given number of load applications and/or the occurrence of distress due to pavement material properties, subgrade type, climate and traffic conditions.

Performance models typically takes the following form (4):

$$Y = A + (B_1)(X_1)^{c1} + (B_2)(X_2)^{c2} + \text{-----} \ (B_n)(X_n)$$

Where

Y = The predicted performance variable, such as rutting, cracking, serviceability, etc.

X_1, X_2, ...X_n = Independent design variables, such as traffic volume and composition, climate, material properties, layer thickness, etc.

A, B's, C's = Constants.

Examples of empirical models might include:-

1. Estimation of predicted loss of serviceability for a given pavement design, traffic and climatic conditions over a period of time.
2. Prediction of the rutting that will be found on a particular pavement given traffic volumes and compositions, pavement materials properties, subgrade type, climate, etc.
3. Prediction of the number of 18-kip ESAL'S that a pavement can withstand before fatigue cracking reaches an unacceptable level.

2.5.1.2 Limitations of Empirical design Procedures

Empirical procedures are accurate only for the exact conditions and ranges of independent variables (climate, material properties, traffic etc) under which they were developed and may actually be invalid outside of these ranges.

2.5.2 Mechanistic-Empirical Design Approach

In general, mechanistic-empirical design procedures consists of two models; theoretical and empirical (statistical). The theoretical model is mainly used to calculate the pavement mechanistic responses (i.e., stresses, strains, and deflections) based on a theoretical model. Some methods use the linear elastic theory, some others employee the nonlinear elastic theory, and still others use the viscoelastic theory. The empirical/statistical model relate the mechanistic responses to various types of load-related distress such as rutting and fatigue cracking. Therefore, the differences between the various mechanistic-empirical design procedures are mainly related to the theory employed in the method, the boundary conditions, and to the statistical models (pavement performance models) embedded in the method. Mechanistic design offers the only direct analytical consideration of the numerous variables that influences pavement performance in a design procedure. A disadvantage of such an approach to pavement design is that it typically requires more comprehensive data than the empirical design techniques (2).

2.5.2.1 Mechanistic-Empirical Design Concept

The basic components of mechanistic-empirical method consists of a structural analysis of the pavement system and the incorporation of distress or performance functions into the method.

Structural analysis refers to the calculation of stress, strain and deflection in a pavement that has been subjected to external loads or the effects of temperature or moisture. Once these values are determined at critical locations (see Figures 2.1 and 2.2), comparisons can be made to the maximum allowable values obtained from experimental or theoretical studies. The pavement can be designed by adjusting the different layer thicknesses so that the calculated stresses, strains and deflections are a fraction of the maximum allowable values (2).

2.5.2.2 Advantages of Mechanistic-Empirical Design Procedures.

Important advantages of this design philosophy are:-

1. Ability to analyze a pavement for several different failure modes, such as cracking and rutting.
2. Ability to improve the reliability of pavement design.
3. Ability to more accurately model the behavior of pavement sections.

2.5.2.3 Commonly used Empirical Statistical Models

1. **Fatigue Models.** The most commonly used fatigue prediction models are:-

1 Compressive strain - rutting

2 Tensile strain - fatigue or alligator cracking

3 Compressive strain - rutting

4 Compressive strain - rutting, depressions

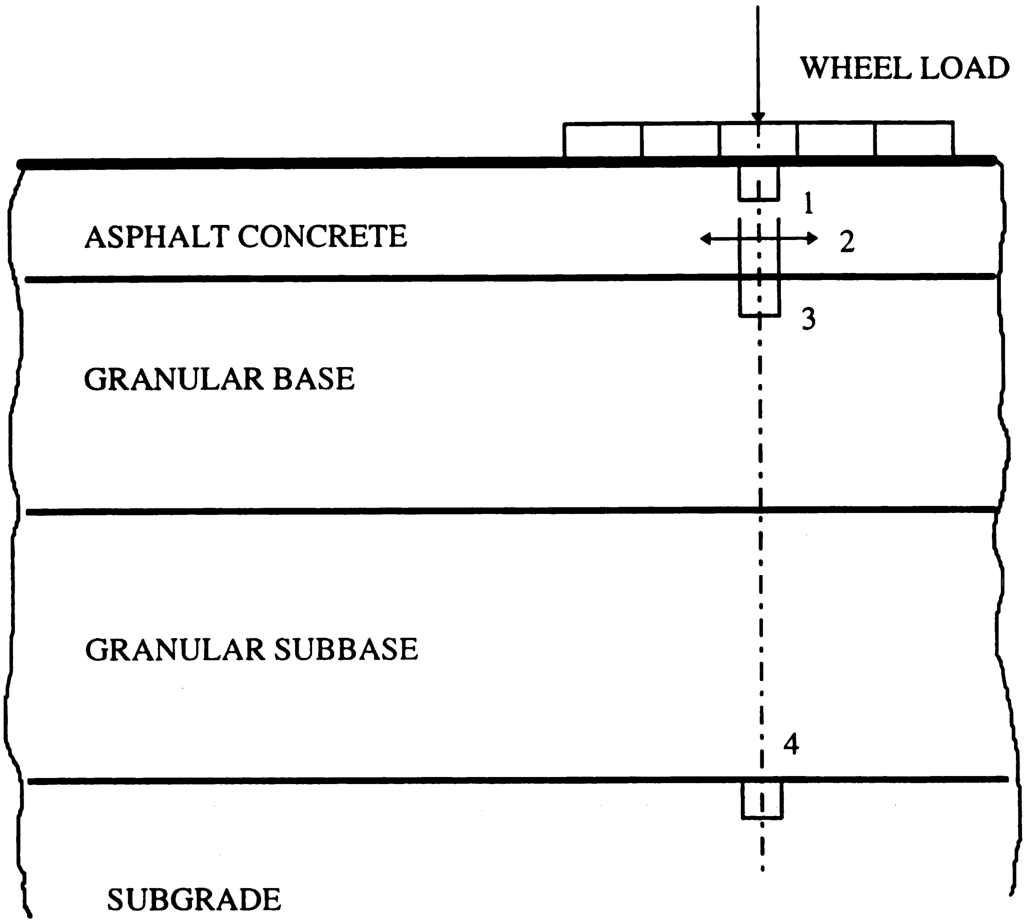

Figure 2.1: Typical asphalt pavement with a granular base showing the critical stress/strain locations

1 Compressive strain - rutting

2 Tensile strain - transverse reflective cracking or fatigue cracking

3 Compressive strain - rutting

4 Compressive strain - rutting, depressions

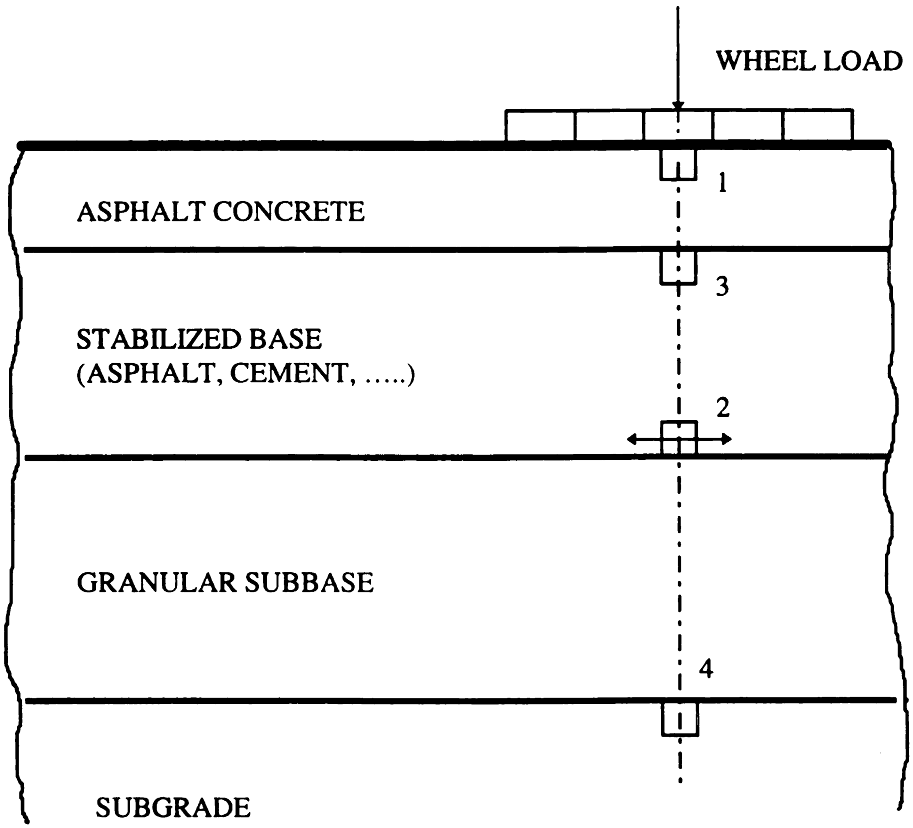

Figure 2.2: Typical asphalt pavement with a stabilized base showing the critical stress/strain locations

a. **Asphalt Institute Fatigue Model.** The Asphalt Institute model uses the following relationship to determine the permissible strain at the bottom of the asphalt layer (6).

Permissible strain = $\mathbf{240(N/10^6)^{-3.29}}$

Or $\mathbf{N_f = 10^6\ (240/\epsilon_r)^{3.29}}$

b. **Monsimith Fatigue Model.** Monsimith developed the following relationship to find the fatigue life of a pavement structure (5).

$$\mathbf{FL = K(1/\epsilon)^c}$$

The approximate values of K and C are tabulated below:

AC Modulus	C	Log_{10} K
100	2.86	-5.08
250	2.96	-5.95
500	3.53	-8.14
1000	4.06	-10.20

The above values of c and K are to be used in the following form of the model:

$$\mathbf{Log_{10}FL = Log_{10}(K) + c[Log_{10}(1/\epsilon)]}$$

c. **MICH-PAVE Model.** The MICHPAVE program was developed for the Michigan department of transportation (12). The program utilizes the following fatigue model.

$$\begin{aligned}\textbf{Log FL} = &-2.25 - 2.8 \log(D_0) + 2.3(B_1) + 0.92 \log(E_B) \\ &+ 0.15\ (T)_{AC} - 0.26\ AV + 0.0000\ E_{RB} - 1.096 \\ &\log(TS) + 1.17 \log\ (CS) - 0.001\ KV \\ &+ \log[(1+F)/32]\end{aligned}$$

Where

D_0 = peak surface deflection

B_1 = function of base and subbase thickness

E_B = modulus of base

T_{AC} = Ac thickness

AV = percent air voids in AC

E_{RB} = modulus of roadbed soil

TS = tensile strain at the bottom of the AC

CS = compressive strain at the top of the AC

KV = kinematic viscosity of the asphalt

F = average annual air temperature

d. **NAASRA Model** (Australian Model). N A A S R A developed the following relationship to predict the fatigue life (N_f) of the pavement structure(7).

$$N_f = 10^6\ (225/\epsilon_r)^5$$

Where ϵ_r = radial strain (microstrain)

2. **Rut Models.** The most common rut prediction models are:-

a. **The Asphalt Institute Rut Model.** Asphalt Institute developed the following relationship to predict the number of load repetitions to 13 mm rut depth (7):-

$$\mathbf{N = 10^6\ (482/\epsilon_v)^{4.48}}$$

Where ϵ_v = vertical compressive strain (microstrain)

b. **The TRRL Rut Model.** The following TRRL rut model predicts the number of load repetitions to 10 mm rut depth (7):-

$$\mathbf{N = 10^6\ (453/\epsilon_v)^{3.95}}$$

Where ϵ_v = vertical compressive strain (microstrain)

c. **The ERES Rut Model.** ERES developed following rut model which limits the vertical strain on the roadbed soil to a value that will not overstress the soil. However the literature is quite on the maximum allowable rut depth (2):-

$$\mathbf{N = 1.365 \times 10^{-9}\ (\epsilon_v * 10^{-6})^{-4.477}}$$

Where ϵ_v = vertical compressive strain (microstrain)

2.6 DESIGN PROCEDURES

Two design procedures can be found: empirical and mechanistic-empirical.

2.6.1 Empirical Procedures

Two of the more popular empirical design methods are, the AASHTO and the Asphalt Institute methods:-

2.6.1.1 AASHTO Design Procedure

The AASHTO design procedure was developed as the result of the AASHO Road Test that was conducted under a particular set of environment, one roadbed soil, and a limited load/traffic conditions. The method has been modified and revised several times. The most significant revision was made in 1986. The 1993 revision of the AASHTO design procedure did not include any further modification of the 1986 version. However, the design of the asphalt overlay was totally revised.

The 1993 AASHTO design procedure for flexible pavements begin with the determination of the required structural number (SN) as a function of design reliability and standard deviation, the number of 18-kip equivalent single axle load (ESAL), the effective resilient modulus of the roadbed soil (M_R) and the total allowable serviceability loss in terms of PSI. Trial pavement designs are then identified by using different layer thicknesses that provide the required structural number, meet minimum layer thickness criteria, and provide adequate protection for the underlying materials (2).

2.6.1.2 Road Note 29

Road Note 29 was first published in 1960 to provide a guide to the structural design of roads carrying medium to heavy traffic under British conditions of climate, materials, traffic loading etc.

This note deals solely with the construction of new roads and not with the resurfacing and maintenance of existing roads (8).

2.6.2 Mechanistic-Empirical Design Procedures

Few of the more commonly used design procedure under this approach are the VESYS, Finite element, and elastic layered system methods.

2.6.2.1 VESYS (Visco-Elastic System) Method

The VESYS structural subsystem computer program is designed in a modular form based on the theory of viscoelasticity. It includes routines for the computations of the pavement deformation in each of the N layer. The VESYS computer program consists of four major interactive models as follows (2):

1. Primary response model in terms of stress, strain and displacement under static loading. The model produces a probablistic linear viscoelastic solution for the mean and variance of the time dependent stress, strain and deflection at prescribed positions of a layered pavement

system.

2. General response model that is defined as that response of a mathematical model resulting from any type of loading input.
3. Damage model that consists of three submodels: rut, cracking and roughness. The outputs of the primary and the general response models are used for the prediction of pavement distress.
4. Performance model in terms of present serviceability index (PSI). In this model, the rut depth and roughness prediction models are used in conjunction with the AASHO developed PSI equation.

2.6.2.2 Finite Element Method

The finite element method is used for the structural analysis of pavements, specially when the nonlinear behavior of granular and cohesive materials is to be considered in the mechanistic modeling. In the method it is necessary to impose side and bottom boundaries at a reasonable distances from the loaded area. Weak roadbed soils require deep finite element mesh which increases the computational efforts and in case of nonlinear problems, requires a mainframe computer (2).

Several finite element (FEM) programs have been developed, some popular programs are:-

1. **ILLI-PAVE**, a stress dependent program developed at the University of Illinois, U.S.A. The ILLI-PAVE computer program considers the pavement as an axisymmetric solid.

The program uses stress-dependent resilient modulus and failure criteria for granular materials and fine grained soils. The principle stresses in the granular and subgrade layers are modified at the end of each iteration, so that they do not exceed the strength of the materials as defined by Mohr-Coulomb failure criteria (9).

2. The **MICH-PAVE** is very similar to ILLI-PAVE and uses similar methods to characterize granular materials and fine grained soils. A major improvement is the use of flexible boundary at a limited depth beneath the surface of the subgrade, instead of a rigid boundary at a large depth below the surface. The subgrade below the flexible boundary is considered as a homogeneous half-space, whose stiffness matrix can be determined and superimposed to the stiffness matrix of the pavement above the flexible boundary to form the overall stiffness matrix. The use of flexible boundary greatly reduces the number of finite elements required, especially those oblong elements at the bottom. Consequently the storage requirement is significantly reduced and the program can be implemented on personal computers. The fewer number of simultaneous equations to be solved and the elimination of those oblong elements also yield more accurate results (2,12).

2.6.2.3 Elastic Layered Methods

2.6.2.3.1 Asphalt Institute Method

The Asphalt Institute method for flexible pavement design can be used to design an asphalt pavement composed of various combinations of asphalt surface and base. emulsified asphalt surface and base, and untreated aggregate base and subbase. The procedure uses multi layer elastic theory for the determination of the required pavement thickness. In the development of the design procedure, two critical stress-strain conditions were examined. The first is the maximum vertical compressive strain induced at the top of the roadbed soil (rutting) and the second is the maximum horizontal tensile strain induced at the bottom of the asphalt concrete layer (fatigue cracking). For a given set of design variables, the larger of either the rut potential or the fatigue life governs the thickness requirement (2). The method uses 20 to 25 percent of fatigue crack in the asphalt surface and 0.5 inch of rut as the limiting criteria.

Parameters relevant to design are traffic in terms of 18 kips single axle load, environment (design charts are prepared for 45°F, 60°F, 75°F) and material characteristics.

2.6.2.3.2 ELSYM5

ELSYM5 is a computer program that models a three dimensional idealized elastic layered pavement system. The pavement may be loaded with one or more identical uniform circular loads normal to the surface of the pavement. The program computes various component, strains and displacements along locations specified by the user, within the layered pavement. It is a modification of the layer 5 program allowing consideration of multiple loads as well as the presence of a rigid base below the subgrade (13).

1. **Development of the ELSYM5 Procedure.** ELSYM5 was developed by Gale Ahlborn of the Institute of Transportation and Traffic Engineering (ITTE) at the University of California, Berkeley. It is based on the elastic layered system, with the ability to consider multiple loads as well as the presence of a rigid base below the subgrade. The coordinate system in ELSYM5 is a three dimensional cartesian system.

   The program assumes that each layer is composed of a weightless, homogeneous, isotropic material. The material behaves in an ideally elastic manner, according to Hook's Law. Each layer is of uniform thickness and infinite width in all horizontal directions. The bottom elastic layer may be semi-infinite in thickness or may be given a finite thickness, in which case the program assumes the bottom elastic layer is supported by a rigid base. The boundaries between the layers are assumed to develop full friction, with the exception of the interface between the bottom layer and the rigid base where zero friction can be specified. The surface is free of shear and the applied loads are assumed to be identical, vertical, and uniform over circular areas. The principle of superposition is used to determine the response at any given point when the multiple loads are specified. The input data consists of layer property, load, and evaluation coordinate data, as shown in Figures 2.3, 2.4 and 2.5. The output of ELSYM5 contains a summary of all the responses calculated at each point. These include principal stresses and strains as well as the normal stresses, strains, and displacements. The output result menu and the output options are presented in Figures 2.6, 2.7, 2.8 and 2.9.

2. **Data Required by ELSYM5.** The input data required for ELSYM5 is divided into the following three categories:-

   a. **Layer Properties.** Each pavement analyzed by ELSYM5 may be composed of one to five elastic layers. The three properties required for each layer are the thickness (in inches), Poisson's ratio, and modulus of elasticity. The thickness is set equal to zero for the bottom elastic layer which is assumed to be a semi-infinite. If a thickness is given, it is assumed that the layer is resting on a rigid base and the user is prompted to determine if the base is a full friction rigid base or a no friction base.

   b. **Load Data.** Loading is applied to the pavement by a series of up to ten uniform circular loads applied

Screen 1.2.2

ELASTIC LAYER DATA

Number of Layers: 3

Layer Number	(top to bottom)	Thickness inches)	poisson's Ratio	Modulus of Elasticity
1		8.00	.15	4000000.00
2		6.00	.40	30000.00
3		.00	.45	5000.00

Note: Enter Zero thickness when bottom layer is semi-infinite.

Which one layer will be deleted (if NONE, enter 0)? Ω

Figure 2.3 Terminal Screen : Elastic Layer Data

```
                                                          Screen 1.2.3

                              LOAD DATA


Enter two of the following, the third is calculated.

Load:    4500.00lbs  Pressure:    75.00 Psi   Load Radius    .00Inches

Number of load location:    2
Location                                        Coordinates
Number =                                   X =                Y =
        1                                       .00               .00
        2                                     13.11               .00



CR:  To Next Data Field: F2: Skip to End of Screen
```

Figure 2.4 Terminal Screen : Load Data

Screen 1.2.4

EVALUATION LOCATION DATA

Results are evaluated for all combinations of X-Y coordinates and Depths of Z.
Number of X-Y positions: 2
Number of Z position : 1

Position	X	Y
1	.00	.00
2	6.56	.00

Position	Z
1	8.00

CR: To Next Data Field: F2: Skip to End Screen

Figure 2.5 Terminal Screen : Evaluation Location Data

```
                 Normal Strains                      Shear Strains
XP     YP         EXX        EYY        EZZ        EXY        EXZ        EYZ
 .00    .00     .267E-04   .343E+04 -.111E-04   .000E+00   .179E-06   .000E+00
6.56    .00     .231E-04   .348E+04 -.105E-04   .000E+00 -.303E-09   .000E+00

               Principal  --  Strains           Shear Strains

XP     YP         PEI        PE2        PE3       PSE1       PSE2       PSE3
 .00    .00     .345E+04   .267E+04 -.111E+04   .454E+04   .758E+05   .379E+04
6.56    .00     .348E+04   .231E+04 -.105E+04   .458E+04   .117E.04   .386E+04

               RESULTS MENU FOR ELSYM 5
               -----------------------------
                LAYER  =  1      Z   =    8.00

  1. - Stresses Normal & Shear & Principal
  2. - Strains  Normal & Shear & Principal
  3. - Desplacements
  4. - Return or continue with Next Layer

    Selection = = >
```

Figure 2.6 Terminal Screen : Output Screen
Stresses Normal, Shear and Principal

```
                 Normal Stresses                     Shear Stresses
XP     YP          SXX        SYY        SZZ       SXY       SXZ        SYZ
 .00    .00    .130E+03  .156E+03 - .158E+01  .000E+00  .311E+00  .000E+00
6.56    .00    .116E+03  .106E+03 - .141E+01  .000E+00 -.527E-01  .000E+00

               Principal  --  Stresses               Shear Stresses

XP     YP          PS1        PS2        PS3      PSS1      PSS2       PSS3
 .00    .00    .156E+03  .130E+03 - .159E+01  .790E+02  .132E+02  .650E+02
6.56    .00    .156E+03  .116E+03 - .142E+01  .786E+02  .204E.02  .585E+02

               RESULTS MENU FOR ELSYM 5
               -----------------------------
                LAYER  =  1      Z   =    8.00

  1. - Stresses Normal & Shear & Principal
  2. - Strain a Normal & Shear & Principal
  3. - Desplacements
  4. - Return or continue with Next Layer

    Selection = = >
```

Figure 2.7 Terminal Screen : Output Option
Strains Normal, Shear and Principal

```
                 Displacement
XP     YP        UX           UY         UZ
 .00    .00   - .172E-03  .000E+00 .145E-01
6.56    .00     .174E-06  .000E+00 .142E-01

           RESULTS MENU FOR ELSYM 5
           -----------------------------
           LAYER  = 1      Z    =   8.00

  1. - Stresses Normal & Shear & Principal
  2. - Strains  Normal & Shear & Principal
  3. - Displacements
  4. - Return or continue with Next Layer

    Selection = = >
```

Figure 2.8 Terminal Screen : Output Option 3 Displacements

```
        RESULTS MENU FOR ELSYM 5
       -----------------------------
       LAYER  =  1      Z    =    8.00

1. - Stresses Normal & Shear & Principal
2. - Strains  Normal & Shear & Principal
3. - Displacements
4. - Return or continue with Next Layer

Selection = = >
```

Figure 2.9 Terminal Screen : Results Menu normal to the surface of the pavement. The loads are defined by any two of the following three properties: load force in pounds, load pressure in psi, or load radius in inches. ELSYM5 calculates the third property based on the two entered. The location is defined by X and Y coordinates along the surface of the top layer of the pavement. All load values must be positive, but the coordinates may be positive or negative distances.

c. **Evaluation Coordinate.** ELSYM5 evaluates stresses, strains and displacements at locations determined by the user. These locations are entered as a series of XYZ coordinates. All combinations of XY and Z coordinates can be evaluated.

3. **Program Limitations.** There are several limitations imposed on the ELSYM5 procedure. The first two are based on the analysis procedure itself and the remaining are based on array size limits in the coding. The limitations are as follows:-

a. Poisson's ratio for any layer must not have a value of one. In addition, Poisson's ratio for a bottom layer on a rigid base must not equal to 0.75 and therefore, should not be in range of 0.748 to 0.752. These values lead to impossible results or run time errors because of the equations used in the analyses.

b. The program uses a truncated series for the integration process that leads to some approximation of the results at and near the surface and at points located at some distance from the load.

c. The number of different pavement systems for solution is limited only by the size of the data file on the diskette. Each pavement is analyzed individually and thus there is no program limitation.

d. The number of elastic layers in the pavement cannot exceed five.

e. The number of identical uniform circular loads applied to the pavement cannot exceed ten.

f. The number of evaluation coordinates where results are desired is limited to a maximum of ten XY coordinates pairs and ten Z coordinates, for a combined maximum of 100 points. The minimum number would be one XY pair and one Z for a total of one point.

g. For pavements with a rigid base specified, the maximum value for coordinate Z cannot exceed the depth to the rigid base.

h. All values except for the XY coordinates must be positive.

CHAPTER 3

RESEARCH PLAN

3.1 RESEARCH OBJECTIVES

As stated in chapter 1, the research objectives are:-

1. Establish a series of AC pavement structural design by using the AASHTO procedure (DNPS-86) for various combinations of roadbed soil modulus, structural layer material properties and traffic levels existent in Pakistan (see Table 3.1).

2. Compute the mechanistic responses of each pavement section using ELSYM5 for a standard 18,000-lb single axle load (80 psi tire pressure) and analyze their sensitivity to the assigned range of variables (roadbed and layer moduli and traffic levels) and subsequently verify SHRP study results (see section 4.10.2) for ranges of variables in Pakistan.

3. Select AASHTO designed pavement sections from Table 3.1 with the constant variables as given below and then calculate "critical pavement responses" using ELSYM5 for 23,000-lb and 28,000-lb single axle load (120 psi tire pressure).

   - AC layer coefficient, $a_1 = 0.44$

Table 3.1: Study Variables for Sensitivity Analyses

Test Variable	Test Level		
	I	II	III
AC Modulus (ksi)	150	300	450
Base Modulus (ksi)	20	30	40
Subbase Modulus (ksi)	10	15	20
Roadbed Soil Modulus (ksi)	7.5	10	20
18,000-lb ESAL's (million)	25	50	75

- Base layer coefficient, a_2 = 0.14
- Base drainage coefficient, m_2 = 1.00
- Subbase layer coefficient, a_3 = 0.11
- Subbase drainage coefficient, m_3 = 1.00
- Design reliability, R = 95%
- Overall standard deviation, S_o = 0.45 (Traffic errors included)
- Performance period = 10 years
- Loss in serviceability = 1.9

4. Calculate the "fatigue and rut life" for each pavement section (for loading conditions of 18,000 lb, 23,000 lb and 28,000 lb) using various fatigue and rut performance prediction models.

5. Re-compute adopting combinations of strategies mentioned below, the fatigue and rut life of the AASHTO designed pavement sections after changing the material properties and using different combinations of layer thicknesses and check them against various other existent fatigue and rut criterion.
   a. Use asphalt stabilized base with layer moduli values ranging between 250,000 and 450,000 psi.
   b. Eliminate subbase layer and use asphalt treated base (elastic modulus value up to 200,000 psi).
   c. Use granular base and subbase but with increased layer moduli (increase in layer moduli to be

achieved through compaction and better gradation of the materials).

To accomplish the above objectives a 3-part research plan was formulated. These parts are presented in the next section.

3.2 RESEARCH PLAN AND METHODOLOGY

As stated early, a 3-parts research plan was formulated and executed as presented below:-

3.2.1 PART I -Sensitivity Analysis of outputs from AASHTO design procedure (DNPS-86 computer program) and verification of SHRP study results (11) for ranges of variables in Pakistan. This part consists of two phases as follows:-

PHASE I - In this phase a series of AC pavement structures was designed by using the AASHTO design guide (the AASHTO DNPS-86 computer program was used). In the design, a range of variables (roadbed and layer moduli and traffic levels) similar to that existing in Pakistan was used. Table 3.2 and Figure 3.1 provide a list of the values of these variables. As it can be seen from Figure 3.1, the design matrix consists of 243 cells. Each cell representing a pavement section. Table 3.3 provides a list of the constant values of the other design input required by the AASHTO. These constant values have no impact

Table 3.2: Sensitivity analysis - Study variables.

Design Variables	Ranges of values		
	Low	Nominal	High
Traffic in terms of 18-kips ESALs (millions)	25	50	75
Asphalt concrete resilient modulus (ksi)	150	300	450
Base resilient modulus (ksi)	20	30	40
Subbase resilient modulus (ksi)	10	15	20
Roadbed resilient modulus (ksi)	7.5	10	20

	(1)	150									300									450								
	(2)	20			30			40			20			30			40			20			30			40		
(4)	(3)	10	15	20	10	15	20	10	15	20	10	15	20	10	15	20	10	15	20	10	15	20	10	15	20	10	15	20
7.5	25	1	10	19	28	37	46	55	64	73	82	91	100	109	118	127	136	145	154	163	172	181	190	199	208	217	226	235
	50	2	11	20	29	38	47	56	65	74	83	92	101	110	119	128	137	146	155	164	173	182	191	200	209	218	227	236
	75	3	12	21	30	39	48	57	66	75	84	93	102	111	120	129	138	147	156	165	174	183	192	201	210	219	228	237
10	25	4	13	22	31	40	49	58	67	76	85	94	103	112	121	130	139	148	157	166	175	184	193	202	211	220	229	238
	50	5	14	23	32	41	50	59	68	77	86	95	104	113	122	131	140	149	158	167	176	185	194	203	212	221	230	239
	75	6	15	24	33	42	51	60	69	78	87	96	105	114	123	132	141	150	159	168	177	186	195	204	213	222	231	240
20	25	7	16	25	34	43	52	61	70	79	88	97	106	115	124	133	142	151	160	169	178	187	196	205	214	223	232	241
	50	8	17	26	35	44	53	62	71	80	89	98	107	116	125	134	143	152	161	170	179	188	197	206	215	224	233	242
	75	9	18	27	36	45	54	63	72	81	90	99	108	117	126	135	144	153	162	171	180	189	198	207	216	225	234	243

Figure 3.1: Full factorial design matrix showing layer moduli and levels of traffic volume in terms of 18-kip ESAL's.

(1) = AC MR (ksi) (2) = BASE MR (ksi) (3) = SUBBASE MR (ksi) (4) = ROADBED MR (ksi)

Table 3.3: Sensitivity analysis - Constant design variables

Design Variables	Value
Design and analysis period (years)	10
Loss in serviceability	1.9
Reliability	95%
Standard deviation	0.45
Drainage coefficient (all layers)	1.0
Wheel load (lbs)	9000
Tire pressure (psi)	80
Poisson's ratio	
AC	0.40
Base	0.35
Subbase	0.35
Roadbed	0.45

on this study. The sensitivity of the AASHTO outputs (layer thicknesses) to the assigned range of variables was then determined.

PHASE II- In this phase the mechanistic responses of each pavement section of Figure 3.1 to 18,000 lb axle load (80 psi tire pressure) were determined using the ELSYM5 computer program. The mechanistic responses were then analyzed to verify the accuracy and applicability of SHRP results (11) to conditions in Pakistan. Initially it was planned to verify the results of the study using field data. Unfortunately such data was not available and consequently this alternate plan was formulated.

3.2.2 **PART II -** In this part the performance of some of the pavement sections of Figure 3.1 was compared relative to the roughness, rut and fatigue cracking. In the comparison several existing rut and fatigue performance models and the AASHTO roughness models were used and relative performance of 9 pavement sections (9 cells) of Figure 3.1 was predicted. These 9 pavement sections were chosen because the material properties (layer coefficient and moduli) are equivalent to those used in Pakistan for the design of pavement structures. During the analysis 3 additional pavement sections with 15 ksi roadbed modulus were also designed by using the AASHTO design guide and their relative performance were predicted. The reason for addition of these three cells is to narrow the gap in the values of the roadbed modulus. Figure 3.2 shows the original 9 cells of Figure 3.1 and the 3 new cells alongwith the material properties used in the design. The analysis in this part consists of the following 3 steps.

STEP 1- The ELSYM5 computer program was used to calculate the radial tensile strain at the bottom of the AC layer and the vertical compressive strain at the top of the roadbed soil for the pavement sections of Figure 3.2. The following combinations of axle loads and tire pressures were used in the analysis:-

Axle Load(lbs)	Tire Pressure(psi)
18000	80
23000	120
28000	120

STEP 2- The fatigue life of each of the 12 pavement sections of Figure 3.2 was then estimated by using the following models:-

a) **Asphalt Institute Fatigue Model**

b) **Monismith Fatigue Model**

c) **MICH-PAVE Fatigue Model.** The parameters used in the MICH-PAVE model are:
Percent air voids in Asphalt mix = 6.5%, the

AC M_R (ksi)	450 ($a_1 = 0.44$)			
BASE M_R (ksi)	30 ($a_2 = 0.14$)			
SUBBASE M_R (ksi)	15 ($a_3 = 0.11$)			
ROADBED	7.5	10	15*	20
TRAFFIC $25x10^6$	199	202	205a	205
TRAFFIC $50x10^6$	200	203	206a	206
TRAFFIC $75x10^6$	201	204	207a	207

* Three additional pavement sections

Figure 3.2: Matrix representing nine pavement sections from Figure 3.1 and three additional pavement sections with roadbed modulus of 15 ksi

average value used by the National Highway Authority (NHA).

The kinematic viscosity of the asphalt binder of 270.00 centistoke.

An average annual temperature of 88°F (This is the average annual temperature observed in Risalpur area for the year 1993).

d) **NAASRA Fatigue Model**

STEP 3 - The number of load repetitions to cause a specific rut depth for the 12 cells of Figure 3.2 was calculated by using the following three rut models (It is to be noted that each model was caliberated for different rut depth as mentioned in chapter 2):

a) **Asphalt Institute Rut Model**

b) **TRRL Rut Model**

c) **ERES Rut Model**

3.2.3 PART III - ENHANCEMENT OF THE PERFORMANCE OF THE AASHTO DESIGNED PAVEMENT SECTIONS

In this part, the performance of each of the 12 pavement sections of Figure 3.2 was reassessed by using the following alternatives:-

1. **Alternative** 1. Replace the granular base layer with

asphalt stabilized layer with a range of elastic moduli from 250 to 450 ksi.

2. **Alternative 2.** Eliminate the subbase layer and use asphalt treated base with a modulus value of 200 ksi.

3. **Alternative 3.** Increase the layer moduli of the granular base and subbase layer. The modulus of the base layer will be increased to a maximum value of 75 ksi and the modulus of the subbase layer to a maximum value of 40 ksi.

The 3 alternatives provide the means to the highway engineer to optimize the material selection process relative to pavement performance and cost.

CHAPTER 4

AASHTO FLEXIBLE PAVEMENT DESIGN PROCEDURE

4.1 INTRODUCTION

The design procedure recommended by the American Association of State Highway and Transportation Officials (AASHTO) is based on the results of the extensive AASHO Road Test conducted in Ottawa, Illinois, in the late 1950s and early 1960s. The AASHO Committee on Design first published an interim design procedure in 1961. It was revised in 1972 and 1981. In 1984-85, the subcommittee on Pavement Design and a team of consultants revised and expanded the interim procedure under NCHRP Project 20-7/24 and issued the 1986 Design Guide.

The empirical performance equations obtained from the AASHO Road Test are still being used as the basic models in the current guide but were modified and extended to make them applicable to other regions in U.S.A. It should be kept in mind that the original equations were developed under a given climatic setting with a specific set of pavement materials and subgrade soils. The climate at the test site is temperate with an average annual precipitation of about 34 in. The subgrade soils consisted of A-6 and A-7-6 that are poorly drained, with CBR values ranging from 2 to 4.

4.2 CHANGES IN THE 1986 AASHTO Design Guide

The 1986 AASHTO Design Guide presents major changes in several areas including (6):-

1. **Reliability.** A reliability factor based on variations in the input variables was introduced into the 1986 AASHTO guide.
2. **Soil Support Value.** The soil support value has been replaced with the effective resilient modulus of the roadbed soil.
3. **Layer coefficients.** The 1986 AASHTO Guide suggests the use of the resilient moduli of the layers to assigned layer coefficients to both stabilized and unstabilized materials.
4. **Regional factor.** The subjective regional factor was replaced by a rational approach to account for the effects of environmental factors such as moisture, temperature, and freeze-thaw cycles on pavement design.
5. **Traffic and Load Equivalency Values.** Extensive information concerning methods for calculating equivalent single axle loads are provided. Load equivalency values have been extended to include heavier loads, more axles, and terminal serviceability levels of up to 3.0.
6. **Mechanistic-Empirical Design Procedure.** A state of knowledge concerning mechanistic-empirical design concepts is provided in the guide.

4.3 OVERVIEW OF THE AASHO ROAD TEST

The AASHO Road Test was conducted near Ottawa, Illinois, U.S.A, located about 80 miles southwest of Chicago. The site was chosen because the soil within the area was uniform and representative of the country. The climate was typical of that found in the northern United States.

The Test facilities consisted of six two lane test loops, constructed as shown in Figure 4.1. The north tangent of each loop was constructed of flexible pavement sections and the south tangent was constructed of rigid pavement sections. Most of the 234 flexible pavement structural design sections (468 test sections each 160 feet in length) comprised a complete replicated factorial experiment to investigate the effects of varying the thicknesses of surface, base and subbase layers. Several additional studies were conducted to evaluate surface treatments, shoulders, and four different types of base layers: crushed stone,gravel, cement-treated gravel, and bituminous-treated gravel.

All vehicles assigned to any one traffic lane in loops 2 through 6 (no traffic operated over lane 1) had the same axle arrangement and axle load combinations, as described in Table 4.1. The tire pressure and steering axle loads were representative of normal practice at that time. The test was conducted over a two year period which was sufficient to allow the application of 1,114,000 load applications to each loop (2).

Several measurements were taken at regular intervals to assess pavement performance. These include transverse pavement profile to determine rutting, cracking, patching, deflections, strains, layer thickness, and temperature. This information was used directly in the development of the performance models

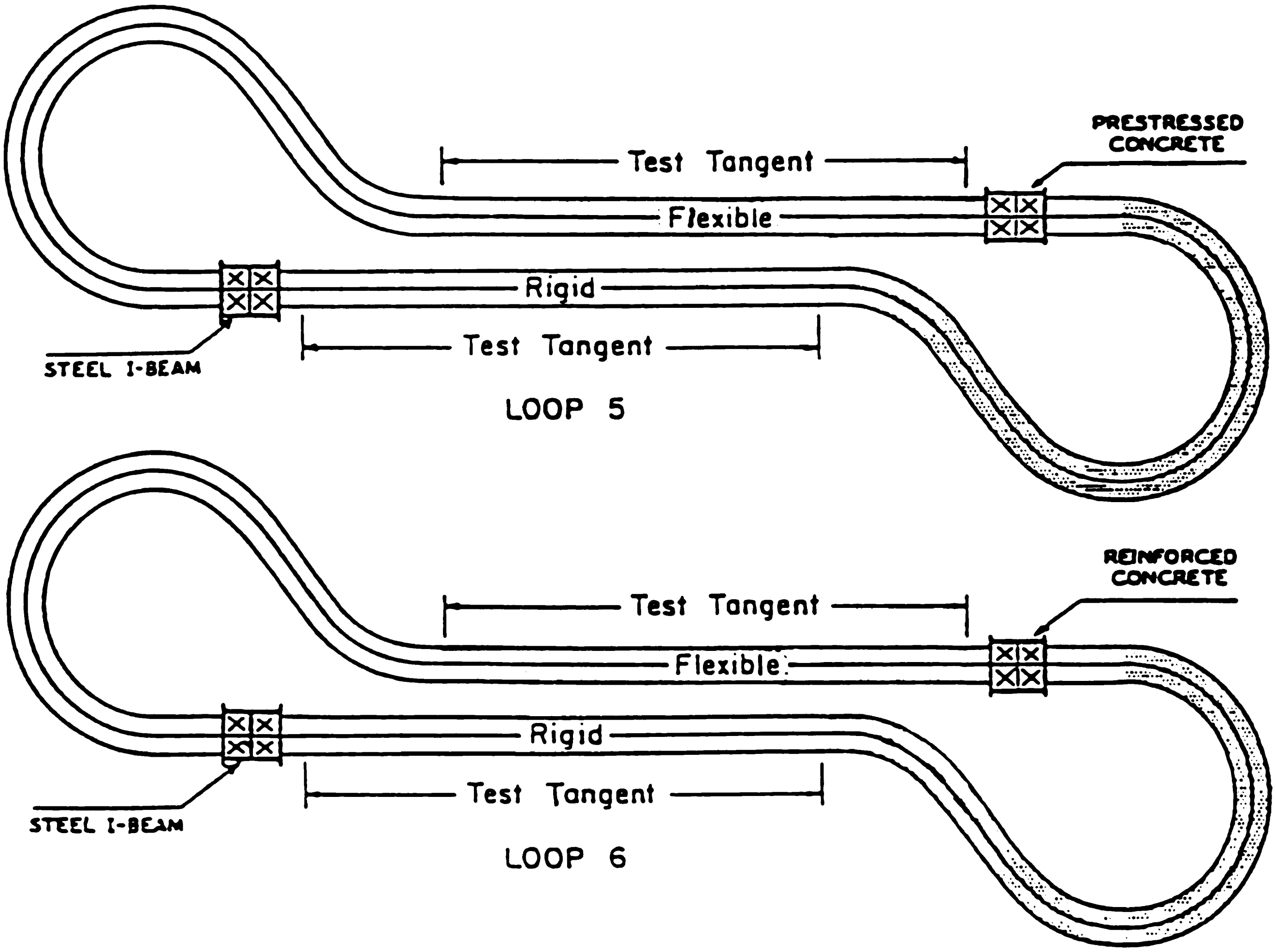

Figure 4.1 Layout of the ASSHO road test

Table 4.1 Axle weights and distributions used on various loops of the AASHO road test

LOOP LANE	WEIGHT IN KIPS		
	FRONT AXLE	LOAD AXLE	GROSS WEIGHT
2	2	2	4
	2	6	8
3	4	12	28
	6	24	54
4	6	18	42
	9	32	73
5	6	22.4	51
	9	40	89
6	9	30	69
	12	48	108

that eventually became the basis for the current AASHTO Design Guide.

4.4 DESIGN VARIABLES

The general design variables considered in the design and construction of any pavement structure are presented below (6).

1. **Time constraints.** Time constraints permit the designer to select from strategies ranging from the initial structure lasting the entire analysis period (i.e., performance period equals the analysis period) to stage construction with an initial structure and planned overlays (6). To achieve the best use of available funds, the AASHTO Design Guide encourages the use of a longer analysis period (for high-volume facilities), that include at least one rehabilitation period. Thus, the analysis period should be equal to or greater than the performance period (9).

    a. **Performance Period.** This refers to the period of time that an initial pavement structure will last before it needs rehabilitation. It also refers to the performance time between rehabilitation operations. In the AASHTO design guide, the performance period is equal to the time elapsed as the new, reconstructed, or rehabilitated pavement deteriorates from its initial serviceability to its terminal serviceability. For the performance period, the designer must select minimum and maximum bounds that are established by the agency experience (6). The selection of performance period can be affected by such factors as the functional classification of the pavement, the type and level of maintenance applied, the available funds for initial construction, life cycle cost, and other engineering considerations (9).

b. **Analysis Period.** This refers to the period of time for which the analysis is to be conducted, i.e., the length of time that any design strategy must cover. Because of the consideration of the maximum performance period, it may be necessary to consider and plan for stage construction (i.e., an initial pavement structure followed by one or more rehabilitation operations) to achieve the desired analysis period. In the past, pavements were typically designed and analyzed for a 20-year performance period (6).

2. **Traffic.** The design procedures for both highways and low volume roads are all based on cumulative expected 18-kip equivalent single axle loads (ESAL) during the performance and analysis periods (6). If a pavement is designed for the analysis period without any rehabilitation or surfacing, all that is required is the

total ESAL over the analysis period. However, if stage construction is considered and rehabilitation or resurfacing is anticipated, a graph or equation of cumulative ESAL versus time is needed so that the ESAL traffic during any given stage can be obtained. Hence, an accurate traffic forecasting model is crucial in the pavement design process.

3. **Reliability.** The reliability of a pavement design-performance process is the probability that a pavement will perform satisfactorily during its design life. Basically, it is a means of incorporating some degree of certainty into the design process to ensure that the various design alternatives will last the analysis period. The reliability design factor accounts for variations in both traffic prediction, performance prediction, material, and construction.

   Table 4.2 presents recommended levels of reliability for various pavement functional classifications. Application of reliability concept requires the selection of a standard deviation that is representative of local conditions. Table 4.3 presents the recommended values of standard deviation. Values of S_0 developed at the AASHO Road Test did not include traffic error. However, the performance prediction error developed at the Road Test was 0.25 for rigid and 0.35 for flexible pavements. This corresponds to a total standard deviation of 0.35 and 0.45 for rigid and flexible pavements, respectively (6).

Table 4.2: Recommended level of reliability for various pavement functional classifications.

Functional classification	Reliability (%) Urban	Rural
Interstate and Other Freeways	85-99.9	80-99.9
Principal Arterials	80-99	75-95
Collectors	80-95	75-95
Local	50-80	50-80

Table 4.3: Recommended values of standard deviation.

Design Condition	Standard Deviation	
	Flexible	Rigid
Variation in pavement performance prediction without traffic error	0.35	0.25
Total variation in pavement performance prediction and in traffic estimation	0.45	0.35

When stage construction is considered, the reliability of each stage must be compounded to achieve the overall reliability:

$$R_{stage} = (R_{overall})^{1/n}$$

in which n is the number of stages being considered. For example, if two stages are contemplated and the desired level of overall reliability is 95 percent, the reliability of each stage must be $(0.95)^{1/2}$, or 97.5 percent (9).

4. **Environmental Effects.** The environment can affect pavement performance in several ways. Temperature and moisture changes can have an effect on the strength, durability and load carrying capacity of the pavement and roadbed materials. Another major environmental impact is the direct effect of roadbed swelling, frost heave, etc. on loss of ride quality and serviceability. Additional effects such as aging, hardening and overall material deterioration due to weathering, have been considered in the AASHTO Design Guide only in terms of their inherent influence on the pavement performance prediction models (6).

5. **Serviceability.** The AASHTO Design Guide defines serviceability of a pavement as its ability to serve the traffic during its design life. The primary measure of serviceability is the Present Serviceability Index (PSI),

which ranges from 0 (impassible road) to 5 (perfect road). The basic design philosophy of this guide is the serviceability-performance concept, which provides a means of designing a pavement based on a specific total traffic volume and a minimum level of serviceability desired at the end of the performance period (6).

Initial and terminal serviceability indexes must be established to compute the changes in serviceability, ▲PSI, to be used in the design equation. The initial serviceability is a function of pavement type and construction quality. Typical values from the AASHO Road Test are 4.2 for flexible pavements and 4.5 for rigid pavements. The terminal serviceability index is the lowest index that will be accepted before rehabilitation or reconstruction become necessary. An index of 2.5 or higher is suggested for design of major highways and 2.0 for highways with lower traffic (9).

4.5 MATERIAL PROPERTIES FOR STRUCTURAL DESIGN

4.5.1. Effective Roadbed Soil Resilient Modulus

The basis for material characterization in AASHTO Design Guide is its elastic or resilient modulus. For roadbed materials, laboratory resilient modulus test (AASHTO T274) should be performed on representative samples in stress and moisture conditions simulating those of the primary moisture seasons. Alternatively, the seasonal resilient modulus values may be determined by correlations with soil properties i.e., clay content, moisture, PI, etc. The purpose of identifying seasonal moduli is to quantify the relative damage a pavement is subjected to during each season of the year and treat it as a part of the overall design. An effective roadbed soil resilient modulus is then established which is equivalent to the combined effect of all the seasonal modulus values. (The development of the procedure for generating roadbed soil resilient modulus is presented in Appendix HH of volume 2 of the 1986 AASHTO Design Guide).

Two different procedures for determining the seasonal variation of the modulus are offered as guidelines. One method is to obtain a laboratory relationship between resilient modulus and moisture content. With an estimate of the in situ moisture content of the soil beneath the pavement, the resilient modulus for each of the seasons may be estimated. An alternate procedure is to backcalculate the resilient modulus for different seasons using nondestructive deflection test data conducted on in- service pavements. These may be used as adjustment factors to correct the resilient modulus for a reference condition (6).

4.5.2. Pavement Layer Materials Characterization

The 1986 AASHTO Design Guide relies more heavily on the determination of material properties for the estimation of appropriate layer coefficient values. Although there are many types of material properties and laboratory test procedures for assessing the strength of the pavement materials, the

AASHTO Guide recommends that for a relatively low stiffness material, the AASHTO T274 standard test procedure be used to determine its resilient modulus. For stiff materials the AASHTO Guide recommends the use of the repeated load indirect tensile test (ASTM D4123).

Because of the small displacements and brittle nature of the highly stiff materials (e.g., portland cement concrete and those materials stabilized with a high cement content) The Guide recommends that the elastic modulus of such high stiffness materials be determined according to the procedure described in ASTM C469 (6).

4.6 LAYER COEFFICIENTS

The AASHTO flexible pavement layer coefficient (a_i) is a measure of the relative ability of a unit thickness of a given material to function as a structural component of the pavement (2). A value of this coefficient is assigned to each layer in the pavement structure in order to convert the actual layer thicknesses into a structural number (SN). This layer coefficient expresses the empirical relationship between SN and thickness. The following general equation relates the structural number (SN), layer coefficients (a_i), thicknesses (D_i), and drainage coefficients (m_i):

$$SN = \Sigma \, a_i \, D_i \, m_i$$

Although the elastic or resilient modulus has been adopted as the standard material quality measure, it is still necessary to identify layer coefficients because of their roles in the structural number design approach. The discussion of how these coefficients are estimated is presented below in five categories, depending on the type and function of the layer material (6).

1. **Asphalt Concrete Surface Course.** Figure 4.2 provides a chart that may be used to estimate the structural layer coefficient of a dense-graded asphalt concrete surface course based on its elastic (resilient) modulus (E_{AC}) at 68° F. Caution is recommended for modulus values above 450,000 psi.

2. **Granular Base Layer.** Figure 4.3 provides a chart that may be used to estimate the layer coefficient of a granular base layer(a_2). The following relationship may also be used to estimate the layer coefficient provided that the elastic/resilient modulus (E_{BS}) is known:

$$a_2 = 0.249 (\log_{10} E_{BS}) - 0.977$$

3. **Granular Subbase Layers.** Figure 4.4 provides a chart that may be used to estimate the layer coefficient of the subbase layer (a_3). The following relationship may also be used to estimate the layer coefficient provided that the elastic/resilient modulus (E_{SB}) is known:

$$a_3 = 0.227(\log_{10} E_{SB}) - 0.839$$

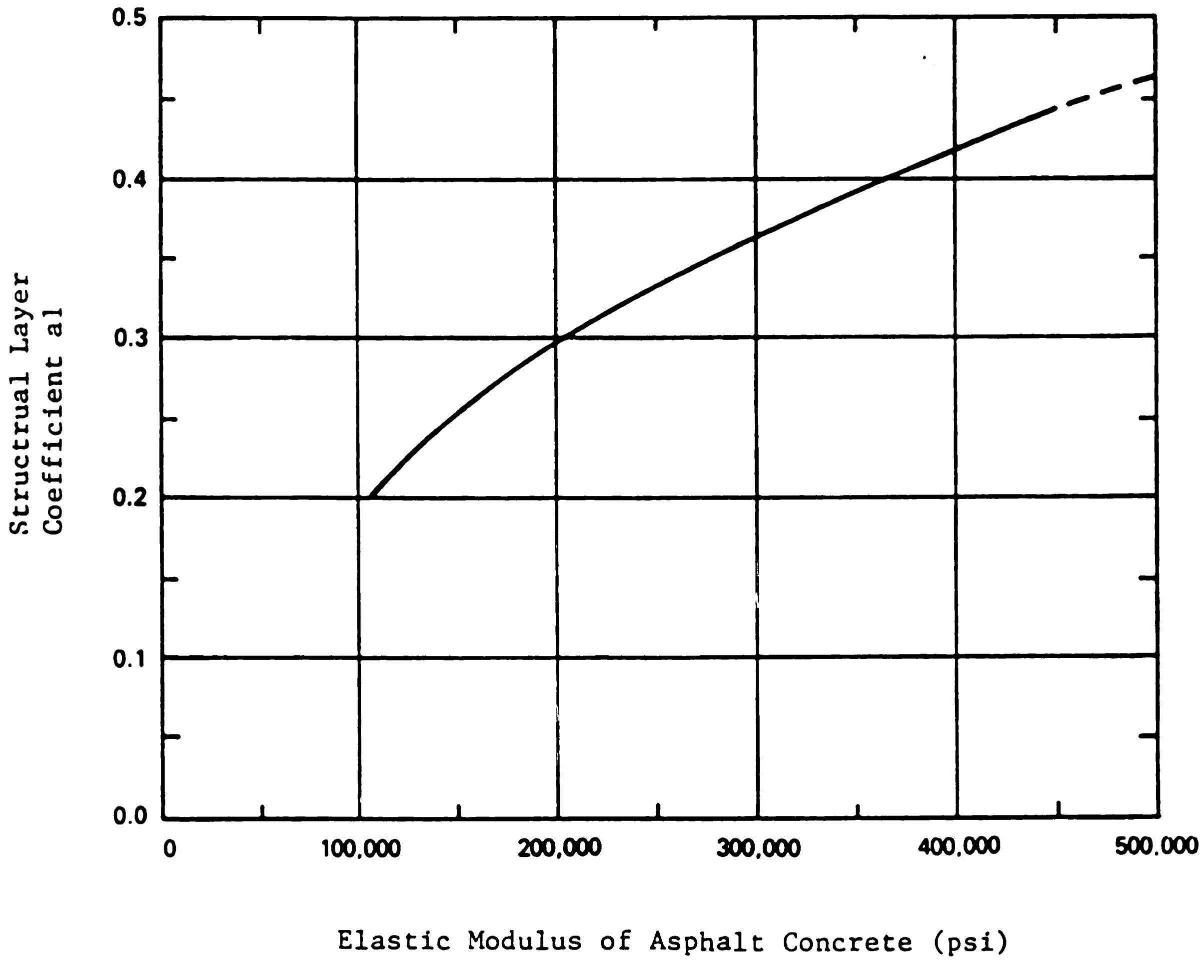

Figure 4.2 Chart for estimating structural layer coefficient of dense-graded asphalt concrete based on the elastic (resilient)modulus

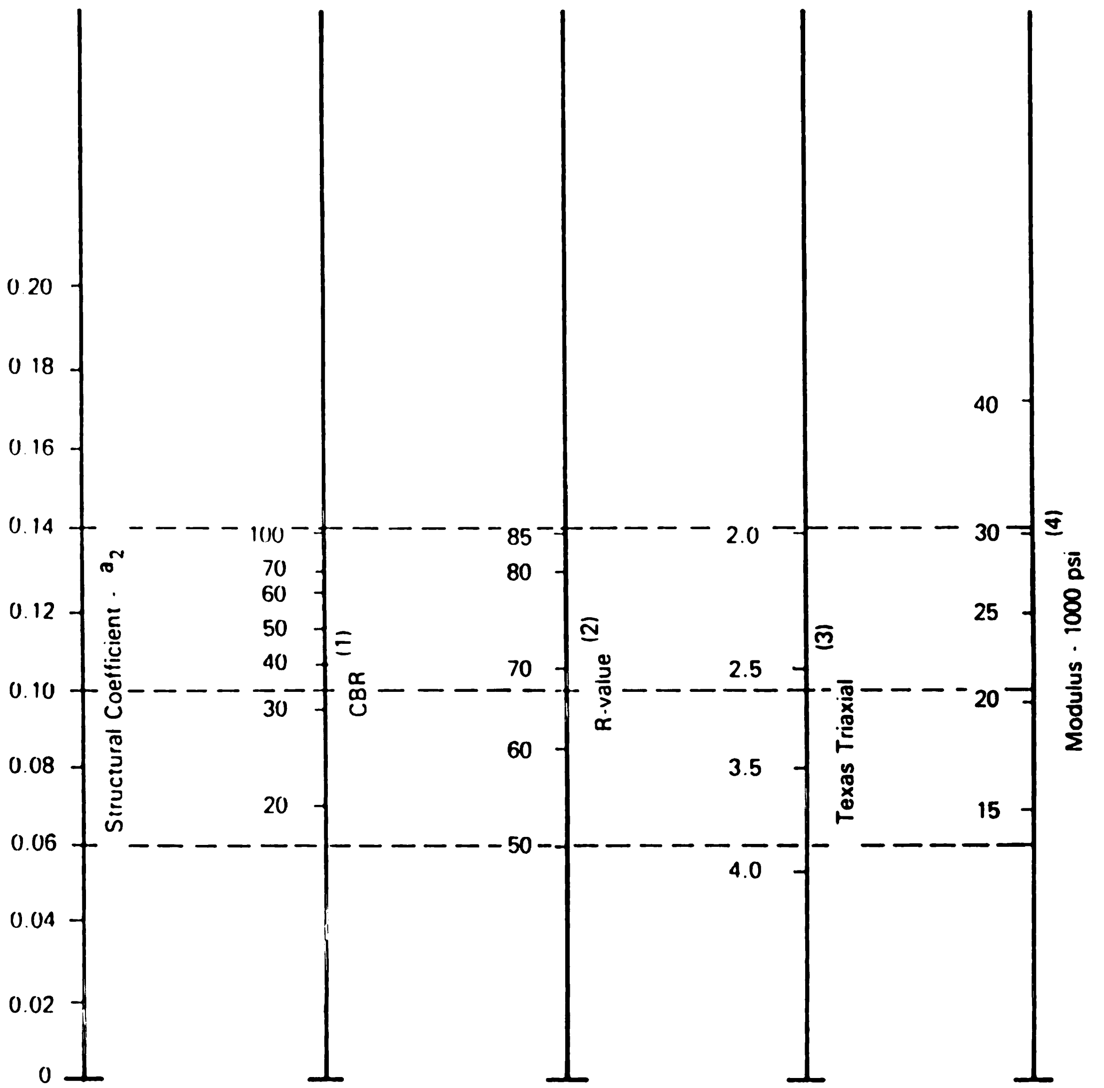

(1) Scale derived by averaging correlations obtained from Illinois.
(2) Scale derived by averaging correlations obtained from California, New Mexico and Wyoming.
(3) Scale derived by averaging correlations obtained from Texas.
(4) Scale derived on NCHRP project

Figure 4.3: Variation in granular base layer coefficient (a_2) with various base strength parameters.

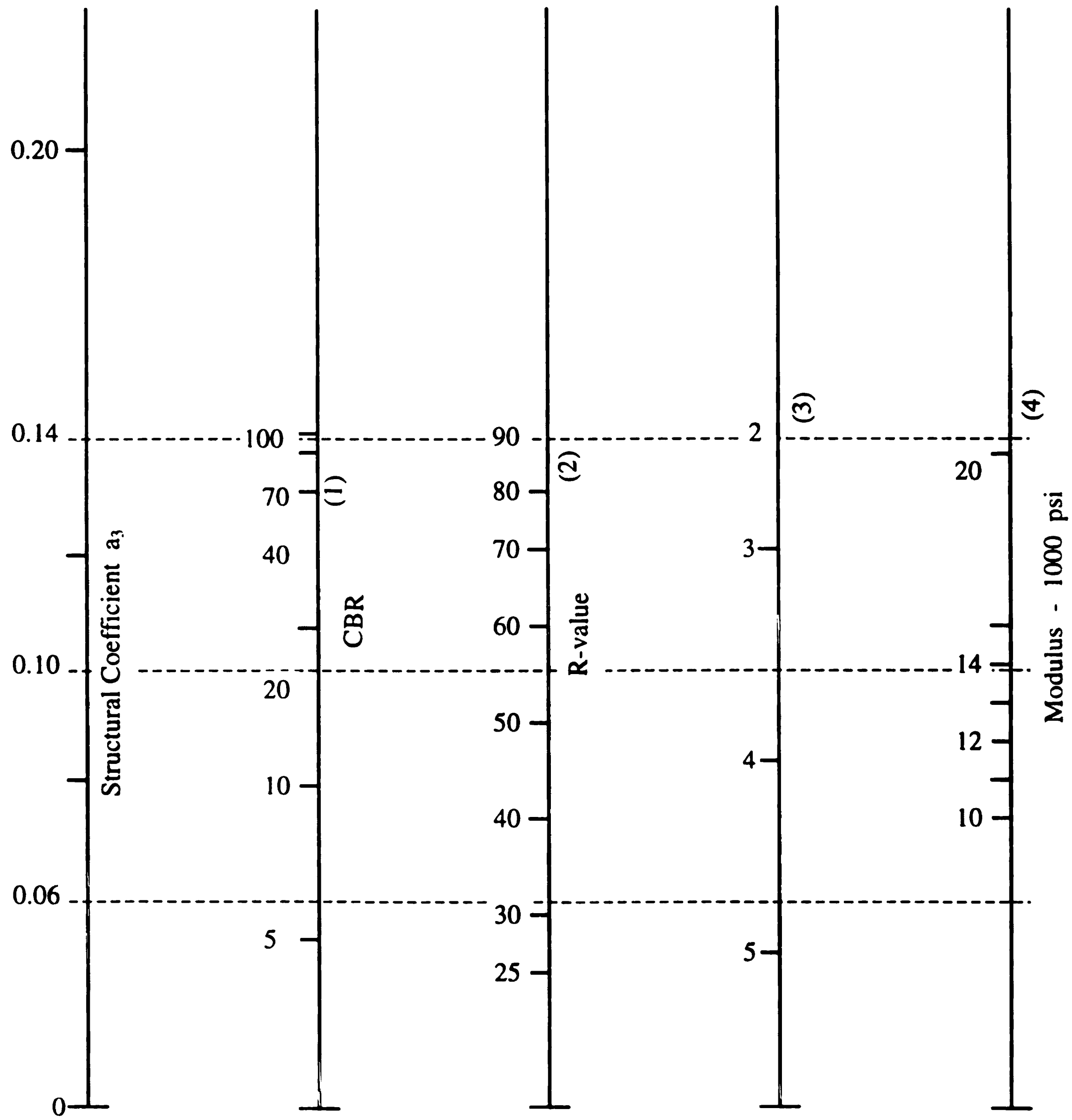

(1) Scale derived from correlation from Illinois.
(2) Scale derived from correlations obtained from the Asphalt Institute, California, New Mexico and Wyoming
(3) Scale derived from correlations obtained fromTexas
(4) Scale derived on NCHRP project (3)

Figure 4.4 : Variation in granular subbase layer coefficient (a_3) with various subbase strength parameters

4. **Cement Treated Bases.** Figure 4.5 provides a chart that may be used to estimate the structural layer coefficient of cement treated bases.

5. **Bituminous Treated Bases.** Figure 4.6 presents a chart that may be used to estimate the structural layer coefficient of bituminous treated bases. The elastic modulus or the Marshal Stability can be used as a input to the chart.

4.7 PAVEMENT STRUCTURAL NUMBER

The treatment for the expected level of drainage for a flexible pavement is through the use of modified layer coefficients (e.g., a higher effective layer coefficient would be used for improved drainage conditions). The factor for modifying the each layer coefficient is referred to the drainage coefficient (m_i) which has been integrated into the structural number (SN) equation along with layer coefficients (a_i) and layer thicknesses (D_i); thus:

$$\mathbf{SN = a_1\ D_1 + a_2\ D_2\ m_2 + a_3\ D_3\ m_3} \quad \text{......Eq 4.1}$$

Table 4.4 presents recommended m_i values as a function of the quality of the drainage and the percent of time during the year the pavement structure would normally be exposed to moisture levels approaching saturation. As a bases for comparison, the m_i, value for conditions at the AASHO Road

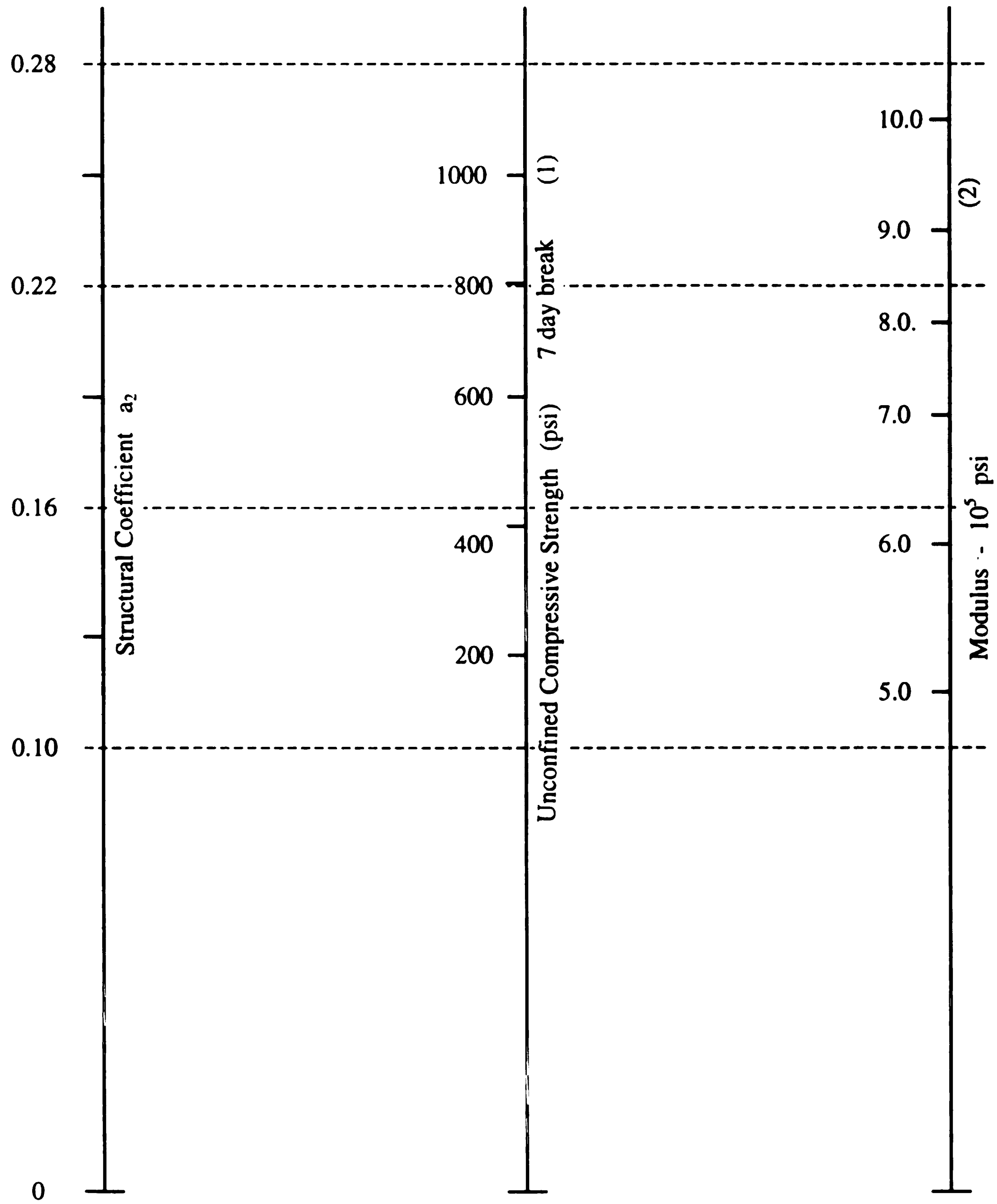

(1) Scale derived by averaging correlations from Illinois, Louisiana and Texas
(2) Scale derived on NCHRP project (3)

Figure 4.5 Variation in a_2 for cement-treated base with base strength parameters

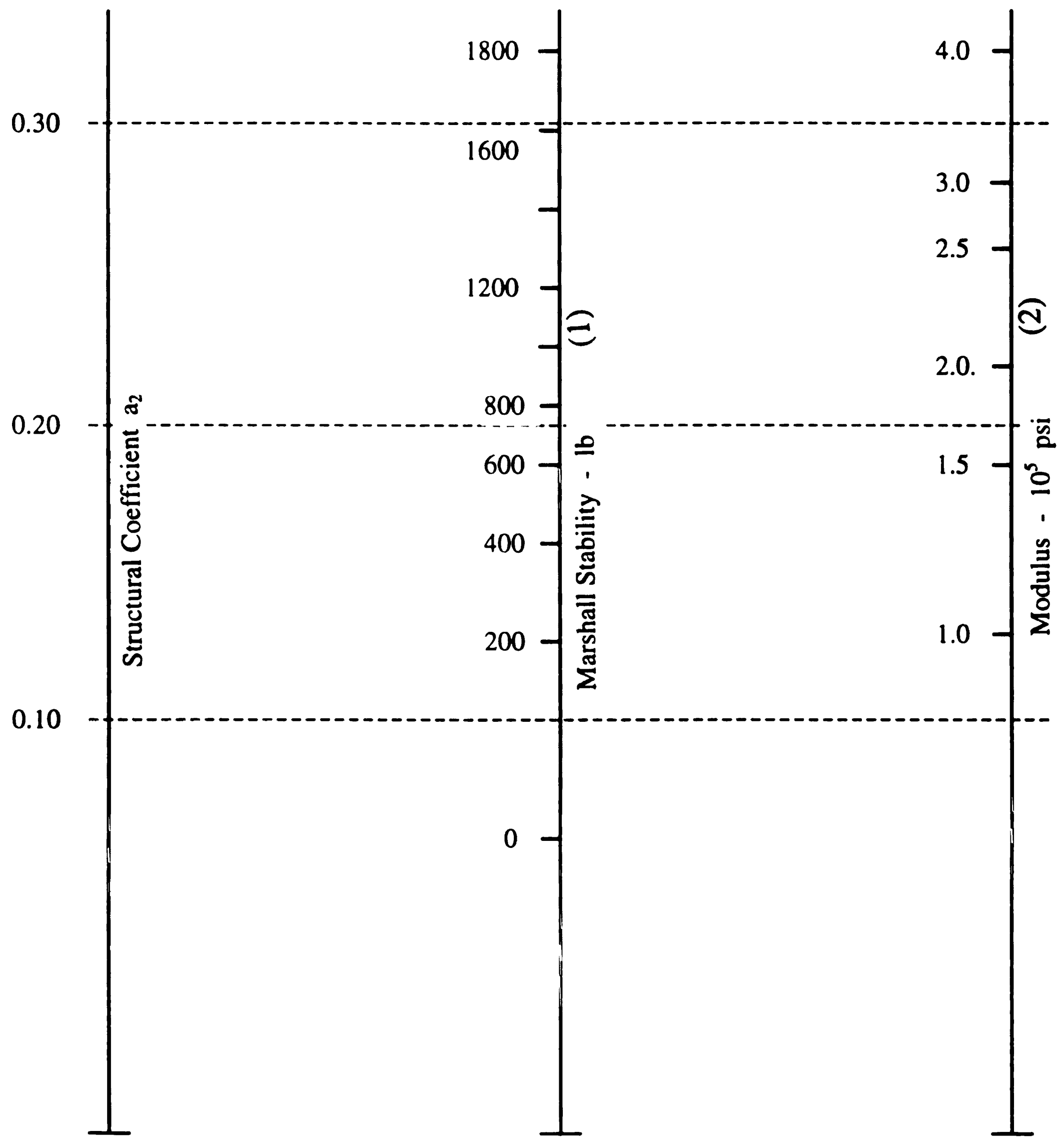

(1) Scale derived by averaging correlation obtained from Illinois.
(2) Scale derived on NCHRP project (3)

Figure 4.6 Variation in a_2 for bituminous-treated base with base strength parameters

Table 4.4: Recommended m_1 values for modifying structural layer coefficients of untreated base and subbase materials in flexible pavements.

Quality of Drainage	Percent of Time Pavement structure is Exposed to Moisture Levels Approaching Saturation			
	Less than 1%	1-5%	5-25%	Greater than 25%
Excellent	1.40 - 1.35	1.35 - 1.30	1.30 - 1.20	1.20
Good	1.35 - 1.25	1.25 - 1.15	1.15 - 1.00	1.00
Fair	1.25 - 1.15	1.15 - 1.05	1.00 - 0.80	0.80
Poor	1.15 - 1.05	1.05 - 0.80	0.80 - 0.60	0.60
Very Poor	1.05 - 0.95	0.95 - 0.75	0.75 - 0.40	0.40

Test is 1.0. Finally it is also important to note that these values apply to the effects of drainage on untreated base and subbase layers. Although improved drainage is certainly beneficial to stabilized or treated materials, the effects on performance of flexible pavements are not as profound as those quantified in Table 4.4 (6) .

4.8 COMPUTATION OF REQUIRED PAVEMENT THICKNESS

For both the asphalt concrete pavements (AC) and surface treatments surface types, the design is based on identifying a flexible pavement structural number (SN) to withstand the projected level of axle load (6).

4.8.1. Determination of the Required Structural Number.

Figure 4.7 presents a nomograph for determining the design structural number (SN) required for specific conditions. The nomograph solves the following equation:-

$$\log_{10}(W_{18}) = Z_R\, S_0 + 9.36 * \log_{10}(SN + 1) - 0.20 + \frac{\log_{10}[\,\Delta PSI/4.2-1.5\,]}{0.4 + 1094/(SN+1)^{5.19}} + 2.32 * \log_{10}(M_R) - 8.07 \qquad \text{Eq 4.2}$$

The required data to be substituted into this equation

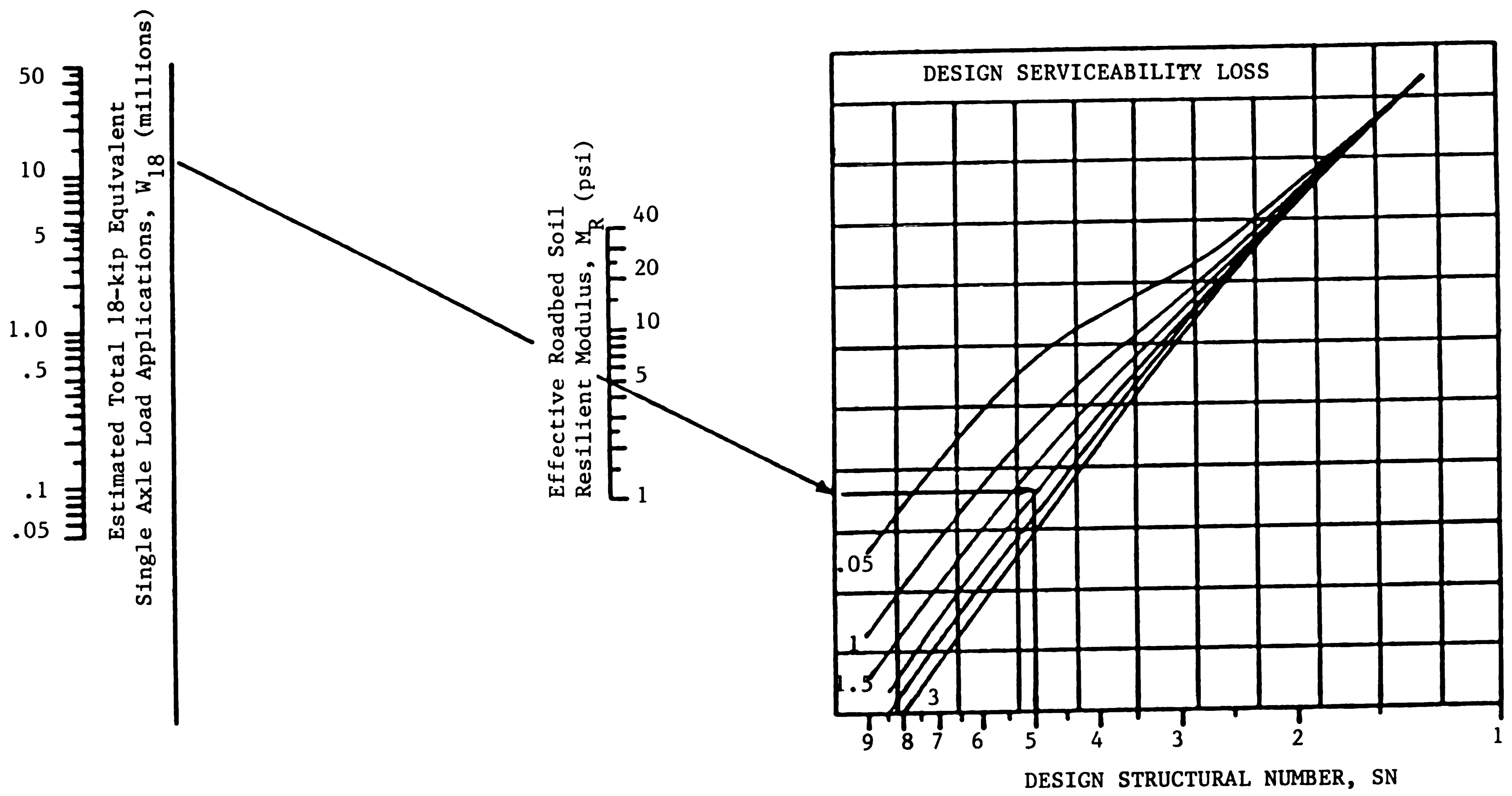

Figure 4.7 : Design chart for flexible pavement based on mean values for each input

is:-

a. The estimated future traffic, W_{18}, for the performance period.

b. The reliability, R, which assumes that average values are used for all inputs. For hand calculation, Z_R can be obtained from Table 3.2.

c. The overall standard deviation, S_o.

d. The effective resilient modulus of roadbed material, M_R.

e. The design serviceability loss, $\Delta PSI = p_o - p_t$.

4.8.2. Selection of Trial Pavement Thickness Design.

Once the design structural number of an initial pavement has been determined, the designer must identify a set of pavement layer thicknesses that will provide the required structural number (2).

4.8.3. Layered Design Analysis.

Flexible pavement structures are layered system and should be designed accordingly. Each unbound or aggregate layer must be protected from excessive vertical stresses, which could result in permanent deformation. This requires that a minimum layer thickness value be established. Table 4.5 (6) provides a list of suggested minimum thicknesses for surface and base layers for various traffic conditions. The minimum thickness values should be modified for local conditions.

The AASHTO design nomograph presented in Figure 4.7 can

Table 4.5: Minimum Layer Thickness

	Minimum Thinkness (inches)	
Traffic (ESAL)	Asphalt Concrete Surface	Aggregate Base
Less than 50,000	1.0(or surface treatment)	4
50,000 - 150,000	2.0	4
150,000 - 500,000	2.5	4
500,000 - 2,000,000	3.0	6
2,000,000 - 7,000,000	3.5	6
Greater than 7,000,000	4.0	6

1 inch = 2.54 cm

be used to determine the design structural number required for the protection of any unbound layer by substituting the resilient modulus of that layer for the roadbed resilient modulus in the nomograph. Hence, the nomograph can be used to determine the thickness of the AC layer that is required to protect the base course. It can also be used to determine the required thicknesses of the AC and base layers to protect the subbase layer. Such use is termed as layer design analysis.

This procedure, however, should not be applied to determine the required layer thickness above materials having a modulus higher than 40,000 psi. Layer thickness above such materials should be established on the bases of cost-effectiveness and minimum practical thickness considerations.

4.9 LIMITATIONS OF THE AASHTO FLEXIBLE PAVEMENT DESIGN PROCEDURE

The AASHTO design procedure is being used by many highway agencies of the world for the design of flexible and rigid pavements. Roads designed by using the AASHTO Guide have exhibited premature failure in many parts of the world, especially in Pakistan. In the light of the advancements in the pavement design procedures, the researchers have carried out analytical studies of the AASHTO Design Procedure and pointed out certain limitations/inadequacies in the Procedure, which are summarized below:-

1. **Materials.** The AASHO Road Test used a specific set of

pavement materials and one roadbed soil. The extrapolation of the performance of these materials to general applications is a questionable proposition because the materials and soils available in Pakistan are not identical to those used at the road test site and therefore should perform differently. The pavement design agencies in Pakistan do not seem to recognize this as is evidenced by the widespread use of $a_1 = 0.44$, $a_2 = 0.14$, and $a_3 = 0.11$. These structural layer coefficients values represent the relative strength of the construction materials used at the AASHO road test and do not represent the strength properties of the materials available locally (10).

2. **Traffic.** The AASHO Road Test sections were subjected to 1.1 million applications of axle loads ranging from 2000 lbs to 30,000 lbs on single axles and 24,000 lbs to 48,000 lbs on tandem axles. No tridem axle were included in the Road Test experiment. Each test section was exposed to axle loads of only one particular magnitude and configuration, as opposed to mixed traffic. Tire pressures were representative of normal practice at the time i.e., 80 psi.

In Pakistan, like in many other developing countries of the world, the economics of truck transportation have contributed to an increase in the average gross weight of trucks such that the majority of the trucks are operating well above the legal axle load limits. A recent axle load survey carried out by the Military College of Engineering (4) indicates gross overloading as may be seen from the truck factor ranges presented in Table 4.6. Table 4.7 presents a comparison of traffic loading conditions of the AASHO Road Test and Pakistan. As axle loads have increased, the use of higher tire pressure has become more popular in the trucking industry.

3. **Climate.** AC pavements constructed in hot climatic zones like Pakistan undergo greater permanent deformation due to softening of the bitumen. The AASHTO empirical model was developed in a temperate climate where the mean monthly air temperature varies between -4°C during january to 24°C during july. Thus, the AASHTO empirical model is not applicable to the hot climatic conditions of Pakistan.

Moreover, the use of the AASHTO empirical model for climatic conditions in Pakistan has resulted in inaccurate predictions of environmental deterioration over time i.e., aging or weathering of the AC. These processes result in the loss of volatile material in the bitumen and are primarily a function of temperature. Therefore a greater loss of serviceability (ride quality) in AC pavements in Pakistan would be expected due to rapid aging of the AC than accounted for by the AASHTO empirical model.

Table 4.6: Truck Factors at Texila on N-5 (Loaded Vehicles)

Vehicle Type	Axle Configuration	Truck Factor	Truck Factors Range in USA
2 Axle	Both single axles	4.757	0.15 - 0.21
3 Axle	One single & one tandem	11.850	0.29 - 1.59
4 Axle	All single axles	6.996	0.43 - 1.32
5 Axle	One single & two tandem	4.380	0.43 - 1.32
6 Axle	One single, one tandem &	14.730	0.71 - 1.39
	one tridem	15.820	0.71 - 1.39

Table 4.7: Traffic Loading Comparison AASHO Road Test and PAKISTAN

	Maximum Tandem Axle Load (lbs)	Maximum Tandem Axle Load (lbs)	Maximum Tridem Axle Load (lbs)	Maximum Truck Load (lbs)	Maximum Tire Pressure (lbs)
AASHO	30,000	48,000	None	108,000	70
PAKISTAN	47,000	95,000	110,000	174,000	145

4. **Quality control.** The AASHTO Road Test sections were short in length (160 ft) and an extraordinary effort was put forth to ensure uniformity of all pavement components. Thus construction quality control was extremely high. Typical highway projects are normally several miles long, contain much greater construction and material variability. In Pakistan, the variability is even more due to poor quality control and construction practices (10). Since the AASHTO model is based on the performance of the AASHTO test sections with very little variability, therefore AC pavements in Pakistan designed using this model would tend to show not only overall rapid deterioration but also more variability in performance along the project in the form of localized failures.

4.10 Mechanistic Evaluation/Calibration

Baladi and Mckelvey (11) conducted mechanistic evaluation and calibration of the AASHTO flexible design equations by using artificial pavement sections with various layer properties, roadbed soil modulus, and traffic volumes. Throughout the analysis it was assumed that the mechanistic responses (stresses, strains, and deflections) of the pavement sections due to an applied 18000-lb single axle load are indicative of the level of damage delivered to these sections. The work plan consisted of five phases as follows:-

PHASE-1. Establish a full factorial experiment design matrix that consists of 243 cells (each cell represents a pavement section). Design each pavement section by using the 1986 AASHTO design procedure and establish the layer thicknesses. The full factorial experiment design matrix is shown in Figure 4.8.

PHASE-2. Conduct mechanistic analysis of each pavement section of step 1 by using MICHPAVE computer program and determine its mechanistic responses due to an 18-kip single axle load.

PHASE-3. Compare the resulting mechanistic responses to determine whether or not the outputs of the AASHTO design procedure are reasonable.

PHASE-4. Select pavement sections from Figure 4.8. Redesign (by using the AASHTO design procedure) the layer thicknesses based on four additional values of the drainage coefficients of the base layer and two values of the drainage coefficients of the subbase layer. Conduct mechanistic analysis of each redesigned section and then mechanistically evaluate the concept of drainage coefficients.

PHASE-5. Select pavement sections from Figure 4.8. Redesign (by using the AASHTO design procedure) the layer thicknesses based on two additional values of loss of serviceability due to environmental factors. Conduct mechanistic analysis of each redesigned section and then mechanistically evaluate the

		100									300									500								
		10			25			40			10			25			40			10			25			40		
		10	15	25	10	15	25	10	15	25	10	15	25	10	15	25	10	15	25	10	15	25	10	15	25	10	15	25
1	5	1	10	19	28	37	46	55	64	73	82	91	100	109	118	127	136	145	154	163	172	181	190	199	208	217	226	235
	10	2	11	20	29	38	47	56	65	74	83	92	101	110	119	128	137	146	155	164	173	182	191	200	209	218	227	236
	20	3	12	21	30	39	48	57	66	75	84	93	102	111	120	129	138	147	156	165	174	183	192	201	210	219	228	237
5	5	4	13	22	31	40	49	58	67	76	85	94	103	112	121	130	139	148	157	166	175	184	193	202	211	220	229	238
	10	5	14	23	32	41	50	59	68	77	86	95	104	113	122	131	140	149	158	167	176	185	194	203	212	221	230	239
	20	6	15	24	33	42	51	60	69	78	87	96	105	114	123	132	141	150	159	168	177	186	195	204	213	222	231	240
10	5	7	16	25	34	43	52	61	70	79	88	97	106	115	124	133	142	151	160	169	178	187	196	205	214	223	232	241
	10	8	17	26	35	44	53	62	71	80	89	98	107	116	125	134	143	152	161	170	179	188	197	206	215	224	233	242
	20	9	18	27	36	45	54	63	72	81	90	99	108	117	126	135	144	153	162	171	180	189	198	207	216	225	234	243

Figure 4.8: Full factorial design matrix showing layer moduli and levels of traffic volume in terms of 18-KIP ESAL.

concept of loss of serviceability.

Each of the five phases were accomplished in several steps. Details for each phase and the corresponding steps are presented else where (11). Important conclusions/concepts brought out by the study are presented below.

4.10.1 Observations of the AASHTO Outputs

For a given value of the resilient modulus of the roadbed soil, a constant traffic volume, a constant design reliability level, and a constant overall standard deviation, the AASHTO design procedure produces:-

1. Pavement sections with a constant SN which presumably provides an equal level of protection against traffic loading to all pavement layers regardless of the type and quality of the AC, base, and subbase layer.
2. An AC layer thickness that is independent of the properties (modulus or layer coefficient) of the subbase material and roadbed soil. It depends on the layer coefficients of the AC and base materials.
3. A base layer thickness that is independent of the resilient modulus of the AC layer and roadbed soil. It depends on the layer coefficient of the base and subbase materials.
4. A subbase thickness that is independent of the resilient modulus of the AC and base layers. It depends on the layer coefficient of the subbase material and the modulus of the roadbed soil.

4.10.2 Mechanistic Evaluation of the AASHTO Design Equation

The 243 pavement sections were analyzed by using the linear option of the MICHPAVE computer program. The mechanistic responses of the 243 pavement sections are provided in the matrices given elsewhere (11).

Table 4.8 summarizes the AASHTO and mechanistic response outputs of the seven pavement sections from the above study. Based on the data presented in the table and the range of the material properties used in this study, the following conclusions were drawn:-

1. Based on the pavement surface peak deflection data listed in Table 4.8 and shown in Figure 4.9 and on the assumption that the peak surface deflection can be used as a measure of the level of damage delivered to a pavement section (higher deflection causes higher compression and higher rut and/or fatigue cracking potential), one can conclude that:-

   For a constant traffic level and one type of roadbed soil, the AASHTO design procedure produces pavement sections (layer thicknesses) such that the peak surface deflection is constant. Hence, the amount of overall damage delivered to the pavement section (or the overall protection level) is constant and independent of the layer properties.

2. Based on the amount of vertical compression (the

Table 4.8: The outputs of the AASHTO design method and the mechanistic responses of pavement sections 60, 87, 141, 150, 159 and 222

Section Number	Layer thicknesses (in)			Layer moduli (Ksi)				Deflection (mills) at top of				Amount of compression (mill)			
	AC	Base	Subbase	AC	Base	Subbase	Roadbed	AC	Base	Subbase	Roadbed	AC	Base	Subbase	Roadbed
60	17.75	12.09	18.00	100	40	10	5	21.14	15.31	13.58	11.05	5.83	1.73	2.53	11.05
141	8.41	12.09	18.00	300	40	10	5	21.26	20.13	17.10	13.25	1.13	3.03	3.85	13.25
222	6.94	12.09	18.00	300	40	10	5	21.14	20.60	17.51	13.50	0.54	3.09	4.01	13.05
67	13.80	0.00	18.00	300	40	10	5	19.64	18.03	18.03	14.30	1.61	0.00	3.73	14.3
114	10.04	11.94	18.00	300	40	10	5	20.87	19.57	16.54	13.02	1.30	3.03	3.52	13.08
141	8.41	12.09	18.00	300	40	10	5	21.26	20.13	17.10	13.25	1.30	3.03	3.85	13.25
141	8.41	12.09	18.00	300	40	10	5	21.26	20.13	17.10	13.25	1.30	3.03	3.85	13.25
160	8.41	3.18	17.50	300	40	15	5	21.70	20.58	18.22	14.37	1.20	2.36	3.85	14.37
159	8.41	3.65		300	40	20	5	21.83	20.71	19.43	15.66	1.20	1.28	3.77	16.66
156	8.41	3.66	40.40	300	40	25	1	35.19	34.07	32.79	27.00	1.12	1.28	5.79	27.00
159	8.41	3.66		300	40	25	5	21.83	20.71	19.43	15.66	1.12	1.28	3.77	16.66
162	8.41	3.66		300	40	25	10	16.93	15.79	14.52	12.03	1.40	1.27	2.49	12.03

Table 4.8 (Continued)

Section Number	Layer Thicknesses (in)			Verticle stress (psi) at top of			Tensile stress bottom of AC		Verticle strain top and bottom (0.0001in/in)						
	AC	Base	Subbase	Base	Subbase	Roadbed	stress (Psi)	Stress ratio*	AC		Base		Subbase		Roadbed
									Top	Bottom	Top	Bottom	Top	Bottom	Top
60	17.75	12.09	18.00	7.24	1.71	0.70	10.30	0.10	3.36	1.34	2.14	1.23	1.99	1.15	1.38
141	8.40	12.09	18.00	15.91	2.88	1.01	64.10	0.21	0.30	1.81	4.26	1.98	3.24	1.67	2.01
222	6.94	12.09	18.00	16.27	3.02	1.05	105.50	0.21	0.28	1.59	4.23	2.06	3.37	1.75	2.09
87	13.80	0.00	18.00	N/A	3.20	1.12	52.04	0.17	0.68	1.15	N/A	N/A	3.15	1.68	2.01
114	10.04	11.94	18.00	9.39	2.52	0.97	64.54	0.22	0.42	1.60	4.06	1.95	2.82	1.59	1.91
141	8.41	12.09	18.00	15.91	2.88	1.01	64.10	0.24	0.30	0.81	4.26	1.98	2.24	1.67	2.01
141	8.41	12.09	18.00	15.91	2.88	1.01	64.10	0.21	0.30	1.81	4.26	1.98	3.24	1.67	2.01
150	8.41	8.18	17.50	15.25	4.58	1.21	66.58	0.22	0.26	1.84	4.21	2.38	3.48	1.81	2.40
159	8.41	3.66	16.80	14.71	6.59	1.46	68.46	0.23	0.25	1.86	4.17	3.09	3.77	1.95	2.83
156	8.41	3.66	40.40	15.34	9.44	0.20	66.05	0.21	0.31	1.80	4.16	3.11	3.79	1.09	2.82
156	8.41	3.66	15.80	14.17	8.59	1.46	68.46	0.23	0.25	1.86	4.17	3.89	3.77	1.95	2.83
162	8.41	3.66	8.96	14.38	8.23	3.25	69.81	0.23	0.27	1.88	4.15	3.87	3.75	2.46	3.14

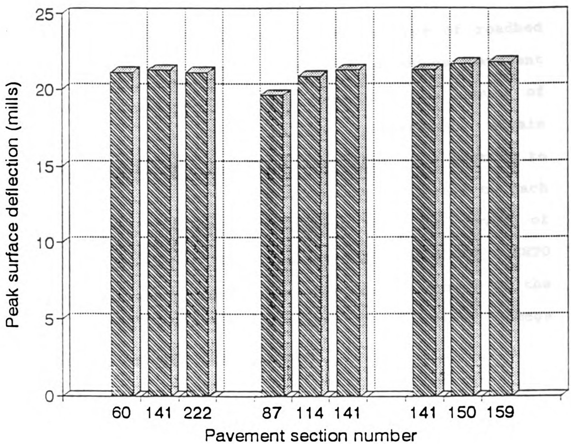

Figure 4.9 Peak pavement surface deflections of the seven indicated pavement sections

difference between the peak deflections at the top of any two consecutive layers) experienced by each pavement layer (see Figures 4.10, 4.11, 4.12, and 4.13, and the resulting vertical strains at the top and bottom of each pavement layer (see Figures 4.14, and 4.15), the following conclusion was drawn:-

For a constant traffic level and one type of roadbed soil, the AASHTO design procedure produces pavement sections (layer thicknesses) such that the amount of compression and the resulting compressive strain experienced by any one layer vary from one section to another. Hence, the amount of damage delivered to each layer of the pavement sections (or the level of protection) varies. This implies that while the AASHTO design procedure insures that the overall damage of the pavement sections is the same, the relative damage delivered to each layer is not.

3. Based on the magnitude of the tensile stress induced at the bottom of the AC layer (of seven pavement sections) due to an 18-kips ESAL and the ratio of that tensile stress to the value of the AC modulus (see Table 4.8 and Figure 4.16, and 4.17), the following conclusion was drawn:-

For a constant traffic level and one type of roadbed

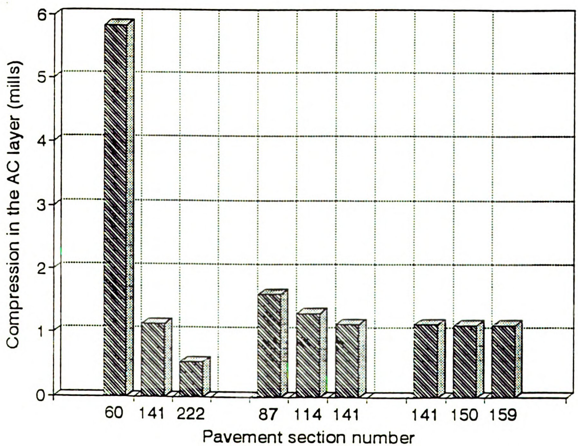

Figure 4.10 The amount of compression in the AC layer of the seven indicated pavement sections

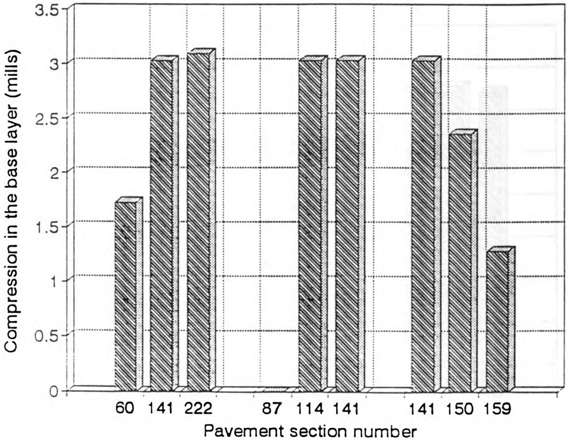

Figure 4.11 The amount of compression in the base layer of the seven indicated pavement sections

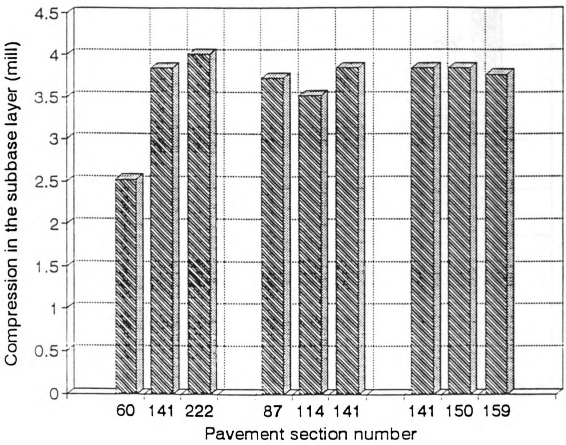

Figure 4.12 The amount of compression in the subbase layer of the seven indicated pavement sections

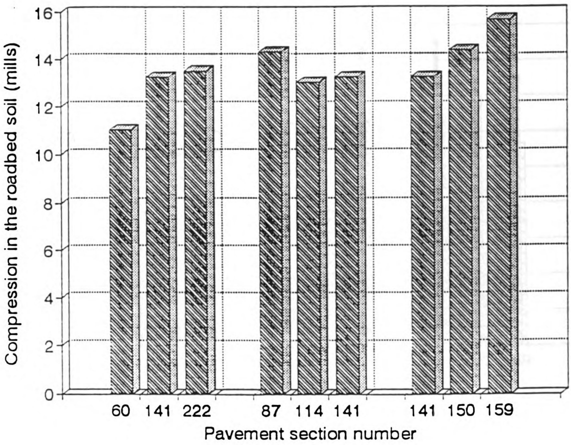

Figure 4.13 The amount of compression in the roadbed soil of the seven indicated pavement sections

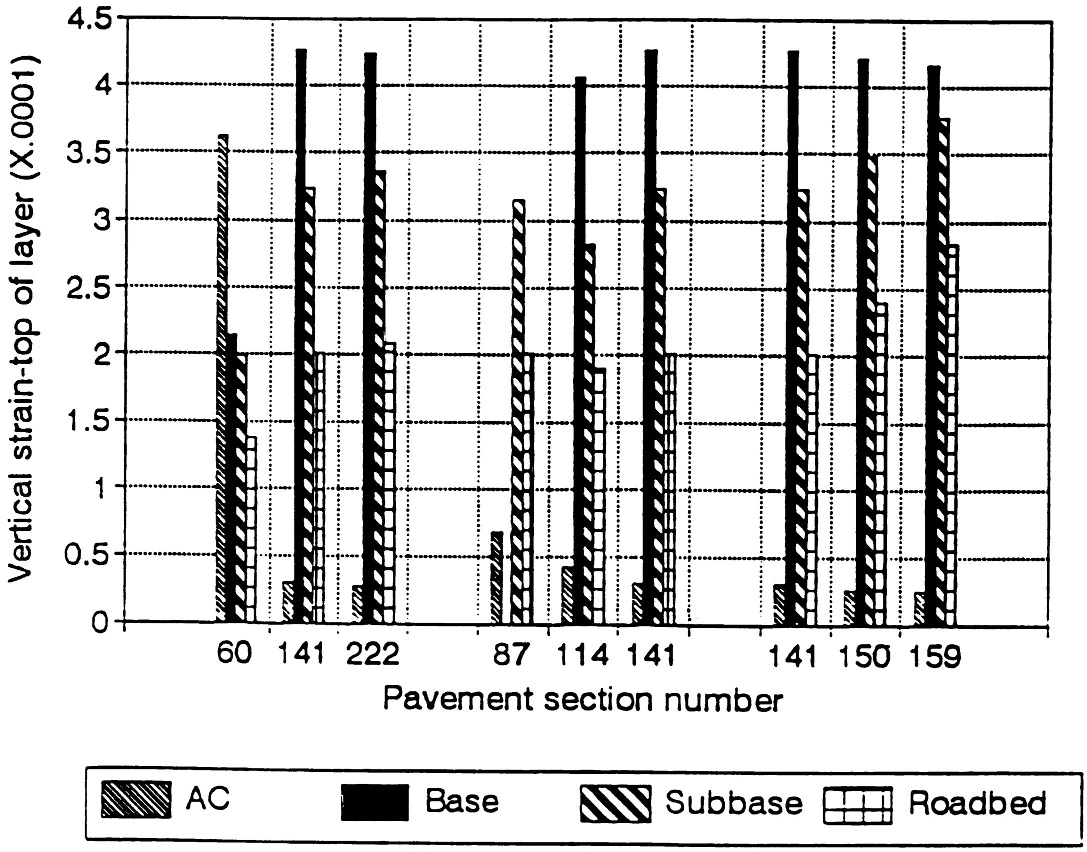

Figure 4.14 The vertical strains induced at the top of each pavement layer for the indicated pavement sections

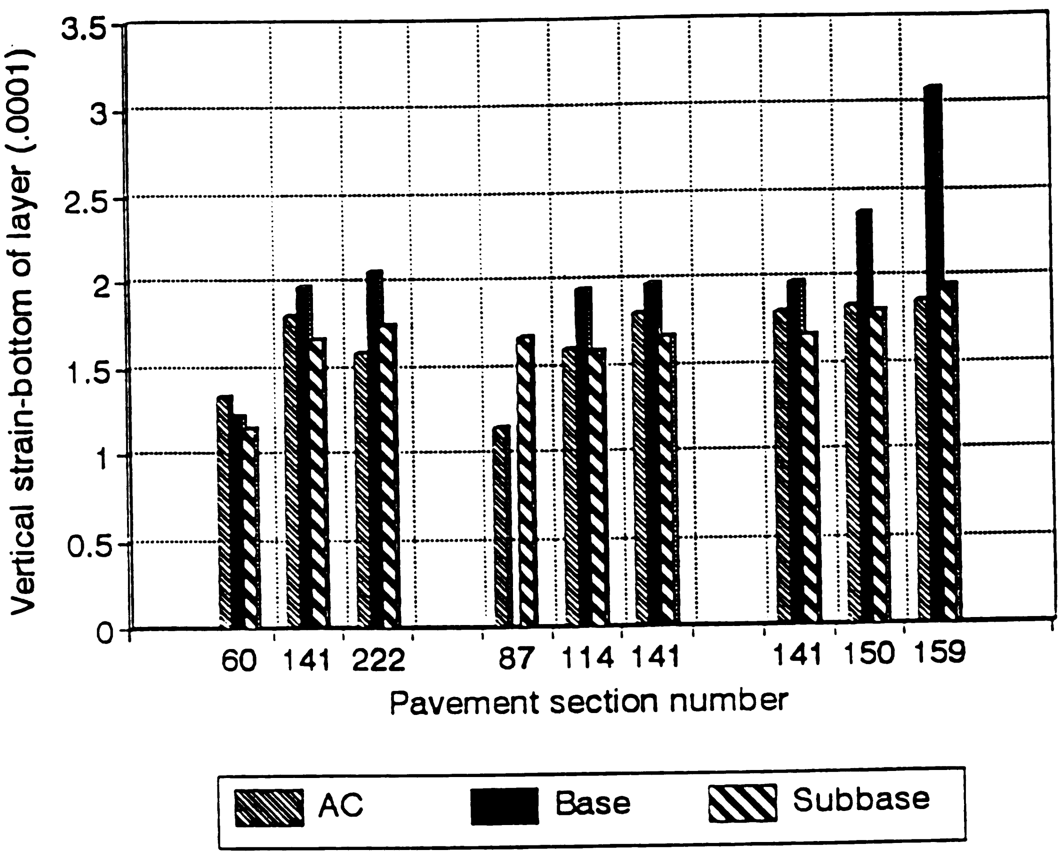

Figure 4.15 The vertical strains induced at the bottom of each pavement layer for the indicated pavement sections

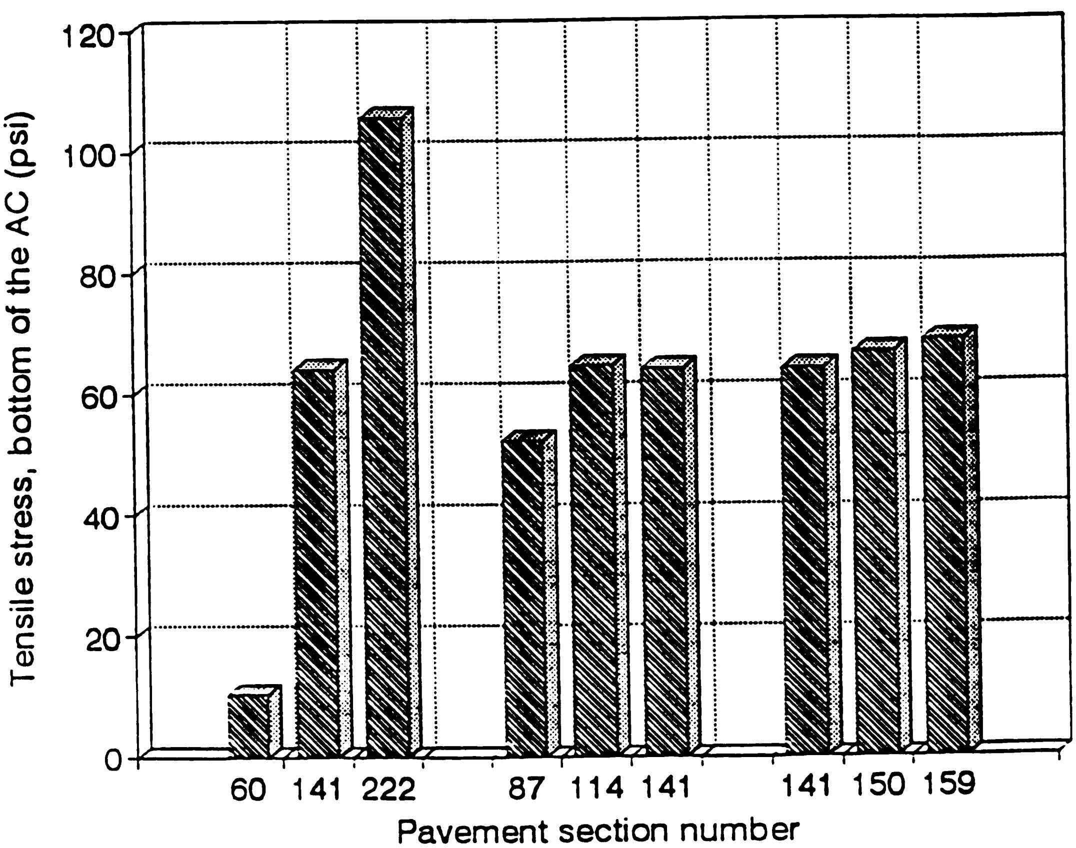

Figure 4.16 Tensile stress at the bottom of the AC layer of the seven indicated pavement sections

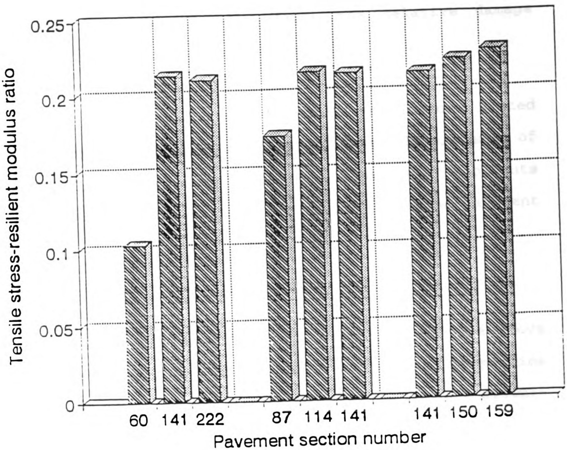

Figure 4.17 The ratio of the tensile stress at the bottom of the AC layer to its resilient modulus for the seven indicated pavement sections

soil, the AASHTO design procedure produces pavement sections (layer thicknesses) such that the tensile stress induced at the bottom of the AC layer vary from one section to another. Hence, the amount of damage delivered to the AC layer of the pavement sections (or the level of protection) varies. This implies that while the AASHTO design procedure insures that the overall damage of the pavement sections is the same, the relative damage delivered to each layer is not.

It should be noted that the three conclusions stated above are strictly based on the outputs (layer thicknesses) of the AASHTO flexible pavement design procedure and the outputs of the mechanistic analysis of the AASHTO designed pavement sections.

4.10.3 Conclusions

Relative to the AASHTO Design Procedure and the above general observations and in the range of material properties used in the SHRP study, the following conclusions were drawn:-

1. Results of the mechanistic evaluation support the first observation (see page 90) of the AASHTO Design Procedure.

2. Results of the mechanistic evaluation do not support observations "2, 3 and 4" (see page 90,) of the AASHTO Design Procedure.

4.10.4 Important Concepts Relative to the calibration of the AASHTO Flexible Design Equations:-

Several important concepts related to the calibration of the AASHTO flexible design equations can be inferred from the mechanistic analysis of those equations. These concepts can be divided (according to the type of the AASHTO equation) into two categories: the concepts of the structural number and the concept of the resilient modulus of the roadbed soil in the AASHTO main design equation (11). These two categories are presented below:-

1. The Concept of the AASHTO Structural Number

The AASHTO equation (note that drainage coefficient is not included yet) can be written as follows:

$SN = a_1D_1 + a_2D_2 + a_3D_3$ **which can also be written as:**

$SN = SN_1 + SN_2 + SN_3$

That is the structural number of a pavement section is the linear sum of the structural numbers of its layers. The following conclusions were made relative to this AASHTO concept.

STRUCTURAL NUMBER AASHTO CONCEPT - 1

The total structural number of any flexible pavement section is the sum of the structural numbers of its

layers. The findings of the mechanistic analysis support this AASHTO concept.

STRUCTURAL NUMBER - AASHTO CONCEPT - 2

The structural number of any flexible pavement layer is the product of its thicknesses and its layer coefficient. For any layer, its coefficient can be obtained from the appropriate equation or chart based on the modulus value of that layer. The results of the mechanistic analysis do not support this AASHTO concept.

2. **The Concept of the AASHTO Main Design Equation**

The number of 18-kips ESAL (W_{18}) is a function of the design reliability (Z_R), the overall standard deviation (S_0) of the materials and traffic data, the structural number (SN) of the pavement section, the resilient modulus (M_R) of the roadbed soil, and the serviceability loss ($\blacktriangle PSI$) expected during the performance period. In practice, however, the number of 18 kips ESAL is used as an input to the equation and the required structural number is obtained.

$$\mathrm{Log}\,(W_{18}) = Z_R\,(S_0) + 9.36[\mathrm{Log}(SN + 1)] - 0.20 + \frac{\mathrm{Log}[(\blacktriangle PSI)/(4.2 - 1.5)}{[0.4 + 1094/(SN + 1)^{5.19}]} + 2.32[\mathrm{Log}(M_R)] - 8.07$$

THE CONCEPT OF THE AASHTO MAIN DESIGN EQUATION

The structural number of a pavement section is a function of only one material property, the resilient modulus of the roadbed soil. Pavement sections with different types of roadbed soil will have different structural numbers such that each section will receive the same amount of damage. The results of the mechanistic analysis do not support this AASHTO concept.

3. Results of the mechanistic evaluation do not support the role of the roadbed soil resilient modulus in the AASHTO main design/ performance equation (the equation does not properly account for the effects of the resilient modulus of the roadbed soil on the structural capacity of the pavement).

4.11 AASHTO Layer Coefficients

Considerable disagreement is apparent about both the definition and the recommended method of measurement of layer coefficients (15). For example, the following statements are from the 1986 AASHTO Design Guide (6):

1. "The structural number is an abstract number.... converted to actual thickness of surfacing, base and subbase, by means of appropriate layer coefficients representing the relative strength of the construction materials"

2. "In effect, the layer coefficients are based on the elastic moduli M_R and have been determined based on stress and strain calculations in a multilayered pavement system" (section 1.2 AASHTO Design Guide 1986).

3. "..... it is not essential that elastic moduli of these materials are characterized. In general, layer coefficients derived from test roads or satellite sections are preferred" (section 2.3.3 AASHTO Design Guide 1986).

At the international conference on the Structural Design of Asphalt Pavements, Shook and Finn (20) stated the following:

"It is believed that the coefficients a_1 , a_2, a_3 are functions of the strengths of the various layers involved. At the present time (1962), however, no entirely satisfactory techniques are available for defining or measuring these strength factors." Persual of existing and current literature reveals (19) that two predominant methods have been adopted for estimating the layer coefficients of bituminous materials:-

a. A power law relating the layer coefficients to the resilient modulus (M_R) (e.g., see Figure 2.5 in the AASHTO Guide).
b. Based on Odemark's equivalent stiffness hypothesis, an analogous relationship is used, wherein the one-third power of the ratio of the material modulus to

that of a reference material (whose layer coefficient is presumed to be known) gives the ratio of the unknown layer coefficient to that of the reference material.

The Assumption of a relationship between strength and layer coefficients is an extrapolation, since no measure of structural strength or adequacy was included in the data used to calibrate the AASHO model (19).

CHAPTER 5

STUDY RESULTS-SENSITIVITY ANALYSIS

5.1 SENSITIVITY OF THE AASHTO EQUATION TO THE DESIGN VARIABLES

A review of the AASHTO design procedure (DNPS 86 Computer Program) results listed in Table 5.1 and presented in Figure 5.1 through 5.5, illustrate the effect of various variables as follows:-

1. For the traffic input values considered a three fold increase in the initial traffic (25 million to 75 million ESALs) causes an 18 percent increase in the AC thickness, 10.66 percent increase in the base thickness, 10 percent increase in the subbase thickness and 13.76 percent increase in the overall thickness. The effect of traffic on thickness is more pronounced for lower values of traffic.

2. A three fold increase in the AC modulus (150 to 450 ksi) yields in about 43 percent decrease in the AC thickness. The overall pavement thickness decreases by about 23 percent. **The thicknesses of the base and sub-base layers are not affected by the changes in the AC modulus.**

3. For two fold increase in the base modulus (20 ksi to 40 ksi) the AC thickness decreases by about 21 percent and

Table 5.1: Effect on thickness of variation in traffic and layer material properties.

Effect of ESALs

ESALs (millions)	25	50	75
Layer Type		Thickness (inches)	
AC	9.76	10.86	11.54
Base	7.03	7.50	7.78
Subbase	5.88	6.25	6.47
Total Thickness	22.67	24.61	25.79

Effect of AC Modulus

AC Modulus (ksi)	150	300	450
Layer Type		Thickness (inches)	
AC	16.07	10.86	9.13
Base	7.50	7.50	7.50
subbase	6.25	6.25	6.25
Total Thickness	29.82	24.61	22.88

Effect of Base Modulus

Base Modulus (ksi)	20	30	40
Layer Type		Thickness (inches)	
AC	12.47	10.86	9.80
Base	5.05	7.50	8.48
Subbase	6.25	6.25	6.25
Total Thickness	23.77	24.61	24.53

Effect of Subbase Modulus

Subbase Modulus (ksi)	10	15	20
Layer Type		Thickness (inches)	
AC	10.86	10.86	10.86
Base	12.41	7.50	4.26
Subbase	0.00	6.25	8.15
Total Thickness	23.27	24.61	23.27

Effect of Roadbed Modulus

Roadbed Modulus (ksi)	7.5	10.00	20.00
Layer Type		Thickness (inches)	
AC	10.86	10.86	10.86
Base	7.50	7.50	7.50
Subbase	11.00	6.25	0.00
Total Thickness	29.36	24.61	18.36

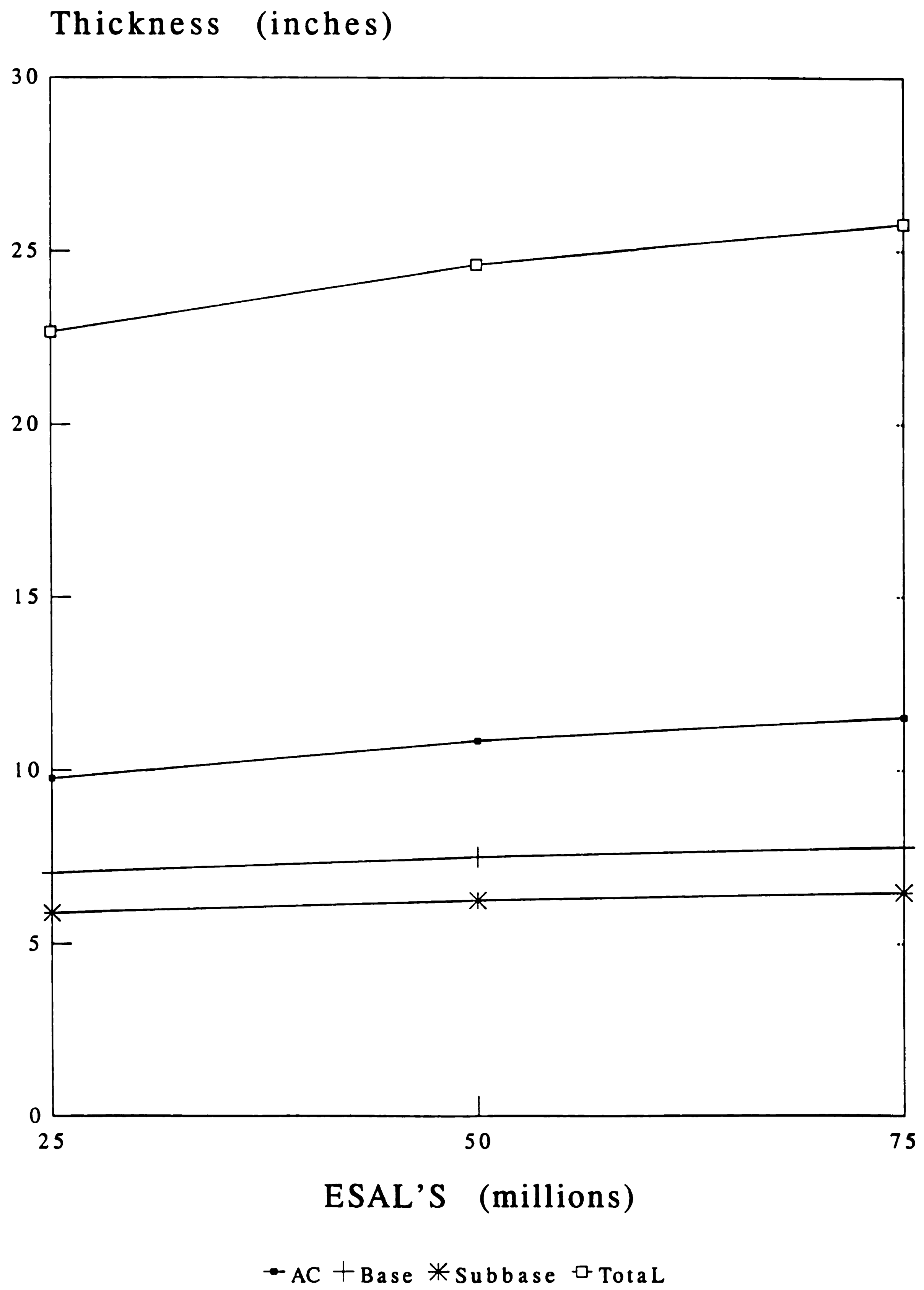

Figure 5.1: Effect of variation in traffic on pavement layer thicknesses

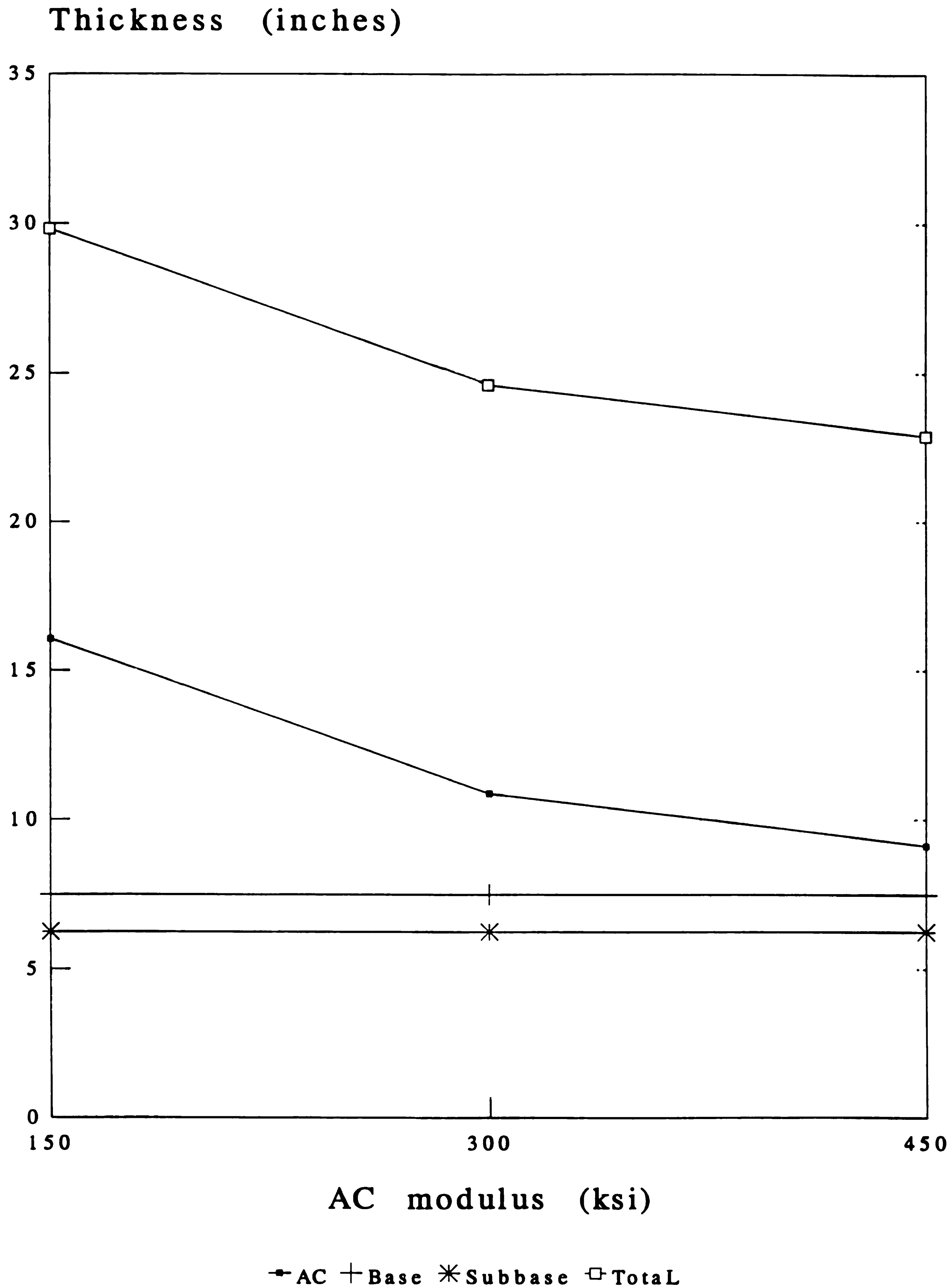

Figure 5.2: Effect of variation in AC modulus on pavement layer thicknesses.

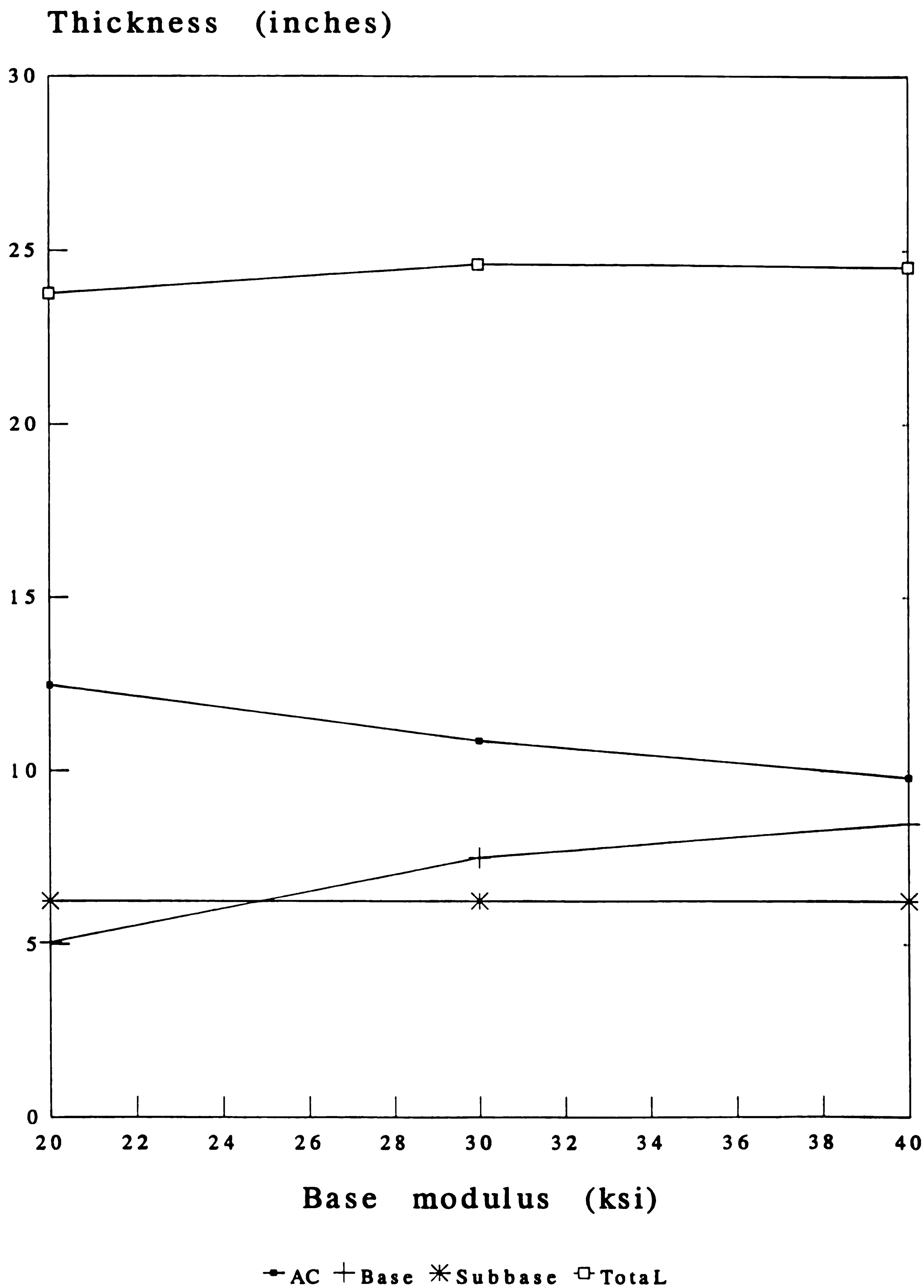

Figure 5.3: Effect of variation in base modulus on pavement layer thicknesses.

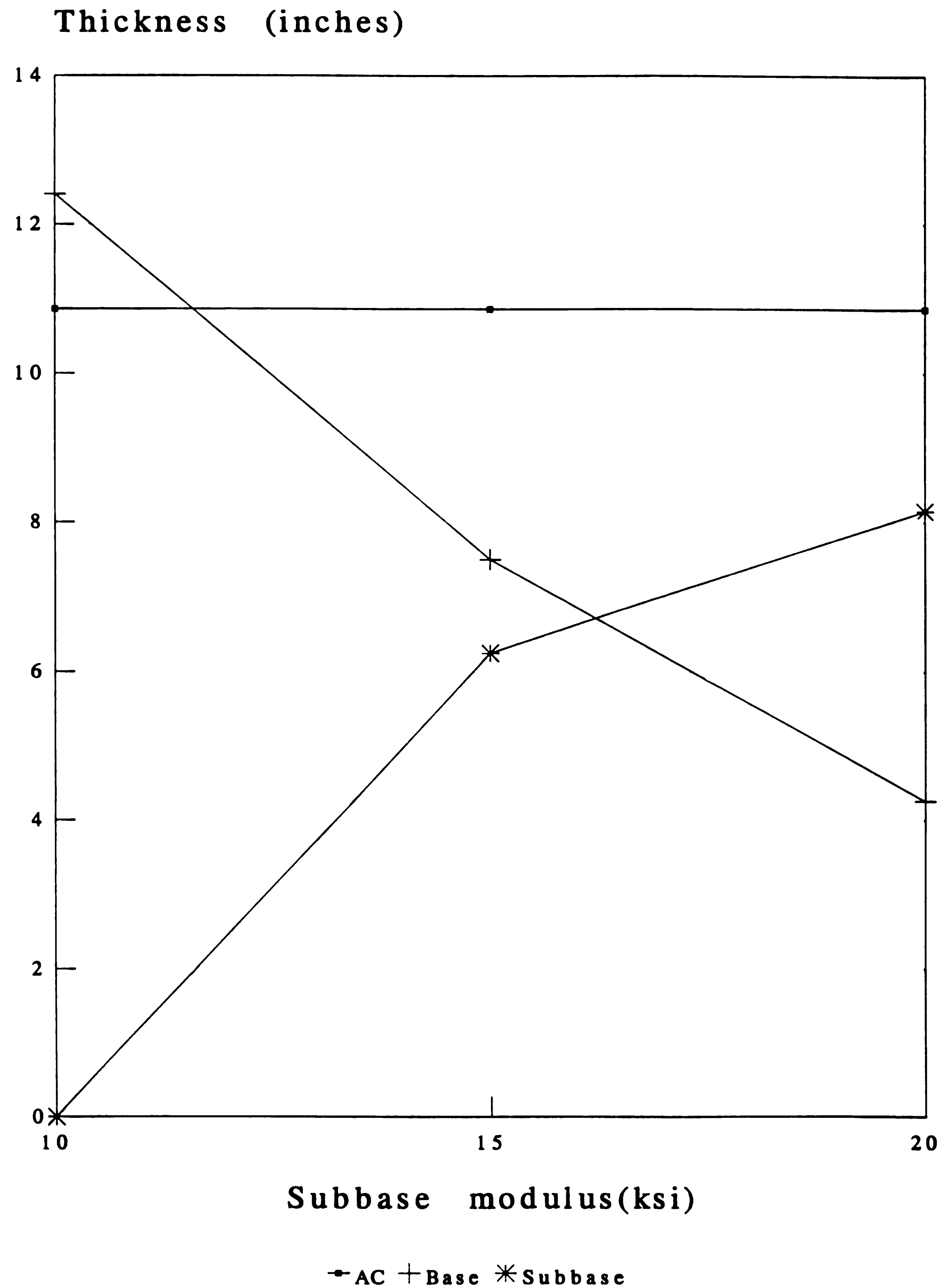

Figure 5.4: Effect of variation in subbase modulus on pavement layer thicknesses.

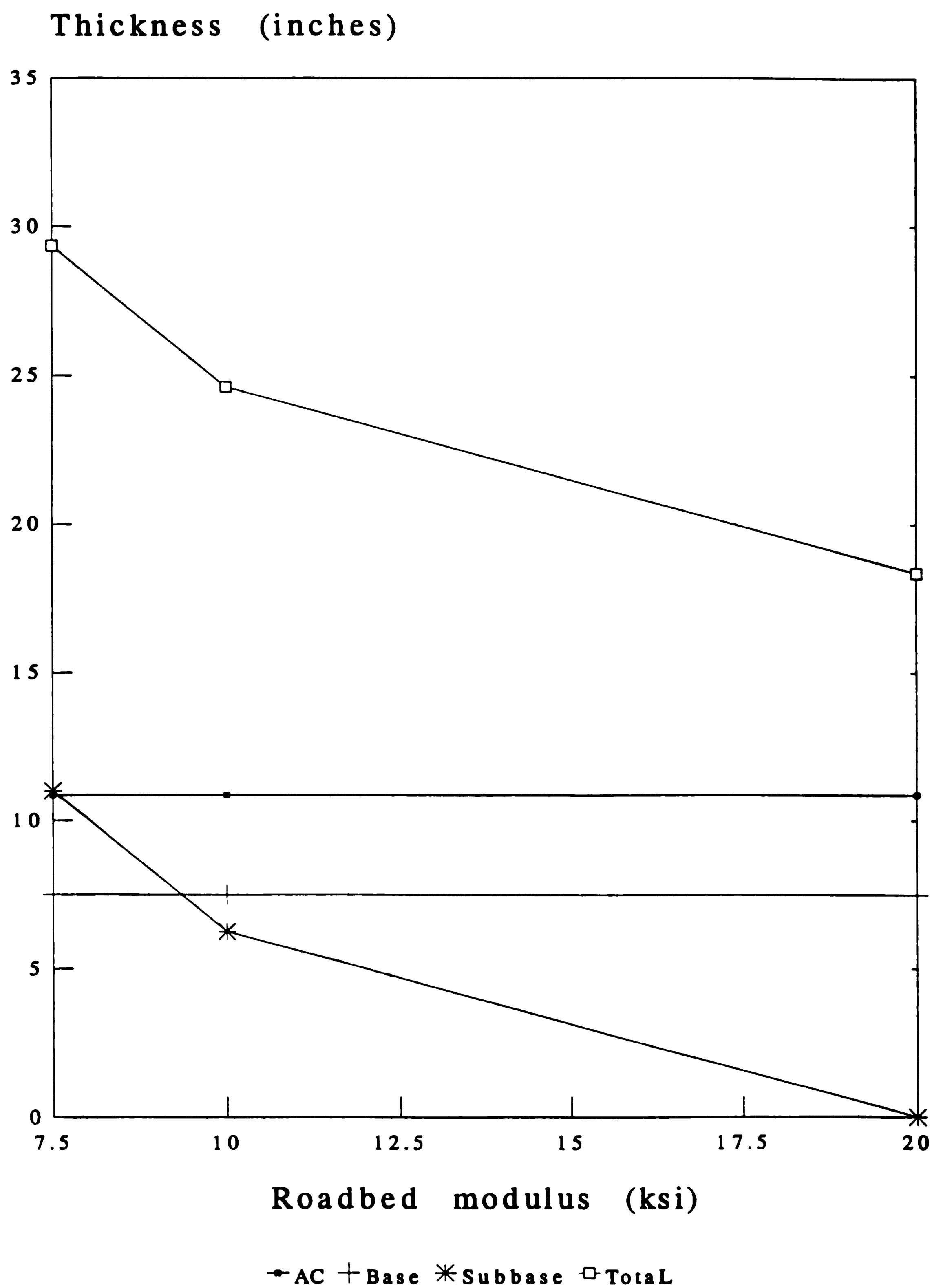

Figure 5.5: Effect of variation in roadbed modulus on pavement layer thicknesses.

the base thickness increases by about 68 percent. The overall pavement thickness is increased by only 3 percent. The Subbase thickness is not affected by the change in the base modulus.

4. An increase in the subbase modulus causes the base thickness to decrease and the subbase thickness to increase. The AC layer thickness is not effected by the changes in the sub-base modulus.

5. Softer road bed soils require more thickness of the subbase and correspondingly greater over all thickness. **The AC and the base thicknesses are not affected by the changes in the road-bed soil modulus.**

5.2 MECHANISTIC EVALUATION OF AASHTO FLEXIBLE PAVEMENT DESIGN PROCEDURE - VERIFICATION OF SHRP STUDY (11) FOR HIGHER LEVELS OF TRAFFIC

5.2.1. Outputs from AASHTO Design Procedure

Figure 5.6 shows the structural number for each of the 243 pavement sections of Figure 3.1. These structural numbers are obtained when a subbase material softer than the roadbed soil is omitted from the analysis. Figure 5.7 also presents the structural numbers of pavement sections of Figure 3.1. These structural numbers are obtained when a subbase material softer than the roadbed soil is included in the analysis.

		150									300									450								
		20			30			40			20			30			40			20			30			40		
		10	15	20	10	15	20	10	15	20	10	15	20	10	15	20	10	15	20	10	15	20	10	15	20	10	15	20
7.5	25	5.74	----	-----	-----	-----	-----																					
	50	6.28	----	-----	-----	-----	-----																					
	75	6.61	----	-----	-----	-----	-----																					
10	25	5.24	----	-----	-----	-----	-----																					
	50	5.75	----	-----	-----	-----	-----																					
	75	6.07	----	-----	-----	-----	-----																					
20	25	4.17	---	----	-----	-----	-----																					
	50	4.61	----	-----	-----	-----	-----																					
	75	4.89	----	-----	-----	-----	-----																					

Figure 5.6: The AASHTO produced structural numbers of 243 pavement sections from design matrix in Figure 3.1 when subbase softer than roadbed soil is omitted from analysis.

		150									300									450								
		20			30			40			20			30			40			20			30			40		
		10	15	20	10	15	20	10	15	20	10	15	20	10	15	20	10	15	20	10	15	20	10	15	20	10	15	20
7.5	25	5.74	----	----	----	----	----																					
	50	6.28	----	----	----	----	----																					
	75	6.61	----	----	----	----	----																					
10	25	5.24	----	----	----	----	----																					
	50	5.75	----	----	----	----	----																					
	75	6.07	----	----	----	----	----																					
20	25	5.24	5.00	4.17	5.24	5.00	4.17	5.24	5.00	4.17	5.24	5.00	4.17	5.24	5.00	4.17	5.24	5.00	4.17	5.24	5.00	4.17	5.24	5.00	4.17	5.24	5.00	4.17
	50	5.75	5.07	4.61	5.75	5.07	4.61	5.75	5.07	4.61	5.75	5.07	4.61	5.75	5.07	4.61	5.75	5.07	4.61	5.75	5.07	4.61	5.75	5.07	4.61	5.75	5.07	4.61
	75	6.07	5.35	4.89	6.07	5.35	4.89	6.07	5.35	4.89	6.07	5.35	4.89	6.07	5.35	4.89	6.07	5.35	4.89	6.07	5.35	4.89	6.07	5.35	4.89	6.07	5.35	4.89

Figure 5.7: The AASHTO produced structural numbers of 243 pavement sections from design matrix in Figure 3.1 when subbase softer than roadbed soil is included in analysis.

Figures 5.8 through 5.11 depicts the thicknesses of the AC, base and subbase layers and the total thickness for all 243 pavement sections, respectively. These thicknesses corresponds to the structural numbers listed in Figure 5.7.

5.2.2 Mechanistic Analysis

After obtaining the layer thicknesses from the AASHTO design procedure using the DNPS86 computer program for all 243 pavement sections of Figure 3.1, a mechanistic analysis was conducted for each section by using ELSYM5 computer program. It should be noted that the mechanistic responses were obtained only for critical locations in the pavement structure. The values of Poisson's ratio, Axle load, and Tire pressure used in the study are listed below.

a) Poisson's Ratio Values

Layer Type	Poisson's Ratio
AC	0.40
Base	0.35
Subbase	0.35
Roadbed	0.45

b) An axle Load of 18000-lbs and the single tire option in ELSYM5 computer program were used. Hence the load on one tire was considered to be 9000-lbs.

c) A typical tire pressure of 80 psi was used.

		150									300									450								
		20			30			40			20			30			40			20			30			40		
		10	15	20	10	15	20	10	15	20	10	15	20	10	15	20	10	15	20	10	15	20	10	15	20	10	15	20
7.5	25	16.7	16.7	16.68	14.45	14.45	14.45	13.01	13.01	13.01	11.27	11.27	11.27	9.76	9.76	9.76	8.79	8.79	8.79	9.48	9.48	9.48	8.21	8.21	8.21	7.39	7.39	7.39
	50	18.4	18.4	18.45	16.07	16.07	16.07	14.51	14.51	14.51	12.47	12.47	12.47	10.86	10.86	10.86	9.80	9.80	9.80	10.5	10.49	10.49	9.13	9.13	9.13	8.24	8.24	8.24
	75	19.6	19.6	19.55	17.07	17.07	17.07	15.44	15.44	15.44	13.21	13.21	13.21	11.54	11.54	11.54	10.43	10.43	10.43	11.1	11.11	11.11	9.70	9.70	9.70	8.77	8.77	8.77
10	25	16.7	16.7	16.68	14.45	14.45	14.45	13.01	13.01	13.01	11.27	11.27	11.27	9.76	9.76	9.76	8.79	8.79	8.79	9.48	9.48	9.48	8.21	8.21	8.21	7.39	7.39	7.39
	50	18.4	18.4	18.45	16.07	16.07	16.07	14.51	14.51	14.51	12.47	12.47	12.47	10.86	10.86	10.86	9.80	9.80	9.80	10.5	10.49	10.49	9.13	9.13	9.13	8.24	8.24	8.24
	75	19.6	19.6	19.55	17.07	17.07	17.07	15.44	15.44	15.44	13.21	13.21	13.21	11.54	11.54	11.54	10.43	10.43	10.43	11.1	11.11	11.11	9.70	9.70	9.70	8.77	8.77	8.77
20	25	16.7	16.7	16.68	14.45	14.45	14.45	13.01	13.01	13.01	11.27	11.27	11.27	9.76	9.76	9.76	8.79	8.79	8.79	9.48	9.48	9.48	8.21	8.21	8.21	7.39	7.39	7.39
	50	18.4	18.4	18.45	16.07	16.07	16.07	14.51	14.51	14.51	12.47	12.47	12.47	10.86	10.86	10.86	9.80	9.80	9.80	10.5	10.49	10.49	9.13	9.13	9.13	8.24	8.24	8.24
	75	19.6	19.6	19.55	17.07	17.07	17.07	15.44	15.44	15.44	13.21	13.21	13.21	11.54	11.54	11.54	10.43	10.43	10.43	11.1	11.11	11.11	9.70	9.70	9.70	8.77	8.77	8.77

Figure 5.8: The AASHTO produced thicknesses (inches) of the asphalt layers for 243 pavement sections of Figure 3.1.

		150									300									450								
		20			30			40			20			30			40			20			30			40		
		10	15	20	10	15	20	10	15	20	10	15	20	10	15	20	10	15	20	10	15	20	10	15	20	10	15	20
7.5	25	11.93	4.75	0.00	11.65	7.03	3.98	11.71	7.90	5.39	11.93	4.75	0.00	11.65	7.03	3.98	11.71	7.90	5.39	11.93	4.75	0.00	11.65	7.03	3.98	11.71	7.90	5.39
	50	12.68	5.05	0.00	12.41	7.50	4.26	12.52	8.48	5.81	12.68	5.05	0.00	12.41	7.50	4.26	12.52	8.48	5.81	12.68	5.05	0.00	12.41	7.50	4.26	12.52	8.48	5.81
	75	13.13	5.22	0.00	12.86	7.78	4.42	12.99	8.81	6.04	13.13	5.22	0.00	12.86	7.78	4.42	12.99	8.81	6.04	13.13	5.22	0.00	12.86	7.78	4.42	12.99	8.81	6.04
10	25	11.93	4.75	0.00	11.65	7.03	3.98	11.71	7.90	5.39	11.93	4.75	0.00	11.65	7.03	3.98	11.71	7.90	5.39	11.93	4.75	0.00	11.65	7.03	3.98	11.71	7.90	5.39
	50	12.68	5.05	0.00	12.41	7.50	4.26	12.52	8.48	5.81	12.68	5.05	0.00	12.41	7.50	4.26	12.52	8.48	5.81	12.68	5.05	0.00	12.41	7.50	4.26	12.52	8.48	5.81
	75	13.13	5.22	0.00	12.86	7.78	4.42	12.99	8.81	6.04	13.13	5.22	0.00	12.86	7.78	4.42	12.99	8.81	6.04	13.13	5.22	0.00	12.86	7.78	4.42	12.71	8.81	6.04
20	25	11.93	4.75	0.00	11.65	7.03	3.98	11.71	7.90	5.39	11.93	4.75	0.00	11.65	7.03	3.98	11.71	7.90	5.39	11.93	4.75	0.00	11.65	7.03	3.98	11.71	7.90	5.39
	50	12.68	5.05	0.00	12.41	7.50	4.26	12.52	8.48	5.81	12.68	5.05	0.00	12.41	7.50	4.26	12.52	8.48	5.81	12.68	5.05	0.00	12.41	7.50	4.26	12.52	8.48	5.81
	75	13.13	5.22	0.00	12.86	7.78	4.42	12.99	8.81	6.04	13.13	5.22	0.00	12.86	7.78	4.42	12.99	8.81	6.04	13.13	5.22	0.00	12.86	7.78	4.42	12.71	7.90	6.04

Figure 5.9: The AASHTO produced thicknesses (inches) of the base layers for 243 pavement sections of Figure 3.1.

		150								
		20			30			40		
		10	15	20	10	15	20	10	15	20
7.5	25	7.03	10.4	11.19	7.03	10.35	11.19	7.03	10.35	11.19
	50	7.47	11.0	11.89	7.47	11.00	11.89	7.47	11.00	11.89
	75	7.76	11.4	12.32	7.76	11.41	12.32	7.76	11.41	12.32
10	25	0.00	5.88	7.67	0.00	5.88	7.67	0.00	5.88	7.67
	50	0.00	6.25	8.15	0.00	6.25	8.15	0.00	6.25	8.15
	75	0.00	6.47	8.44	0.00	6.47	8.44	0.00	6.47	8.44
20	25	0.00	0.00	0.00	0.00	0.00	0.00	0.00	0.00	0.00
	50	0.00	0.00	0.00	0.00	0.00	0.00	0.00	0.00	0.00
	75	0.00	0.00	0.00	0.00	0.00	0.00	0.00	0.00	0.00

		300								
		20			30			40		
		10	15	20	10	15	20	10	15	20
7.5	25	7.03	10.35	11.19	7.03	10.35	11.19	7.03	10.35	11.19
	50	7.47	11.00	11.89	7.47	11.00	11.89	7.47	11.00	11.89
	75	7.76	11.41	12.32	7.76	11.41	12.32	7.76	11.41	12.32
10	25	0.00	5.88	7.67	0.00	5.88	7.67	0.00	5.88	7.67
	50	0.00	6.25	8.15	0.00	6.25	8.15	0.00	6.25	8.15
	75	0.00	6.47	8.44	0.00	6.47	8.44	0.00	6.47	8.44
20	25	0.00	0.00	0.00	0.00	0.00	0.00	0.00	0.00	0.00
	50	0.00	0.00	0.00	0.00	0.00	0.00	0.00	0.00	0.00
	75	0.00	0.00	0.00	0.00	0.00	0.00	0.00	0.00	0.00

		450								
		20			30			40		
		10	15	20	10	15	20	10	15	20
7.5	25	7.03	10.35	11.19	7.03	10.35	11.19	7.03	10.35	11.2
	50	7.47	11.00	11.89	7.47	11.00	11.89	7.47	11.00	11.9
	75	7.76	11.41	12.32	7.76	11.41	12.32	7.76	11.41	12.3
10	25	0.00	5.88	7.67	0.00	5.88	7.67	0.00	5.88	7.67
	50	0.00	6.25	8.15	0.00	6.25	8.15	0.00	6.25	8.15
	75	0.00	6.47	8.44	0.00	6.47	8.44	0.00	6.47	8.44
20	25	0.00	0.00	0.00	0.00	0.00	0.00	0.00	0.00	0.00
	50	0.00	0.00	0.00	0.00	0.00	0.00	0.00	0.00	0.00
	75	0.00	0.00	0.00	0.00	0.00	0.00	0.00	0.00	0.00

Figure 5.10: The AASHTO produced thicknesses (inches) of the subbase layers for 243 pavement sections of Figure 3.1.

		150									300									450								
		20			30			40			20			30			40			20			30			40		
		10	15	20	10	15	20	10	15	20	10	15	20	10	15	20	10	15	20	10	15	20	10	15	20	10	15	20
7.5	25	35.6	31.7	27.87	33.13	31.83	29.62	31.75	31.26	29.59	30.23	26.37	22.46	28.44	27.14	24.93	27.53	27.04	25.37	28.4	24.58	20.67	26.9	25.59	23.38	26.2	25.64	24.0
	50	38.6	34.5	30.34	35.95	34.57	32.22	34.50	33.99	32.21	32.62	28.52	24.36	30.74	29.36	27.01	29.79	29.28	27.50	30.6	26.54	22.38	29.0	27.63	25.28	28.2	27.72	25.9
	75	40.4	36.2	31.87	37.69	36.26	33.81	36.19	35.66	33.80	34.10	29.84	25.53	32.16	30.73	28.28	31.18	30.65	28.79	32.0	27.74	23.43	30.3	28.89	26.44	29.5	28.99	27.1
10	25	28.6	27.3	24.35	26.10	27.36	26.10	24.72	26.79	26.07	23.20	21.90	18.94	21.41	22.67	21.41	20.50	22.57	21.85	21.4	20.11	17.15	19.9	21.12	19.86	19.1	21.17	20.4
	50	31.1	29.7	26.60	28.48	29.82	28.48	27.03	29.24	28.47	25.15	23.77	20.62	23.27	24.61	23.27	22.32	24.53	23.76	23.2	21.79	18.64	21.5	22.88	21.54	20.8	22.97	22.2
	75	32.7	31.2	27.99	29.93	31.32	29.93	28.43	30.72	29.92	26.34	24.90	21.65	24.40	25.79	24.40	23.41	25.71	24.91	24.2	22.80	19.55	22.6	23.95	22.56	21.8	24.05	23.2
20	25	28.6	21.4	16.68	26.10	21.48	18.43	24.72	20.91	18.40	23.20	16.02	11.27	21.41	16.79	13.74	20.50	16.69	14.18	21.4	14.23	9.48	19.9	15.24	12.19	19.1	15.29	12.8
	50	31.1	23.5	18.45	28.48	23.57	20.33	27.03	22.99	20.32	25.15	17.52	12.47	23.27	18.36	15.12	22.32	18.28	15.61	23.2	15.54	10.49	21.5	16.63	13.39	20.8	16.72	14.0
	75	32.7	24.8	19.55	29.93	24.85	22.12	28.43	24.25	21.48	26.34	18.43	13.21	24.40	19.32	15.96	23.42	19.24	16.47	24.2	16.33	11.11	22.6	17.48	14.12	21.8	15.58	14.8

Figure 5.11: The AASHTO produced total thicknesses (inches) for 243 pavement sections of Fig 3.1.

Please note that this is the tire pressure used at the AASHO Road Test sections.

Results of the mechanistic analysis (mechanistic Responses) are provided in Figures 5.12 through 5.21.

5.2.3. Verification of SHRP Study Results

To verify the results of the SHRP study at higher levels of traffic, a traffic level of 75,000,000 ESAL's and roadbed with resilient modulus of 10 ksi is considered. This gives a matrix of 27 cells with variables as shown in Figure 5.22. The cells have been numbered as they appear in the main matrix of Figure 3.1. Table 5.2 shows the outputs (layer thicknesses) of the AASHTO design procedure for the 27 cells of Figure 5.22. Mechanistic responses of these 27 pavement sections are presented in Table 5.3.

According to the AASHTO Design Procedure, the 27 pavement sections are suppose to have the same serviceability loss over the 10-year performance period, they are supported on the same roadbed soil, and they carry the same amount of traffic of 75,000,000 ESAL's over the same performance period. Hence, the amount of damage delivered to each pavement section during the performance period is the same. This implies that the 27 pavement sections receive the same level of protection against damage.

		150									300									450								
		20			30			40			20			30			40			20			30			40		
		10	15	20	10	15	20	10	15	20	10	15	20	10	15	20	10	15	20	10	15	20	10	15	20	10	15	20
7.5	25	16.7	16.9	17.0	17.3	17.5	17.6	17.4	17.7	17.9	16.6	16.9	16.9	17.3	17.6	17.7	17.5	17.9	18.0	16.6	16.9	16.9	17.3	17.7	17.7	17.6	18.0	18.1
	50	15.8	16.0	16.0	16.3	16.5	16.5	16.5	16.7	16.8	15.4	15.4	15.7	16.0	16.3	16.3	16.2	16.6	16.7	15.3	15.5	15.6	16.0	16.3	16.3	16.2	16.6	16.7
	75	15.4	15.5	15.5	15.8	16.0	16.0	15.9	16.2	16.2	14.8	15.0	15.1	15.4	15.6	15.7	15.6	15.9	16.0	14.7	14.9	14.9	15.3	15.5	15.6	15.5	15.8	16.0
10	25	14.7	15.0	15.0	15.2	15.6	15.6	15.3	15.8	15.9	14.4	14.8	14.8	15.0	15.5	15.6	15.2	15.8	16.0	14.3	14.7	14.7	15.0	15.5	15.6	15.2	15.9	16.1
	50	13.9	14.2	14.2	14.3	14.6	14.7	14.4	14.9	15.0	13.4	13.7	13.7	13.9	14.3	14.4	14.1	14.6	14.8	13.2	13.5	13.5	13.8	14.3	14.3	14.0	14.6	14.7
	75	13.5	13.7	13.7	13.9	14.2	14.2	14.0	14.4	14.5	12.8	13.1	13.1	13.3	13.7	13.8	13.5	14.0	14.1	12.6	12.9	12.9	13.2	13.6	13.7	13.4	13.9	14.1
20	25	11.1	11.1	11.1	11.3	11.5	11.7	11.4	11.7	12.0	10.4	10.3	10.3	10.7	10.9	11.1	10.7	11.2	11.5	10.1	10.1	10.0	10.5	10.8	11.0	10.6	11.1	11.4
	50	10.6	10.6	10.5	10.8	10.9	11.1	10.8	11.1	11.3	9.63	9.60	9.57	9.90	10.1	10.3	9.99	10.4	10.6	9.34	9.31	9.26	9.68	9.92	10.1	9.79	10.2	10.5
	75	10.3	10.3	10.3	10.5	10.6	10.8	10.5	10.8	11.0	9.24	9.22	9.18	9.50	9.71	9.88	9.59	9.92	10.2	8.92	8.89	8.84	9.24	9.46	9.63	9.36	9.72	10.0

Figure 5.12: The vertical deflections at the top of the AC layer for the 243 pavement sections Figure 3.1.

		150									300									450								
		20			30			40			20			30			40			20			30			40		
		10	15	20	10	15	20	10	15	20	10	15	20	10	15	20	10	15	20	10	15	20	10	15	20	10	15	20
7.5	25	13.4	13.6	13.6	14.2	14.4	14.5	14.6	14.9	15.5	15.3	15.6	15.6	16.1	16.5	16.5	16.5	16.9	17.0	15.8	16.1	16.2	16.7	17.0	17.1	17.0	17.4	17.6
	50	12.3	12.5	12.5	13.0	13.2	13.3	13.4	13.6	13.7	14.0	14.1	14.3	14.8	15.0	15.1	15.1	15.9	15.5	14.5	14.7	14.8	15.3	15.6	15.6	15.6	16.0	16.1
	75	11.7	11.9	11.9	12.4	12.6	12.6	12.7	13.0	13.0	13.4	13.6	13.6	14.1	14.3	14.4	14.4	14.7	14.8	13.8	14.0	14.1	14.6	14.8	14.9	14.9	15.2	15.3
10	25	11.4	11.6	11.7	12.1	12.4	12.5	12.4	12.9	13.0	13.1	13.5	13.5	13.9	14.4	14.5	14.1	14.8	15.0	13.6	14.0	14.0	14.4	14.9	15.0	14.6	15.3	15.5
	50	10.4	10.6	10.6	11.0	11.3	11.4	11.3	11.7	11.9	12.0	12.3	12.3	12.6	13.1	13.2	12.9	13.5	13.6	12.4	12.7	12.7	13.1	13.6	13.6	13.4	14.0	14.1
	75	9.88	10.1	10.1	10.5	10.8	10.8	10.9	11.1	11.2	11.4	11.6	11.7	12.0	12.4	12.5	12.3	12.8	12.9	11.8	12.1	12.1	12.4	12.8	12.9	12.7	13.2	13.4
20	25	7.71	7.69	NA	8.15	8.36	8.54	8.36	8.71	8.98	9.05	9.02	NA	9.49	9.76	9.97	9.67	10.1	10.4	9.38	9.34	NA	9.83	10.1	10.3	10.0	10.5	10.8
	50	7.00	6.97	NA	7.39	7.57	7.72	7.60	7.89	8.13	8.22	8.19	NA	8.63	8.86	9.04	8.81	9.19	9.48	8.52	8.48	NA	8.95	9.19	9.37	9.14	9.53	9.84
	75	6.67	6.60	NA	6.99	7.16	7.29	7.19	7.46	7.68	7.77	7.75	NA	8.17	8.38	8.54	8.35	80.69	8.96	8.06	8.03	NA	8.48	8.70	8.87	8.66	9.02	9.31

Figure 5.13: The vertical deflections at the top of the base layers for the 243 pavement sections of Figure 3.1.

		150									300									450								
		20			30			40			20			30			40			20			30			40		
		10	15	20	10	15	20	10	15	20	10	15	20	10	15	20	10	15	20	10	15	20	10	15	20	10	15	20
7.5	25	10.1	10.8	11.5	10.6	11.0	11.5	10.9	11.2	11.6	11.2	12.1	13.0	11.7	12.2	12.8	11.9	12.3	12.8	11.5	12.5	13.5	12.1	12.6	13.2	12.3	12.6	13.2
	50	9.36	9.99	10.7	9.86	10.2	10.6	10.1	10.3	10.7	10.3	11.0	12.0	10.8	11.2	11.8	11.0	11.3	11.8	10.7	11.5	12.4	11.2	11.6	12.2	11.3	11.7	12.1
	75	8.98	9.58	10.2	9.45	9.74	10.1	9.68	9.88	10.2	9.92	10.7	11.5	10.4	10.7	11.2	10.6	10.8	11.3	10.2	11.0	11.8	10.7	11.1	11.6	10.9	11.1	11.6
10	25	9.15	9.42	10.1	9.86	9.67	9.99	10.2	9.88	10.1	10.4	10.7	11.5	11.1	10.9	11.3	11.4	11.0	11.3	10.7	11.1	12.0	11.5	11.3	11.7	11.8	11.4	11.7
	50	8.44	8.67	9.23	9.06	8.88	9.16	9.37	9.06	9.27	9.51	9.81	10.5	10.2	9.99	10.3	10.5	10.1	10.4	9.84	10.2	10.9	10.5	10.3	10.7	10.8	10.5	10.7
	75	8.07	8.28	8.80	8.65	8.48	8.74	9.09	8.64	8.84	9.07	9.35	10.0	9.70	9.50	9.83	9.97	9.63	9.88	9.38	9.67	10.4	10.0	9.84	10.2	10.3	9.95	10.2
20	25	5.40	6.54	7.66	5.89	6.78	7.52	6.15	6.99	7.68	6.14	7.56	8.97	6.68	7.77	8.70	6.92	7.96	8.82	6.37	7.84	9.27	6.92	8.07	9.02	7.16	8.26	9.15
	50	4.94	5.95	6.95	5.39	6.16	6.82	5.62	6.35	6.96	5.62	6.88	8.14	6.11	7.08	7.90	6.33	7.25	8.01	5.83	7.14	8.43	6.33	7.35	8.20	6.55	7.52	8.32
	75	4.71	5.65	6.57	5.12	5.84	6.34	5.34	6.02	6.58	5.34	6.52	7.70	5.80	6.70	7.47	6.01	6.87	7.58	5.54	6.77	7.98	6.02	6.96	7.76	6.23	7.13	7.87

Figure 5.14: The vertical deflections at the top of the roadbed soil for the 243 pavement sections of Figure 3.1.

		150									300									450								
		20			30			40			20			30			40			20			30			40		
		10	15	20	10	15	20	10	15	20	10	15	20	10	15	20	10	15	20	10	15	20	10	15	20	10	15	20
7.5	25	4.80	4.56	4.60	7.56	7.21	7.06	10.05	9.98	9.70	6.53	6.21	6.29	10.3	9.83	9.60	14.2	13.5	13.1	6.88	6.54	6.63	10.8	10.3	10.1	14.9	14.2	13.8
	50	3.97	3.77	3.80	6.24	5.94	5.82	8.66	8.25	8.02	5.46	5.23	5.26	8.63	8.23	8.04	12.0	11.4	11.1	5.78	5.49	5.56	9.13	8.70	8.49	12.7	12.1	11.7
	75	3.56	3.38	3.41	5.58	5.31	5.20	7.75	7.39	7.18	4.93	4.88	4.74	7.78	7.42	7.24	10.8	10.3	10.0	5.22	4.96	5.02	8.26	7.87	7.68	11.5	11.0	10.6
10	25	4.91	4.60	4.59	7.69	7.23	7.04	10.6	10.0	9.67	6.67	6.26	6.25	10.4	9.85	9.56	14.3	13.6	13.1	7.02	6.59	6.58	11.0	10.3	10.0	15.1	14.2	13.7
	50	4.06	3.80	3.79	6.34	5.96	5.81	8.76	8.27	8.00	5.58	5.23	5.22	8.75	8.25	8.01	12.1	11.5	11.1	5.90	5.53	5.52	9.25	8.72	8.46	12.8	12.1	11.7
	75	3.64	3.40	3.39	5.67	5.33	5.19	9.15	7.40	7.16	5.03	4.71	4.70	7.89	7.43	7.21	10.9	10.4	10.0	5.33	4.99	4.99	8.37	7.88	7.65	11.6	11.0	10.6
20	25	5.57	5.54	NA	8.47	8.13	7.76	11.4	10.9	10.3	7.44	7.41	NA	11.3	10.9	10.4	15.2	14.6	13.8	7.81	7.79	NA	11.9	11.40	10.90	16.0	15.3	14.4
	50	4.62	4.60	NA	7.01	6.73	6.42	9.47	9.03	8.56	6.24	6.22	NA	9.52	9.15	8.70	12.9	12.3	11.7	6.58	6.56	NA	10.1	9.66	9.18	13.6	13.0	12.3
	75	4.31	4.12	NA	6.28	6.02	5.74	8.49	8.09	7.66	5.63	5.61	NA	8.60	8.26	7.86	11.7	11.2	10.6	5.96	5.94	NA	9.11	8.75	8.32	12.4	11.8	11.2

Figure 5.15. The vertical compressive stress (psi) at the top of the base layer for 243 pavement sections of Figure 3.1.

		150									300									450								
		20			30			40			20			30			40			20			30			40		
		10	15	20	10	15	20	10	15	20	10	15	20	10	15	20	10	15	20	10	15	20	10	15	20	10	15	20
7.5	25	1.02	1.41	1.67	1.37	1.48	1.64	1.46	1.54	1.68	1.50	1.78	2.13	1.69	1.84	2.05	1.78	1.89	2.06	1.60	1.90	2.27	1.80	1.96	2.18	1.88	2.00	2.20
	50	1.02	1.19	1.40	1.16	1.24	1.37	1.23	1.29	1.40	1.26	1.47	1.78	1.42	1.54	1.71	1.50	1.58	1.73	1.34	1.59	1.90	1.52	1.64	1.83	1.59	1.68	1.84
	75	0.93	1.08	1.26	1.05	1.13	1.24	1.12	1.17	1.27	1.15	1.35	1.61	1.29	1.39	1.55	1.36	1.43	1.56	1.22	1.44	1.71	1.37	1.48	1.65	1.44	1.52	1.66
10	25	1.86	1.98	2.31	2.23	2.10	2.26	2.43	2.21	2.33	2.38	2.54	2.99	2.82	2.65	2.86	3.03	2.75	2.90	2.54	2.70	1.18	3.00	2.83	3.05	3.22	2.93	3.09
	50	1.56	1.65	1.92	1.86	1.75	1.88	2.02	1.84	1.93	1.99	2.11	2.49	2.35	2.21	2.38	2.53	2.29	2.42	2.12	2.25	2.65	2.51	2.36	2.54	2.69	2.44	2.58
	75	1.41	1.49	1.73	1.67	1.58	1.69	2.01	1.65	1.74	1.80	1.91	2.24	2.12	1.99	2.14	2.28	2.07	2.18	1.91	2.03	2.39	2.26	2.12	2.29	2.43	2.20	2.32
20	25	2.56	3.89	5.57	3.12	4.18	5.20	3.46	4.48	5.42	3.25	5.05	7.45	3.93	5.33	6.72	4.30	5.66	6.91	3.45	5.34	7.84	4.17	5.66	7.11	4.57	6.01	7.33
	50	2.14	3.24	4.62	2.61	3.47	4.31	2.88	3.72	4.48	2.72	4.23	6.25	3.29	4.46	5.61	3.60	4.72	5.76	2.90	4.48	6.60	3.50	4.74	5.95	3.83	5.02	6.12
	75	1.93	2.91	4.14	2.35	3.12	3.71	2.60	3.34	4.02	2.46	3.82	5.64	2.97	4.02	5.02	3.26	4.26	5.19	2.62	4.05	5.98	3.17	4.27	5.36	3.47	4.53	5.51

Figure 5.16: The vertical compressive stress (psi) at the top of the roadbed soil for 243 pavement sections of Figure 3.1.

		150									300									450								
		20			30			40			20			30			40			20			30			40		
		10	15	20	10	15	20	10	15	20	10	15	20	10	15	20	10	15	20	10	15	20	10	15	20	10	15	20
7.5	25	62.6	60.0	60.0	50.5	46.7	45.4	44.8	39.6	37.4	46.2	49.4	49.5	64.2	68.6	70.0	73.5	79.4	82.0	77.5	80.5	80.7	97.1	101	103	108	114	116
	50	78.0	76.2	76.2	68.3	65.4	64.3	63.6	59.5	57.7	25.6	24.1	28.2	40.5	44.0	45.1	48.6	53.4	55.5	56.3	58.7	58.8	72.9	76.3	77.3	82.3	87.0	89.0
	75	85.8	84.2	84.2	77.0	74.5	73.7	72.9	69.3	67.7	15.2	17.5	17.5	28.6	31.7	32.7	36.0	40.3	42.2	45.6	47.8	47.8	60.6	63.6	64.5	69.3	73.4	75.2
10	25	66.7	63.1	62.7	55.1	49.8	47.9	49.7	42.7	39.8	42.2	46.4	46.8	59.7	65.7	67.6	68.8	76.7	79.7	73.6	77.6	78.0	92.9	89.6	100	103	111	114
	50	81.6	78.8	78.4	72.2	67.9	66.4	67.7	62.1	59.8	22.2	25.7	26.0	36.7	41.7	43.2	44.8	51.2	53.8	53.1	56.4	56.7	69.4	74.1	75.6	78.8	85.0	87.5
	75	89.0	86.6	86.3	80.6	76.8	75.7	76.6	71.7	69.6	12.2	15.3	15.5	25.2	29.6	31.0	32.6	38.3	40.6	42.8	45.7	46.0	57.5	61.7	63.0	66.1	71.6	73.9
20	25	80.2	80.0	80.0	71.7	68.2	64.7	67.8	62.2	57.1	27.4	27.4	27.1	42.0	45.9	49.6	50.1	56.3	62.1	59.6	59.5	59.1	76.2	79.9	83.3	86.0	91.9	97.4
	50	92.4	92.3	92.3	85.6	82.7	79.9	82.4	77.8	73.6	10.3	10.4	10.2	22.3	25.5	28.6	29.4	34.5	39.2	41.8	41.8	41.4	55.7	58.8	61.5	64.3	69.2	73.7
	75	98.6	98.5	98.4	92.5	89.9	87.5	89.6	85.5	81.8	1.76	1.79	1.64	12.5	15.3	18.0	18.9	23.5	27.7	32.8	32.8	32.5	45.3	48.1	50.5	53.2	57.6	61.6

Figure 5.17: The vertical strain (microstrains) at the top of the AC layer for 243 pavement sections of Figure 3.1.

		150								
		20			30			40		
		10	15	20	10	15	20	10	15	20
7.5	25	168	171	171	192	196	198	205	210	213
	50	141	143	142	161	164	165	173	176	178
	75	126	129	128	145	147	149	156	159	161
10	25	167	171	171	191	196	198	205	210	213
	50	139	142	142	160	163	165	172	176	179
	75	125	128	128	144	147	149	143	159	161
20	25	160	161	NA	184	188	192	199	203	208
	50	134	135	NA	154	157	161	168	171	175
	75	115	121	NA	139	142	145	151	154	158

		300								
		20			30			40		
		10	15	20	10	15	20	10	15	20
7.5	25	195	198	198	219	223	225	230	235	238
	50	165	153	168	187	191	192	198	203	205
	75	150	153	152	170	174	175	182	185	188
10	25	193	197	197	217	222	225	228	235	239
	50	164	167	168	155	190	192	197	203	205
	75	149	152	152	169	173	175	181	185	188
20	25	183	184	NA	207	211	216	220	225	231
	50	156	157	NA	177	181	184	190	194	199
	75	142	143	NA	162	165	168	174	178	182

		450								
		20			30			40		
		10	15	20	10	15	20	10	15	20
7.5	25	187	191	191	209	214	216	219	225	228
	50	160	163	163	181	184	186	191	196	198
	75	146	149	149	166	169	170	176	180	182
10	25	185	189	190	207	213	215	218	224	228
	50	159	162	162	179	184	186	190	195	198
	75	145	148	148	164	168	170	175	180	182
20	25	175	176	NA	197	201	205	208	214	219
	50	151	151	NA	171	174	177	182	186	191
	75	138	138	NA	156	159	162	168	172	176

Figure 5.18: The vertical strain (microstrains) at the top of the base layer for 243 pavement sections of Figure 3.1.

		150									300									450								
		20			30			40			20			30			40			20			30			40		
		10	15	20	10	15	20	10	15	20	10	15	20	10	15	20	10	15	20	10	15	20	10	15	20	10	15	20
7.5	25	147	143	153	171	154	153	182	162	159	183	179	191	211	191	189	222	198	194	194	189	201	223	202	200	235	210	206
	50	124	120	128	143	129	127	153	135	132	153	144	159	176	159	158	186	165	162	162	157	167	187	168	167	197	175	172
	75	112	108	115	129	116	115	138	122	119	138	134	143	159	143	142	168	149	146	146	141	150	169	152	150	178	158	155
10	25	143	173	178	150	187	177	151	198	185	178	216	223	186	233	220	186	243	227	187	226	232	196	246	231	196	258	240
	50	119	144	148	125	155	147	126	165	153	149	180	186	155	194	183	155	204	189	156	189	193	163	205	193	164	216	200
	75	107	129	133	112	140	132	109	148	138	134	162	167	140	174	165	140	183	171	141	170	174	147	184	174	148	194	180
20	25	135	206	164	137	183	227	135	175	211	168	259	186	168	226	283	164	215	261	177	168	177	176	236	192	173	225	271
	50	113	172	137	114	152	189	112	145	175	141	217	159	141	190	237	138	180	218	149	226	152	148	198	245	145	188	227
	75	102	155	123	103	137	179	101	131	158	128	197	144	128	171	214	125	163	197	134	204	139	134	179	222	132	170	205

Figure 5.19: The vertical strain (microstrains) at the top of the roadbed soil for 243 pavement sections of Figure 3.1.

		150									300									450								
		20			30			40			20			30			40			20			30			40		
		10	15	20	10	15	20	10	15	20	10	15	20	10	15	20	10	15	20	10	15	20	10	15	20	10	15	20
7.5	25	25.6	26.4	26.3	28.6	27.7	28.3	25.4	26.9	27.7	64.8	66.5	66.3	69.1	71.4	72.4	68.4	71.3	72.9	96.8	99.1	98.9	104	107	109	105	109	111
	50	21.4	22.1	22.0	22.3	23.3	23.7	21.5	22.7	23.4	55.2	50.2	56.4	59.3	61.2	62.0	59.4	61.7	63.1	83.0	84.9	84.7	90.3	92.8	93.9	91.6	94.9	96.7
	75	19.3	19.9	19.2	20.2	21.0	21.4	19.5	20.6	21.2	50.2	51.4	51.2	54.1	55.8	56.5	54.5	56.6	57.8	75.8	77.5	77.4	82.9	85.1	86.0	84.5	87.4	89.0
10	25	25.1	26.2	26.3	26.2	27.6	28.3	25.1	26.8	27.8	63.9	66.0	66.2	68.3	71.1	72.4	67.7	71.1	73.1	95.4	98.3	98.5	103	107	109	104	108	111
	50	21.0	21.9	22.0	22.0	23.2	23.8	21.3	22.7	23.5	54.4	56.2	56.3	58.6	60.9	62.0	58.8	61.6	63.2	81.9	84.2	84.4	89.2	92.4	93.8	90.7	94.7	96.8
	75	18.9	19.7	19.8	19.9	20.9	21.4	15.4	20.5	21.2	49.5	51.1	51.2	53.5	55.6	56.6	54.0	56.5	57.9	74.8	76.9	77.1	81.9	84.8	86.0	83.8	87.3	89.1
20	25	23.1	23.3	NA	24.0	25.0	26.3	23.1	24.5	26.1	59.4	59.7	NA	63.5	65.5	67.9	63.4	66.2	69.4	88.8	89.2	NA	96.0	98.7	102	97.2	101	105
	50	19.4	19.6	NA	20.2	21.0	22.1	19.6	20.8	22.1	50.7	51.0	NA	54.6	56.3	58.3	55.2	57.5	60.1	76.5	76.9	NA	83.4	85.6	88.2	85.3	88.5	92.0
	75	16.2	17.6	NA	18.2	19.0	20.0	17.8	18.8	20.0	46.2	46.5	NA	50.0	51.5	53.2	50.7	52.8	55.1	70.0	70.4	NA	76.6	78.7	81.0	78.8	81.7	84.8

Figure 5.20: The radial stress (psi) at the bottom of the AC layer for 243 pavement sections of Figure 3.1.

		150									300									450								
		20			30			40			20			30			40			20			30			40		
		10	15	20	10	15	20	10	15	20	10	15	20	10	15	20	10	15	20	10	15	20	10	15	20	10	15	20
7.5	25	115	118	117	126	130	132	130	134	137	138	141	141	152	156	158	156	161	163	135	138	138	149	152	154	153	157	160
	50	96.1	94.8	98	106	109	110	109	113	115	118	109	120	130	133	135	135	139	141	116	118	118	129	132	133	133	137	139
	75	86.5	88.6	88.1	95.5	98.2	99.5	98.7	102	104	107	109	109	119	121	123	124	127	129	106	108	108	118	120	122	123	126	128
10	25	114	117	117	125	130	132	129	134	137	137	140	141	150	155	158	155	160	164	133	137	137	147	152	154	151	157	160
	50	94.9	97.8	98	105	109	111	108	113	115	116	119	120	129	133	135	134	139	141	114	117	117	127	131	133	132	137	139
	75	85.4	88.0	88.1	94.6	97.8	99.5	86.2	102	104	106	108	109	118	121	123	123	127	129	104	107	107	117	120	121	122	126	128
20	25	107	108	NA	119	122	126	123	127	132	129	129	NA	142	146	150	147	152	157	125	126	NA	139	142	145	144	148	153
	50	89.7	90.5	NA	99.5	102	106	104	107	111	110	110	NA	122	125	128	128	131	136	108	108	NA	120	123	126	126	130	134
	75	76.3	81.5	NA	89.7	92.1	95.2	93.7	96.8	100	100	101	NA	111	114	117	117	120	124	98.7	99.1	NA	110	113	115	116	119	123

Figure 5.21: The radial tensile strain (microstrains) at the bottom of the AC layer for 243 pavement section of Figure 3.1.

			150			300			450		
			20	30	40	20	30	40	20	30	40
10	75	10	6	33	60	87	114	141	168	195	222
		15	15	42	69	96	123	150	177	204	231
		20	24	51	78	105	132	159	186	213	240

Figure 5.22: 27 cells experiment matrix with material properties and levels of traffic volume in terms of 18-kip ESAL's.

Table 5.2: Layer thicknesses and moduli of the pavement sections of Figure 5.22.

Cell Number	Structural Number (a)	Total Thickness (inches) (b)	Layer Thicknesses (inches)			Layer moduli(ksi)		
			AC (c)	Base (d)	Subbase (e)	AC (f)	Base (g)	Subbase (h)
6	6.07	32.68	19.55	13.13	0.00	150	20	10
15	6.07	31.24	19.55	5.22	6.47	150	20	15
24	6.07	27.99	19.55	0.00	8.44	150	20	20
33	6.07	29.93	17.07	12.86	0.00	150	30	10
42	6.07	31.32	17.07	7.78	6.47	150	30	15
51	6.07	29.93	17.07	4.42	8.44	150	30	20
60	6.07	28.43	15.44	12.99	0.00	150	40	10
69	6.07	30.72	15.44	8.81	6.47	150	40	15
78	6.07	29.92	15.44	6.04	8.44	150	40	20
87	6.07	26.34	13.21	13.13	0.00	300	20	10
96	6.07	24.90	13.21	5.22	6.47	300	20	15
105	6.07	21.65	13.21	0.00	8.44	300	20	20
114	6.07	24.40	11.54	12.86	0.00	300	30	10
123	6.07	25.79	11.54	7.78	6.47	300	30	15
132	6.07	24.40	11.54	4.42	8.44	300	30	20
141	6.07	23.42	10.43	12.99	0.00	300	40	10

Table 5.2: (cont'd)

Cell Number	(a)	(b)	(c)	(d)	(e)	(f)	(g)	(h)
150	6.07	25.71	10.43	8.81	6.47	300	40	15
159	6.07	24.91	10.43	6.04	8.44	300	40	20
168	6.07	24.24	11.11	13.13	0.00	450	20	10
177	6.07	22.80	11.11	5.22	6.47	450	20	15
186	6.07	19.55	11.11	0.00	8.44	450	20	20
195	6.07	22.56	9.70	12.86	0.00	450	30	10
204	6.07	23.95	9.70	7.78	6.47	450	30	15
213	6.07	22.56	9.70	4.42	8.44	450	30	20
222	6.07	21.76	8.77	12.99	0.00	450	40	10
231	6.07	24.05	8.77	8.81	6.47	450	40	15
240	6.07	23.25	8.77	6.04	8.44	450	40	20

Table 5.3: The mechanistic responses for 27 pavement sections of Figure 5.22.

Cell Number	Deflection at top of(Mills)			Vert compressive stress at top of(psi)		Vert strain at top of(Microstrain)			Tensile stress at bottom of AC layer (psi)
	AC (a)	Base (b)	Roadbed (c)	Base (d)	Roadbed (e)	AC (f)	Base (g)	Roadbed (h)	(j)
6	13.50	9.88	8.07	3.64	1.41	89.00	125	107	85.40
15	13.70	10.10	8.28	3 40	1.49	86.60	128	129	88.00
24	13.70	NA/13.7	8.80	NA/3.39	1.73	86.30	128	133	88.10
33	13.90	10.50	8.65	5.67	1.67	80.60	144	112	94.60
42	14.20	10.80	8.48	5.33	1.58	76.80	147	140	97.80
51	14.20	10.80	8.74	5.19	1.69	75.70	149	132	99.50
60	14.00	10.90	9.09	9.15	2.01	76.60	143	109	86.20
69	14.40	11.10	8.64	7.40	1.65	71.70	159	148	102
78	14.50	11.20	8.84	7.16	1.74	69.60	161	138	104
87	12.80	11.40	9.07	5.03	1.80	12.20	149	134	106
96	13.10	11.60	9.35	4.71	1 91	15.30	152	164	108
105	13.10	NA/11.7	10.00	NA/4.70	2.24	15.50	152	167	109
114	13.30	12.00	9.70	7.89	2.12	25.20	169	140	118
123	13.70	12.40	9.50	7.43	1.99	29.60	173	174	121
132	13.80	12.50	9.83	7.21	2.14	31.00	175	165	123
141	13.50	12.30	9.97	10.90	2.28	32.60	181	140	123

Table 5.3: (cont'd)

Cell Number	(a)	(b)	(c)	(d)	(e)	(f)	(g)	(h)	(k)
150	14.00	12.80	9.63	10.40	2.07	38.30	185	183	127
159	14.10	12.90	9.88	10.00	2.18	40.60	188	171	129
168	12.60	11.80	9.38	5.33	1.91	42.80	145	141	104
177	12.90	12.10	9.67	4.99	2.03	45.70	148	170	107
186	12.90	NA/12.1	10.40	4.99	2.39	46.00	148	174	107
195	13.20	12.40	10.00	8.37	2.26	57.50	164	147	117
204	13.60	12.80	9.84	7.88	2.12	61.70	168	184	120
213	13.70	12.90	10.20	7.65	2.29	63.00	170	174	121
222	13.40	12.70	10.30	11.60	2.43	66.10	175	148	122
231	13.90	13.20	9.95	11.00	2.20	71.60	180	194	126
240	14.10	13.40	10.20	10.60	2.32	73.90	182	180	128

Examination of the mechanistic responses of the 27 pavement sections of Figure 5.22 indicates that:-

1. The peak surface deflections listed in Table 5.4 and shown in Figure 5.23 are almost constant for all sections, (the peak pavement surface deflection varies in the range of 1 mill which is negligible). Assuming that the peak surface deflection can be used as a measure of the level of damage delivered to a pavement section (higher deflection causes higher compression and higher rut/or fatigue cracking potential), the following conclusion was made.

   For a constant traffic level and one type of roadbed soil, the AASHTO design procedure produces pavement sections (layer thicknesses) such that the peak pavement surface deflection is constant. Hence the amount of overall damage delivered to the pavement section (or the overall protection level) is constant and independent of the material properties.

2. Based on the amount of vertical compressive stress at the top of the pavement layers and vertical strains at the top of the pavement layers as given in Table 5.5 and shown in Figure 5.24 and 5.25 respectively, the following conclusion from the SHRP study is also verified to the range of conditions found in Pakistan:

Table 5.4: The pavement surface deflections for 27 pavement sections of Figure 5.22.

Cell Number	Deflections at top of layer (Mills)		
	AC (Peak pavement deflection)	Base	Roadbed
6	13.50	9.88	8.07
15	13.70	10.10	8.28
24	13.70	NA/13.70	8.80
33	13.90	10.50	8.65
42	14.20	10.80	8.48
51	14.20	10.80	8.74
60	14.00	10.90	9.09
69	14.40	11.10	8.64
78	14.50	11.20	8.84
87	12.80	11.40	9.07
96	13.10	11.60	9.35
105	13.10	NA/11.70	10.00
114	13.30	12.00	9.70
123	13.70	12.40	9.50
132	13.80	12.50	9.83
141	13.50	12.30	9.97
150	14.00	12.80	9.63
159	14.10	12.90	9.88
168	12.60	12.80	9.38
177	12.90	12.10	9.67
186	12.90	NA/12.10	10.40
195	13.20	12.40	10.00
204	13.60	12.80	9.84
213	13.70	12.90	10.20
222	13.40	12.70	10.30
231	13.90	13.20	9.95
240	14.10	13.40	10.20

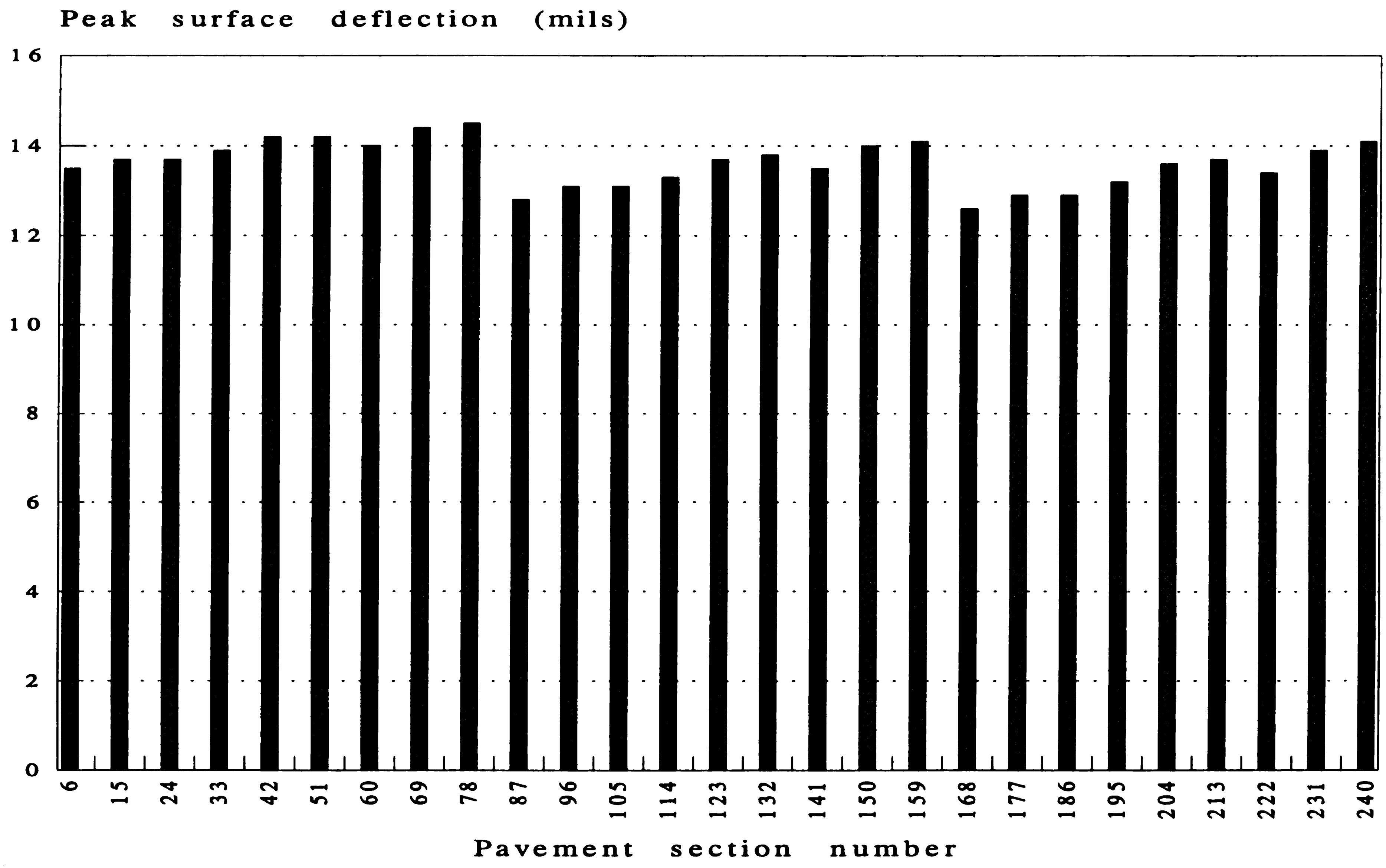

Figure 5.23: The peak pavement surface deflections of indicated pavement sections.

Table 5.5: The vertical compressive stress and vertical strains at the top of layer for 27 sections of Figure 5.22.

Cell Number	Vert compressive Stress (psi)		Vert strains (Microstrains)		
	Base	Roadbed	AC	Base	Roadbed
6	3.64	1.41	89.00	125	107
15	3.40	1.49	86.60	128	129
24	NA/3.39	1.73	86.30	128	133
33	5.67	1.67	80.60	144	112
42	5.33	1.58	76.80	147	140
51	5.19	1.69	75.70	149	132
60	9.15	2.01	76.60	143	109
69	7.40	1.65	71.70	159	148
78	7.16	1.74	69.60	161	138
87	5.09	1.80	12.20	149	134
96	4.71	1.91	15.30	152	162
105	NA/4.70	2.24	15.50	152	167
114	7.89	2.12	55.20	169	140
123	7.43	1.99	29.60	173	174
132	7.21	2.14	31.00	175	165
141	10.90	2.28	32.60	181	140
150	10.40	2.07	38.30	182	183
159	10.00	2.18	40.60	188	171
168	5.33	1.91	42.80	145	141
177	4.99	2.03	45.70	148	170
186	4.99	2.39	46.00	148	174
195	8.37	2.26	57.50	164	147
204	7.88	2.12	61.70	168	184
213	7.65	2.29	63.00	170	174
222	11.60	2.43	66.10	175	148
231	11.00	2.20	71.60	180	194
240	10.60	2.32	73.90	182	180

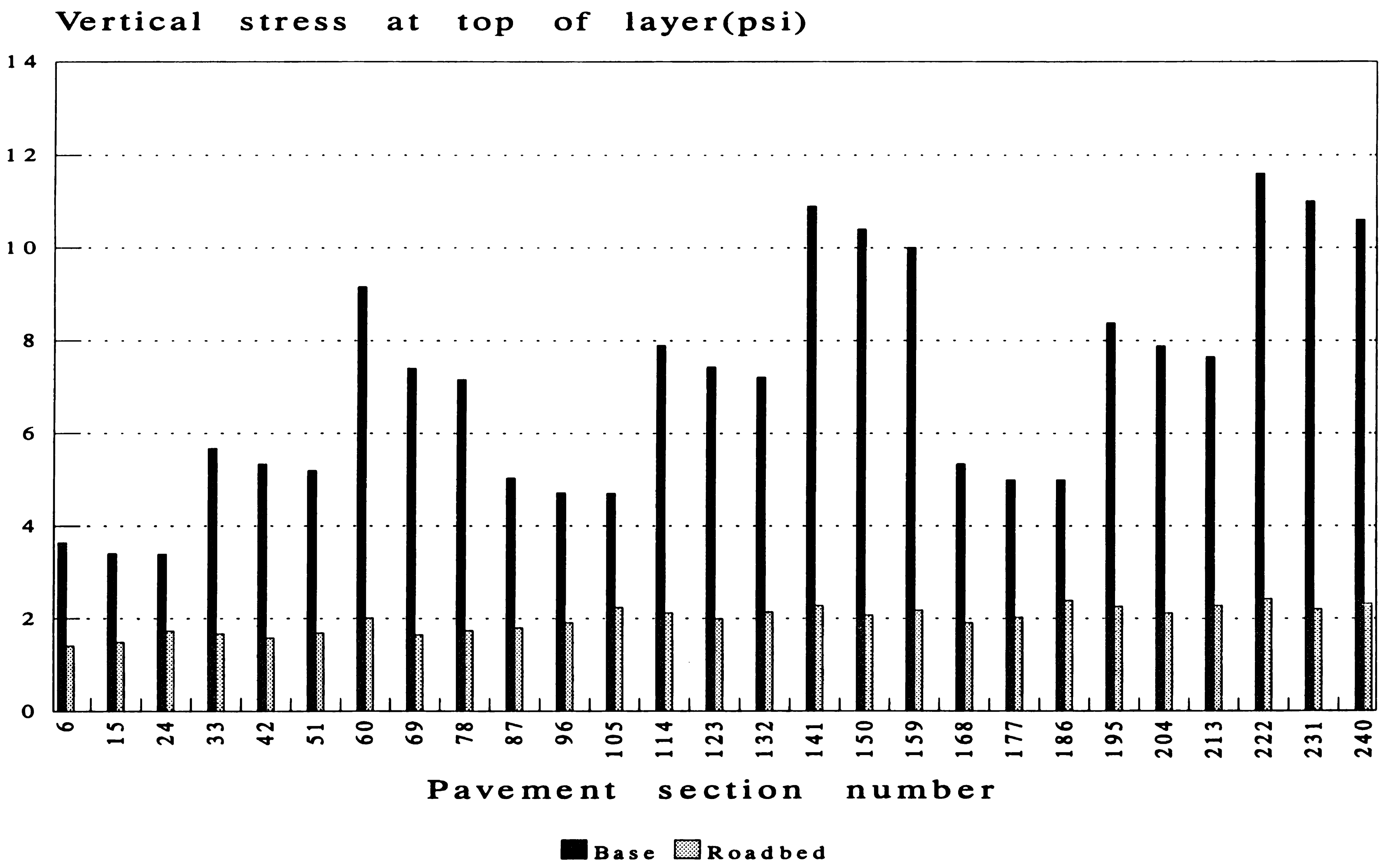

Figure 5.24: The vertical compressive stress at top of layer for indicated pavement sections.

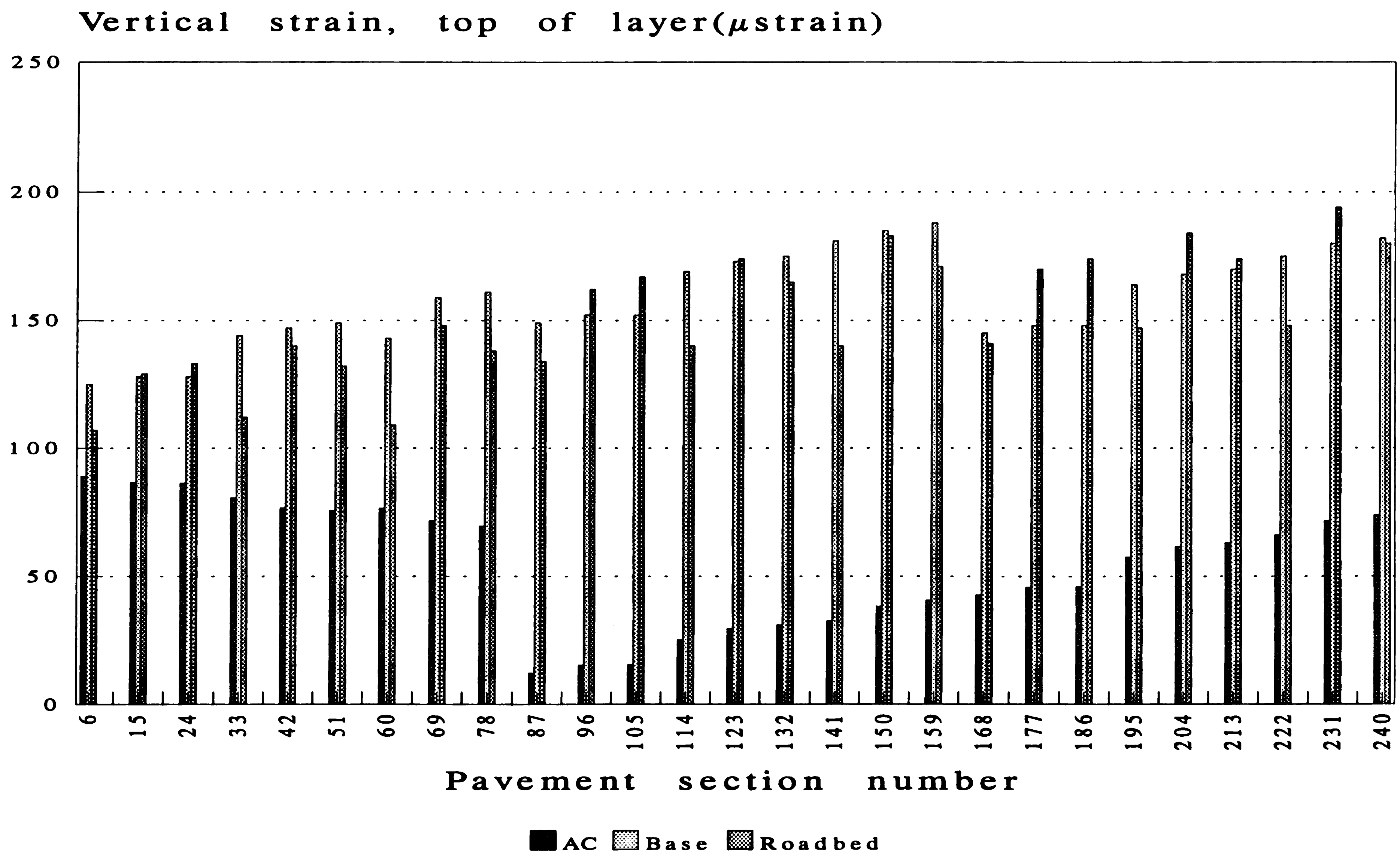

Figure 5.25: The vertical strains at top of pavement layers for indicated pavement sections.

The induced stresses and strains experienced by any one pavement layer vary from one pavement section to another. This implies that the AASHTO design method produces inconsistent results relative to these mechanistic responses. Hence the results of mechanistic analysis do not support the AASHTO concept that the Structural Number (SN) of any one flexible pavement layer is the product of its thickness and its layer coefficient.

3. Based on the magnitude of the tensile stress induced at the bottom of the AC layer of the 27 pavement sections of Figure 5.22 due to an 18-kip ESAL and the ratio of that tensile stress to the value of the AC modulus as given in Table 5.6 and shown in Figures 5.26 and 5.27, the following finding from the SHRP study is verified relative to the conditions in Pakistan.

For a constant traffic level and one type of roadbed soil, the AASHTO design procedure produces pavement sections (layer thicknesses) such that the tensile stress induced at the bottom of the AC layer vary from one section to another. This implies that the AASHTO design procedure produces inconsistent pavement sections relative to fatigue damage. Once again, the results of the mechanistic analysis do not support the AASHTO concept that the structural number of any flexible pavement layer is the product of its thickness and its

Table 5.6: The tensile stress at the bottom of the AC layer and the ratio of the tensile stress to the AC modulus for 27 pavement sections of Figure 5.22.

Cell Number	Tensile stress at bottom of the AC layer (psi)	Ratio of the tensile stress to AC modulus
6	85.40	0.569
15	88.00	0.587
24	88.10	0.587
33	94.60	0.631
42	97.80	0.652
51	99.50	0.663
60	86.20	0.57
69	102	0.680
78	104	0.693
87	106	0.353
96	108	0.360
105	109	0.363
114	118	0.393
123	121	0.403
132	123	0.410
141	123	0.410
150	127	0.423
159	129	0.430
168	104	0.231
177	107	0.238
186	107	0.238
195	117	0.260
204	120	0.267
213	121	0.269
222	122	0.271
231	126	0.280
240	128	0.284

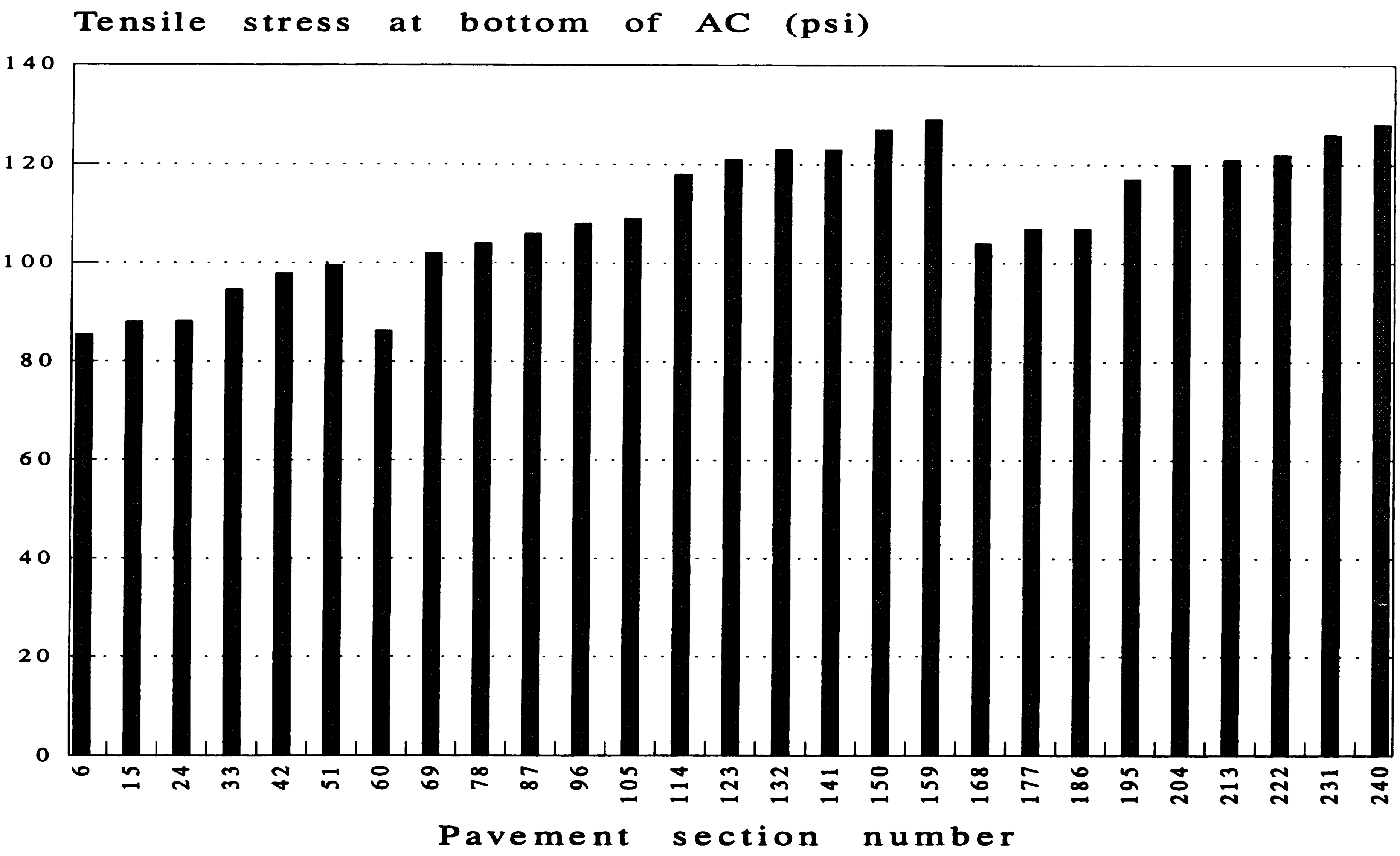

Figure 5.26: The radial tensile stress at the bottom of AC layer for indicated pavement sections.

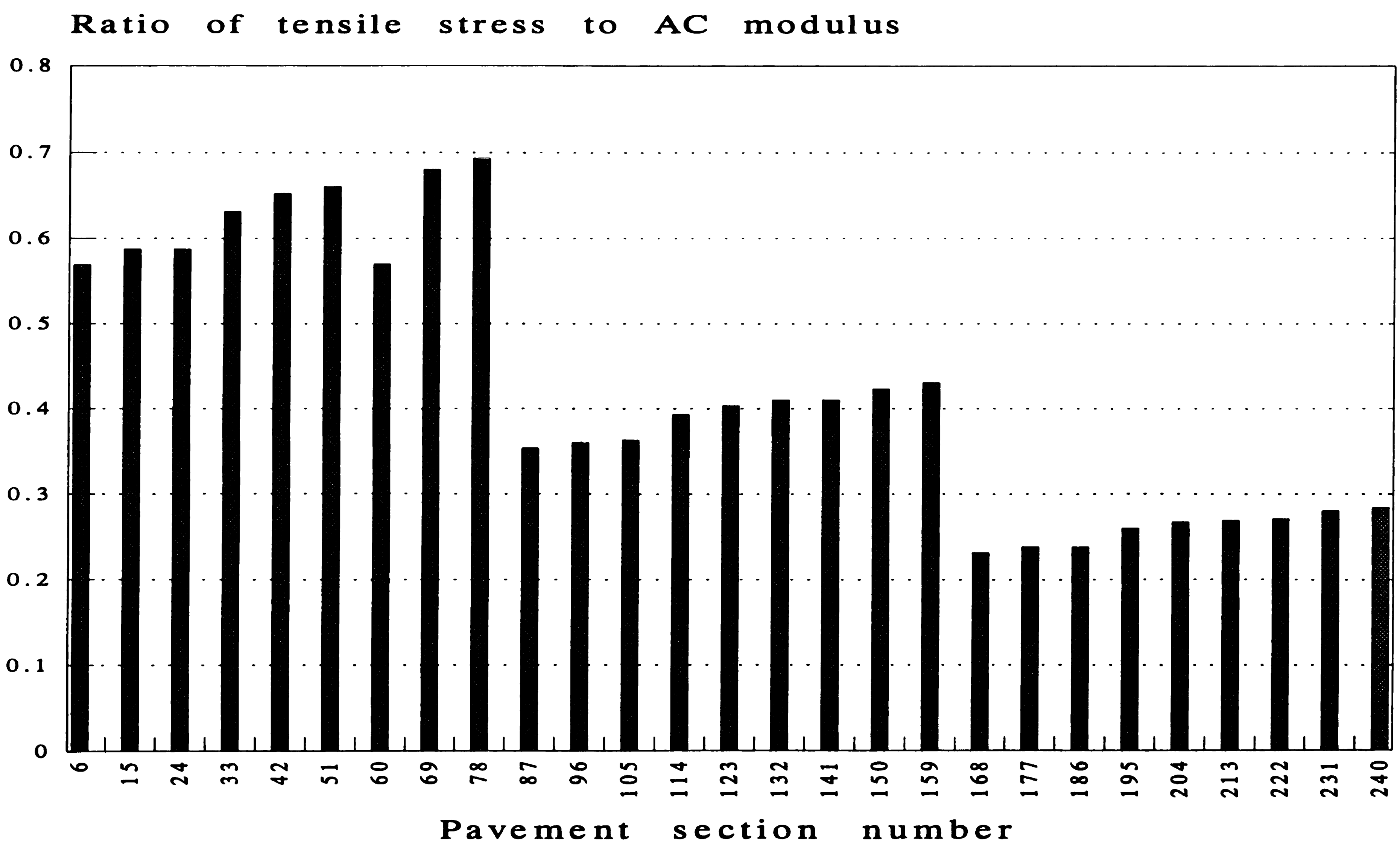

Figure 5.27: The ratio of the tensile stress to the value of AC modulus for indicated sections.

layer coefficient.

4. Sections 156, 159 and 162 (see Figure 3.1) were designed using AASHTO design procedure. The material properties of the AC, base and subbase layers for all three sections are the same. All sections were designed to carry 75,000,000 18-kip ESAL's. The only difference between the three sections is the resilient modulus of the roadbed soil. It varies from 7.5 ksi to 10 ksi and 20 ksi for sections 156, 159 and 162 respectively. The outputs (layer thicknesses) obtained from the AASHTO design procedure are listed in Table 5.7. The mechanistic responses are summarized in Table 5.8. Examination of the mechanistic responses for sections 156, 159 and 162 indicate that:

The peak pavement surface deflection varies from 16.0 mills for pavement section 156 to 11.8 mills for pavement section 162. Figure 5.28 shows the peak deflection at the top of each pavement layer. It can be seen that the peak pavement deflection at top of each layer varies from one section to another which indicates that the amount of the overall damage received by one pavement section is different than that received by the other section.

It is to be noted that for the same traffic level and pavement layer properties, the AASHTO produced structural numbers for various types of roadbed soils do

Table 5.7: The AASHTO outputs of the pavement sections of cells 156,159,and 162 of Figure 3.1 (performance period =10 years, 18-kip ESAL = 75,000,000).

Cell Number	Structural Number	Total Thickness (inches)	Layer Thicknesses (inches)			Layer Moduli (ksi)			
			AC	Base	Subbase	AC	Base	Subbase	Roadbed
156	6.61	28.79	10.43	6.04	12.32	300	40	20	7.5
159	6.07	24.91	10.43	6.04	8.44	300	40	20	10
162	5.36	19.83	10.43	6.04	3.36	300	40	20	15

Table 5.8: Mechanistic responses of the pavement sections of cells 156, 159 and 162 from Figure 3.1.

Cell Number	Deflection at top of (Mills)			Vertical compressive stress at top of (psi)		Vertical strain at top of (microstrains)			Tensile stress at the bottom of the AC layer(psi)
	AC	Base	Roadbed	Base	Roadbed	AC	Base	Roadbed	
156	16.00	14.80	11.30	10.00	1.56	42.20	188	146	57.8
159	14.10	12.90	9.88	10.00	2.18	40.60	188	171	57.9
162	11.80	10.60	8.38	10.10	3.56	35.7	186	221	57.1

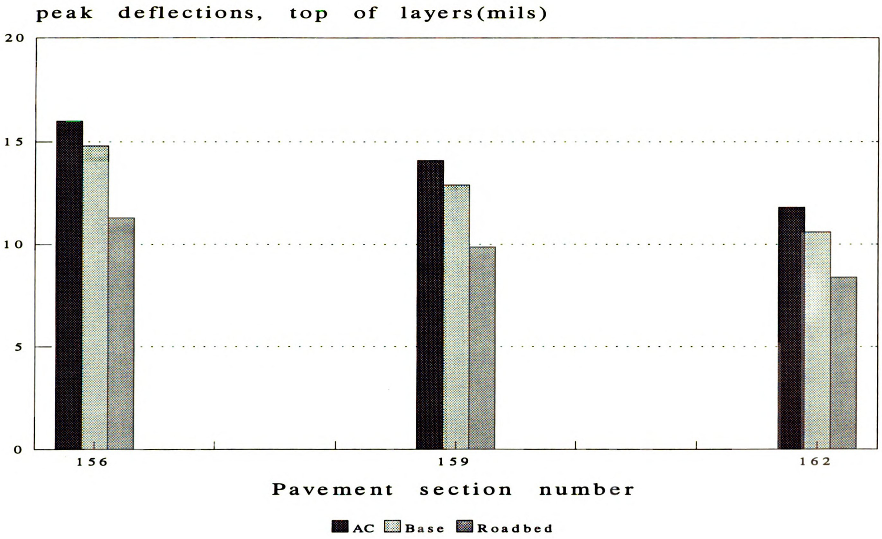

Figure 5.28: Peak surface deflection at top of layer for indicated pavement sections.

not provide the same level of protection to that soil. Since for these three pavement sections, the only factor affecting the calculation of the required structural number is the resilient modulus of the roadbed soil, then the following finding of the SHRP study is verified to the conditions in Pakistan:-

The AASHTO main design equation for flexible pavements does not properly account for the effects of the resilient modulus of the roadbed soil on the structural capacity of the pavement.

5.2.4. Mechanistic Evaluation of the AASHTO Drainage Coefficients

To verify the results of the SHRP study relative to drainage coefficients at higher levels of traffic, mechanistic evaluation of the AASHTO drainage coefficients was conducted by using the data of pavement section 240 from Figure 3.1. Five values of the drainage coefficients were used (0.5, 0.7, 1.0, 1.3, and 1.5). For each design, the same value of the drainage coefficient was used for both base and subbase materials. Two evaluation methods were used: The layer thickness modification method, and the layer coefficient modification method. In the layer thickness modification method, the layer coefficients of the base and subbase materials are not modified but the thickness of the appropriate layer is either reduced or increased depending on the value of the drainage coefficient. In the layer coefficient modification method, the values of the layer coefficient of the base and subbase are modified by multiplying the actual layer coefficient by the drainage coefficient. The modified layer coefficient values are then used to estimate the modified layer moduli (using the appropriate AASHTO layer coefficient equation) which was then used as an input to the AASHTO design method. For further details on these two methods the reader is referred to reference (11). The results of both methods are presented in the subsequent subsections.

5.2.4.1 Layer Thickness Modification Method

Pavement section number 240 was designed using the 1986 AASHTO design procedure (DNPS 86 Computer program). The pavement section was designed once for each of the following values of the drainage coefficients (0.5, 0.7, 1.0, 1.3, and 1.5). The outputs (layer thicknesses, and structural numbers) are listed in Table 5.9. Mechanistic analysis of the AASHTO designed sections was then conducted by using the ELSYM5 computer program. The mechanistic responses are also listed in Table 5.9 and shown in Figures 5.29 through 5.32 as a function of the drainage coefficient. It should be noted that the five pavement sections are supported on the same roadbed soil (M_R = 10 ksi), were designed to carry the same traffic volume (75,000,000, 18-kip ESALs) and to have the same serviceability

Table 5.9: Layer thicknesses, moduli, and mechanistic responses for five values of drainage coefficients for section 159 (thickness modification method).

Results of Analysis	Drainage coefficient (pavement section 159 of Figure 5.1)				
	0.50	0.70	1.00	1.30	1.50
Layer Thicknesses (inches)					
AC	8.77	8.77	8.77	8.77	8.77
Base	12.08	8.63	6.04	4.65	4.03
Subbase	16.88	12.06	8.44	6.49	5.63
Structural Number	6.07	6.07	6.07	6.07	6.07
Layer Moduli (ksi)					
AC	450	450	450	450	450
Base	18.41	25.21	40.00	64.75	88.67
Subbase	10.10	13.42	20.00	31.46	41.79
Roadbed	10.00	10.00	10.00	10.00	10.00
Deflection at top of layer (mills)					
AC	15.40	14.70	14.10	13.50	13.30
Base	14.70	14.00	13.40	12.90	12.60
Subbase	11.40	11.70	12.00	12.00	11.90
Roadbed	8.03	9.17	10.20	10.70	10.90
Vertical stress at top of layer (psi)					
Base	7.79	8.91	10.60	12.50	13.80
Subbase	2.81	3.63	4.61	5.49	5.99
Roadbed	1.36	1.81	2.32	2.63	2.75
Tensile Stress at the bottom of AC (psi)	108	100	89.10	76.60	68.20
Vertical strain at top of layer (microstrain)					
AC	92.70	84.20	73.90	63.40	57.10
Base	209	198	182	164	152
Subbase	207	209	198	176	162
Roadbed	143	171	180	177	172

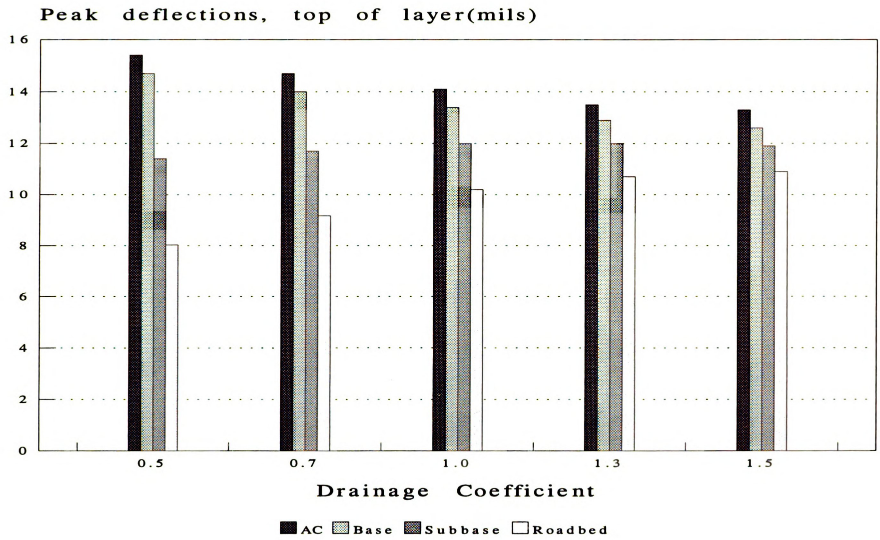

Figure 5.29: The peak deflections at top of layer versus drainage coefficients of base and subbase.

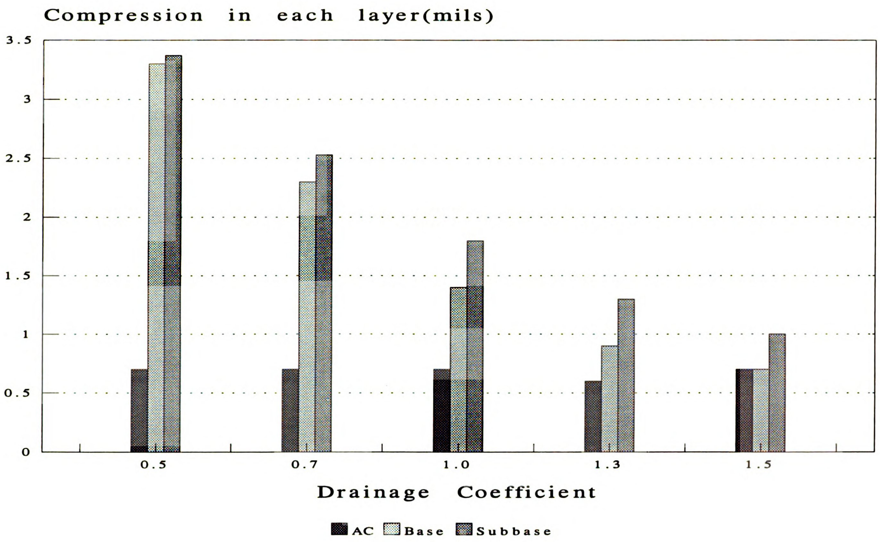

Figure 5.30: The amount of compression in each layer versus drainage coefficient of base and subbase

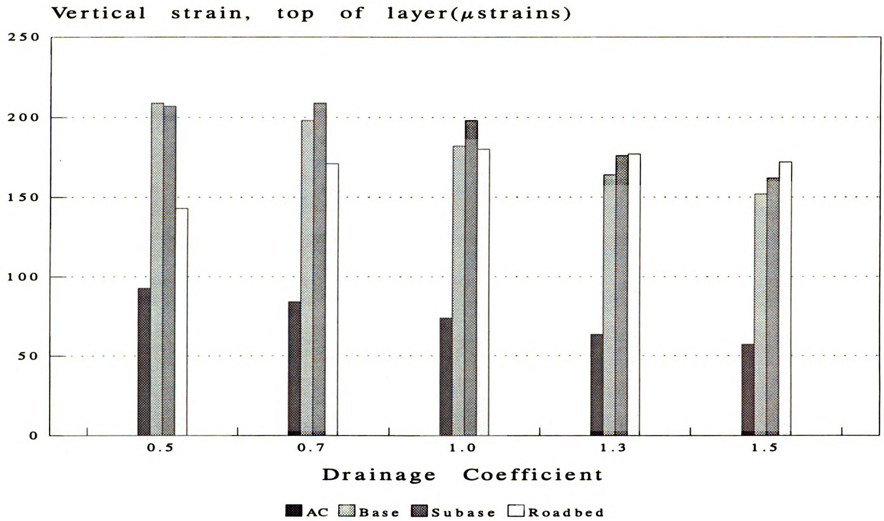

Figure 5.31: The vertical strain at top of layers versus drainage coefficient of base and subbase.

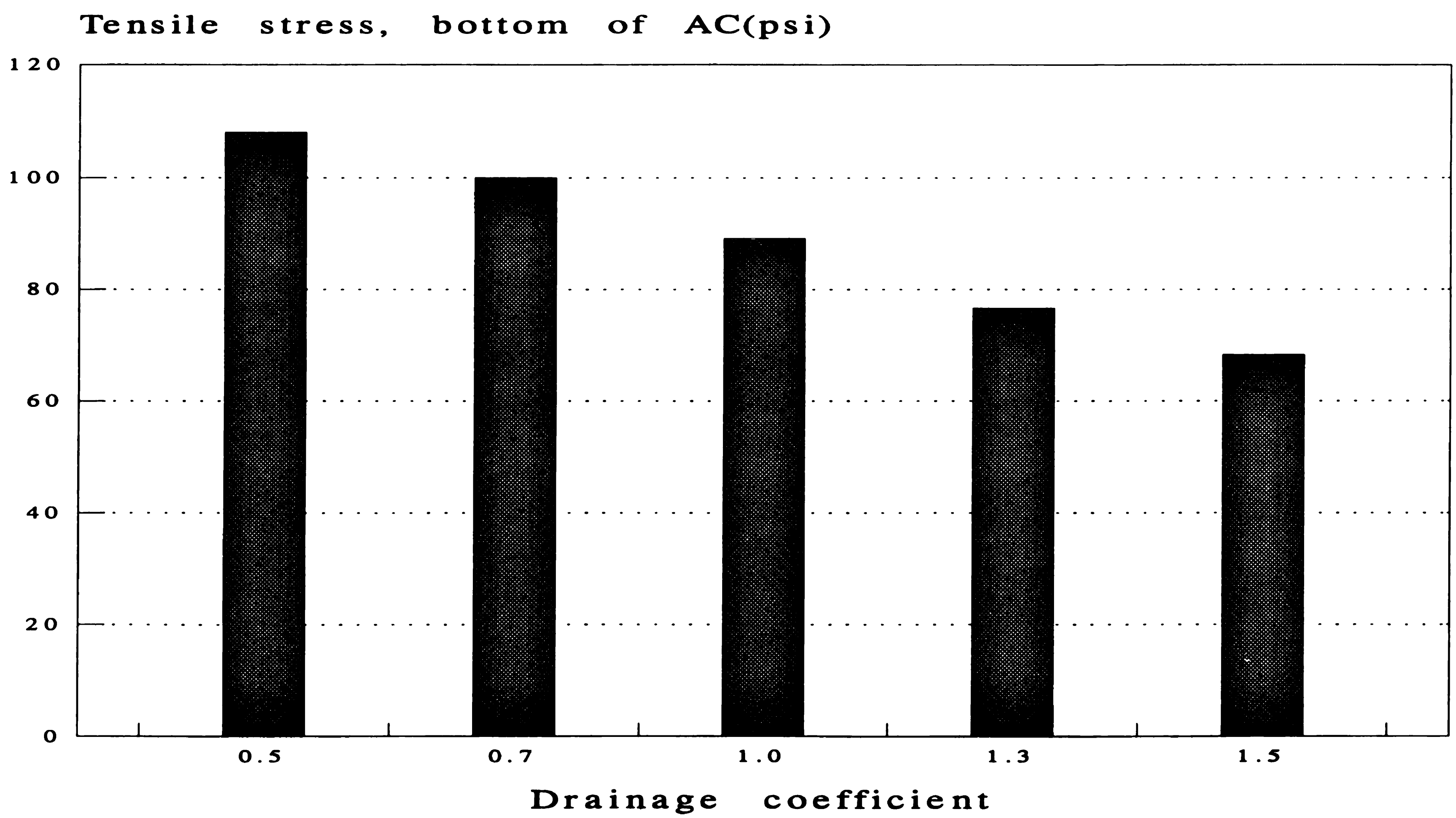

Figure 5.32: The radial tensile stress at bottom of the AC layer versus drainage coefficient of base and subbase

loss (1.9) during a performance period of 10 years. Examination of the mechanistic responses indicate that:

1. The peak deflection at the top of each pavement layer is a function of the drainage quality as shown in Figure 5.29. For example, the peak pavement deflection (deflection at the top of the AC) increases as the quality of the drainage material deteriorates.

2. The amount of compression experienced by each pavement layer is a function of the drainage quality (Figure 5.30). Hence the damage delivered to each layer is affected by the quality of the drainage.

3. The vertical strains (Figure 5.31) at the top of the base and subbase layers increase as the quality of drainage deteriorate. This shows that a higher level of damage is delivered to the layers with poor drainage quality.

4. The tensile stress induced at the bottom of the AC layer (Figure 5.32) due to an 18-kip ESAL increases from 68.2 psi to 108 psi, (an increase of about 60%) as the drainage coefficient decreases from 1.5 to 0.5. This shows that the pavement sections constructed with poorly drainable material will have shorter fatigue life as compared to the sections constructed with good drainable material. The SHRP study (11) showed an increase of about

70% in the radial tensile stress as the drainage coefficient decreased from 1.4 to 0.6.

5.2.4.2 Layer coefficient Modification Method

In this method, the layer coefficients of the base and subbase were modified by multiplying them by the value of the drainage coefficients ($a_i * m_i$). The modified layer coefficients were then used to estimate the modified layer moduli. Pavement section 204 was then redesigned using the AASHTO design procedure (DNPS86 computer program) and the five modified values of the layer coefficient and moduli. The outputs (layer thicknesses, and structural numbers) of DNPS 86 computer program are listed in Table 5.10. The mechanistic analysis of the AASHTO designed sections was then conducted by using ELSYM5 computer program. The mechanistic responses are also listed in Table 5.10 and shown in Figures 5.33 through 5.36 as a function of the drainage coefficient. As before, the five pavement sections are supported on the same roadbed (M_R = 10 ksi), and were designed to carry the same traffic volume (75,000,000, 18-kip ESALs) and to have the same serviceability loss (1.9) during performance period of 10 years. Examination of the mechanistic responses indicate that:-

1. The peak deflections at the top of each pavement layer as function of the drainage coefficient (Figure 5.33) vary with the variation in the drainage quality. It is to be noted that the peak pavement deflection (the deflection

Table 5.10: Layer thicknesses, moduli, and mechanistic responsses for five values of the drainage coefficient of section 159 (Layer coefficient modification method)

Results of Analysis	Drainage coefficient (pavement section 159 of Figure 5.1)				
	0.50	0.70	1.00	1.30	1.50
Layer Thicknesses (inches)					
AC	11.41	10.29	8.77	7.37	6.56
Base	25.78	12.14	6.04	3.34	2.43
Subbase	0.53	7.46	8.44	7.99	7.20
Structural Number	6.06	6.06	6.06	6.06	6.06
Layer Moduli(ksi)					
AC	450	450	450	450	450
Base	18.41	25.21	40.00	64.75	88.67
Subbase	10.10	13.42	20.00	31.46	41.80
Roadbed	10.00	10.00	10.00	10.00	10.00
Deflection at top of layer (mils)					
AC	11.90	12.80	14.10	15.30	16.20
Base	11.10	12.00	13.40	14.80	15.70
Subbase	7.43	9.78	12.00	13.90	15.10
Roadbed	7.37	8.57	10.20	11.90	13.20
Vertical stress at top of layer (psi)					
Base	5.21	6.99	10.60	15.90	20.20
Subbase	1.15	2.30	4.61	8.61	12.10
Roadbed	1.13	1.57	2.32	3.25	3.99
Tensile Stress at the bottom of AC (psi)	70.40	78.50	89.10	95.60	95.80
Vertical strain at top of layer (microstrain)					
AC	20.60	50.20	73.90	100	118
Base	137	155	182	205	215
Subbase	87.60	140	198	245	266
Roadbed	118	143	180	217	246

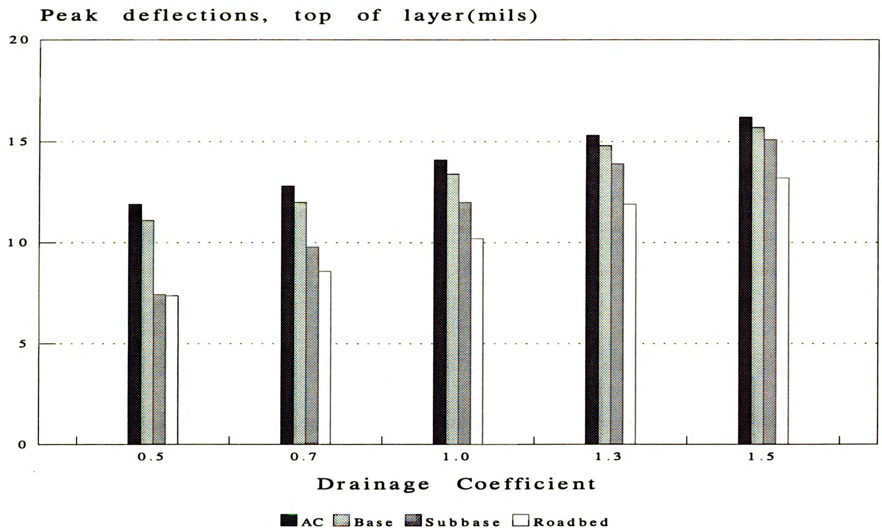

Figure 5.33: The peak deflections at top of layers versus drainage coefficients of base and subbase.

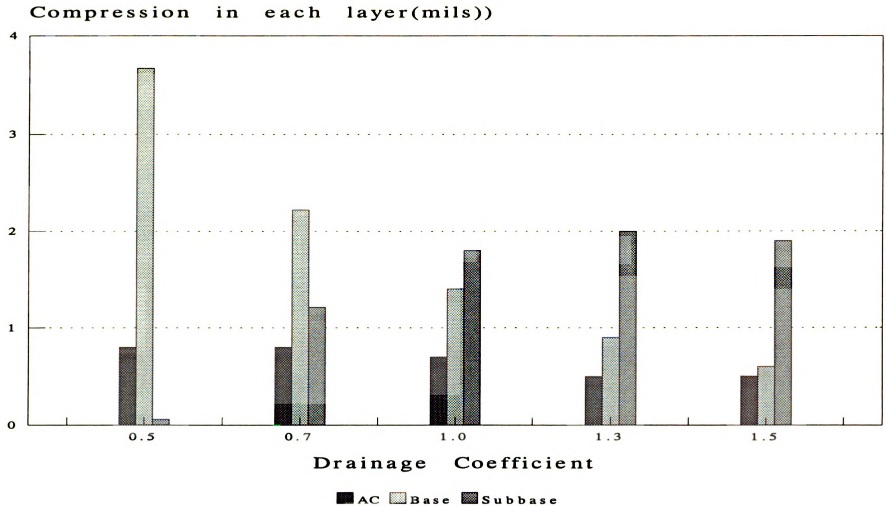

Figure 5.34: The amount of compression in each layer versus drainage coefficients of base and subase.

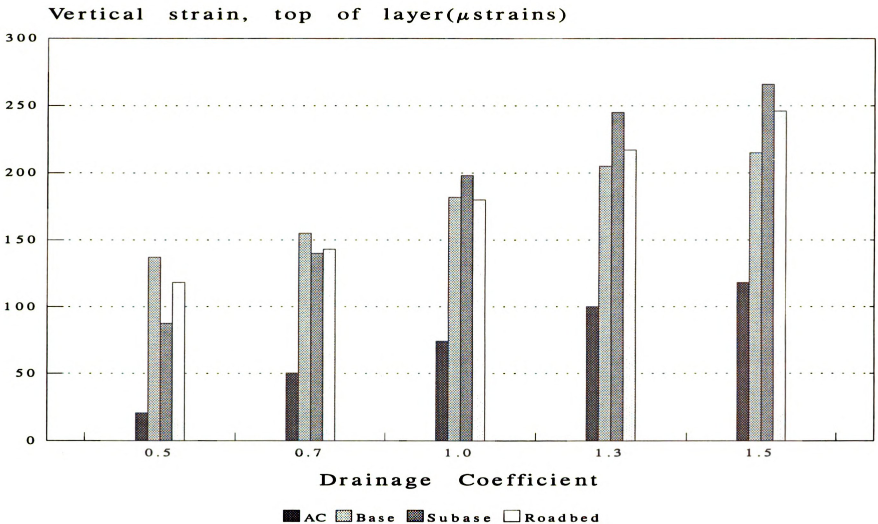

Figure 5.35: The vertical strain at top of layers versus drainage coefficients of base and subbase.

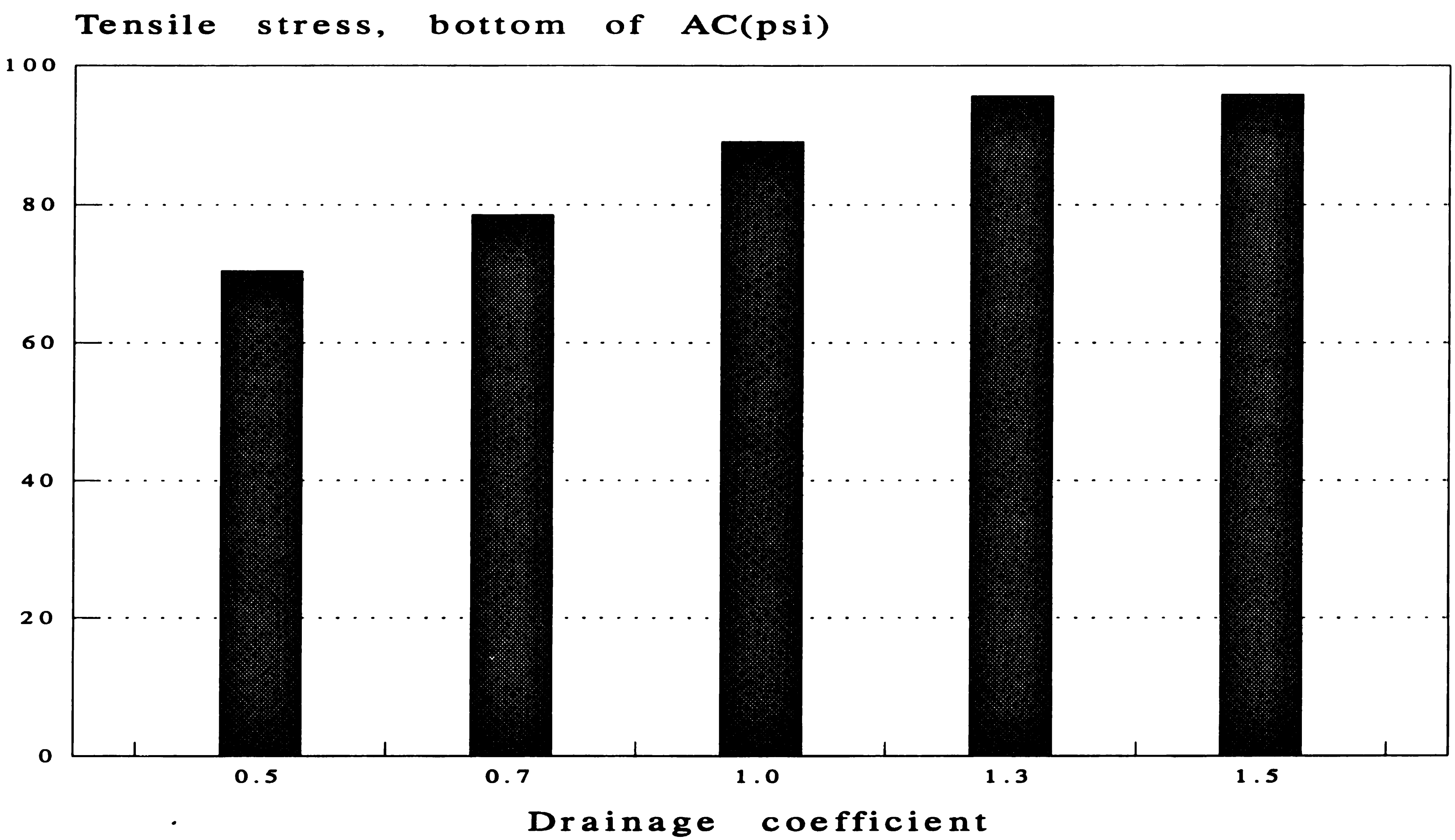

Figure 5.36: The radial tensile stress at the bottom of the AC layer versus drainage coefficients of base and subase.

at the top of the AC layer) decreases with the quality of the drainage which is opposite to the finding of the layer thickness modification method (see page 162 and Figure 5.29).

2. The amount of compression experienced by each pavement layer is a function of the drainage quality (Figure 5.34) is different. Higher drainage coefficient causes lower degree of compression in the AC and base layers and higher compression in the subbase layer.

3. It can be seen that the vertical strains (Figure 5.35) at top of the base and subbase layers decrease as the quality of drainage deteriorate. This shows that the higher level of damage is being delivered to the layers with poor drainage quality. This observation is opposite to what was observed in the layer thickness modification method (see page 162).

4. The tensile stress induced at the bottom of the AC layer (Figure 5.36) due to an 18-kip ESAL is depicted by Figure 5.36.It can be seen that the maximum variation in the magnitude of the tensile stress from one section to another is about 27 percent. For the thickness modification method this variation was about 60 percent (see Figure 5.32). This shows that the layer coefficient modification method tends to produce better thickness

design than the thickness modification method.

The results of the mechanistic responses from both methods i.e. the layer thickness modification method and the layer coefficient modification method verify the following finding of SHRP (11) study:

For pavement sections with the same layer properties but different drainage coefficients that have been designed by using AASHTO procedure to be supported on the same roadbed soil, to carry the same traffic volume and to have the same serviceability loss during an equal performance period, the results of the mechanistic analysis indicate that the magnitudes of the deflections, stresses and strains induced in the various pavement layers vary from one pavement section to another. That is the AASHTO design method does not produce consistent results of the mechanistic responses. Hence the results of the mechanistic analysis do not support the role of the drainage coefficient (in adjusting the layer thicknesses and layer coefficients) in the AASHTO design procedure.

CHAPTER 6

STUDY RESULTS - PREDICTED FATIGUE AND RUT PERFORMANCE OF THE AASHTO DESIGNED PAVEMENT SECTIONS

6.1 OUTPUTS FROM THE AASHTO DESIGN PROCEDURE

Table 6.1 summarizes the outputs from the AASHTO design procedure for the selected pavement sections explained in section 3.2.2 and Figure 3.2 of chapter 3 (page 51) .

6.2 MECHANISTIC RESPONSES FROM ELSYM5

The mechanistic responses (radial tensile strain at the bottom of the AC layer and the vertical compressive strain at the top of the roadbed soil) are listed in Table 6.2. Figure 6.1 presents the variation in radial tensile strain at the bottom of the AC layer due to variation in axle load and Figure 6.2 depicts the variation in the radial tensile strain at the bottom of the AC layer due to variation in the stiffness of the roadbed soil and the design 18-kip ESAL for the pavement sections of Figure 3.2. Examination of the mechanistic responses indicates that:

1. The radial tensile strain at the bottom of the AC layer increases with the increase in axle load (see Figure 6.1). It can be seen from the figure that, in general, the rate of increase in tensile strain decreases as the axle load increases. This however should not be interpreted as the rate of damage (e.g. fatigue life)

Table 6.1: Outputs from AASHTO DNPS86 computer program for the pavement sections of Figure 3.2.

Cell No.	18-Kip ESALS	Roadbed Modulus (ksi)	AASHTO Designed Thicknesses (inches)			
			AC	Base	Subbase	Total
199	25	7.5	8.21	7.03	10.35	25.59
202	25	10	8.21	7.03	5.88	21.12
205a	25	15	8.21	7.03	0.00	15.24
205	25	20	8.21	7.03	0.00	15.24
200	50	7.5	9.13	7.50	11.00	27.63
203	50	10	9.13	7.50	6.25	22.88
206a	50	15	9.13	7.50	0.00	16.63
206	50	20	9.13	7.50	0.00	16.63
201	75	7.5	9.70	7.78	11.41	28.89
204	75	10	9.70	7.78	6.47	23.95
207a	75	15	9.70	7.78	0.00	17.48
207	75	20	9.70	7.78	0.00	17.48

Table 6.2: Mechanistic responses from ELSYM5 for pavement sections of Figure 3.2 for different axle loads and tire pressure.

AASHTO Design ESALS*10^6	Cell No.	Radial Tensile Strain (μ strain) at Bottom of AC Layer for Axle Load/ Tire pressure of			Vertical Compressive Strain (μ strain) at Top of Roadbed soil for Axle Load/Tire pressure of		
		18-kip/ 80 psi	23-kip/ 120 psi	28-kip/ 120 psi	18-kip/ 120 psi	23-kip/ 120 psi	28-kip/ 120 psi
25	199	152	204	234	202	257	314
25	202	152	203	233	246	314	382
25	205a	147	198	227	244	315	378
25	205	142	191	218	236	306	366
50	200	132	175	203	168	214	262
50	203	131	174	202	205	261	319
50	206a	127	170	196	204	263	317
50	206	123	164	189	198	256	307
75	201	120	160	186	152	193	236
75	204	120	159	285	184	235	287
75	207a	117	155	280	184	237	286
75	207	113	150	274	179	231	278

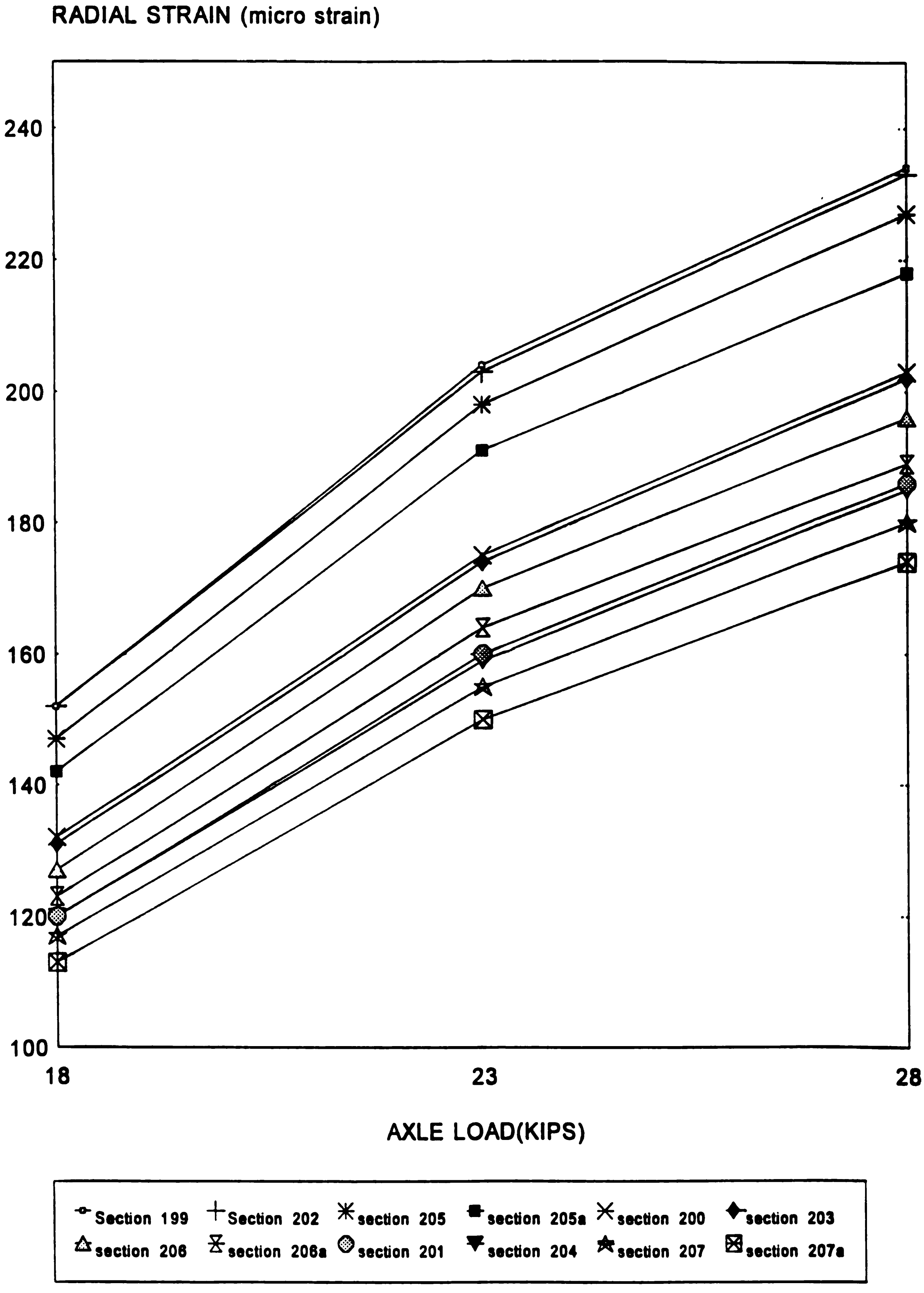

Figure 6.1: Effect of axle load on radial rensile strain at bottom of AC layer for the indicated pavement sections

decreases with increasing axle load. The reason is that the fatigue life in terms of tensile strain follows a power function. Hence a full analysis of the fatigue life must be conducted before a proper conclusion regarding the rate of damage can be made. Nevertheless, the above observation implies, as it was expected, that increasing axle load causes higher fatigue damage.

2. The radial tensile strain at the bottom of the AC layer decreases with the increase in the stiffness (modulus) of the roadbed soil (see Figure 6.2). This implies that stiffer roadbed soils cause a decrease in the tensile strain (though minimal) in the asphalt layer. This finding negates the AASHTO concept that a variation in the roadbed soil strength affects only the layer immediately above it.

4. The vertical compressive strain at the top of the roadbed soil increases almost linearly with increase in axle load (see Figure 6.3). The reason for this is that the ELSYM5 computer program uses the layer elastic theory which produces linear responses. If nonlinear material models are available, one can then use the nonlinear option of the MICHPAVE program to assess the nonlinear effects of the load on the compressive strain.

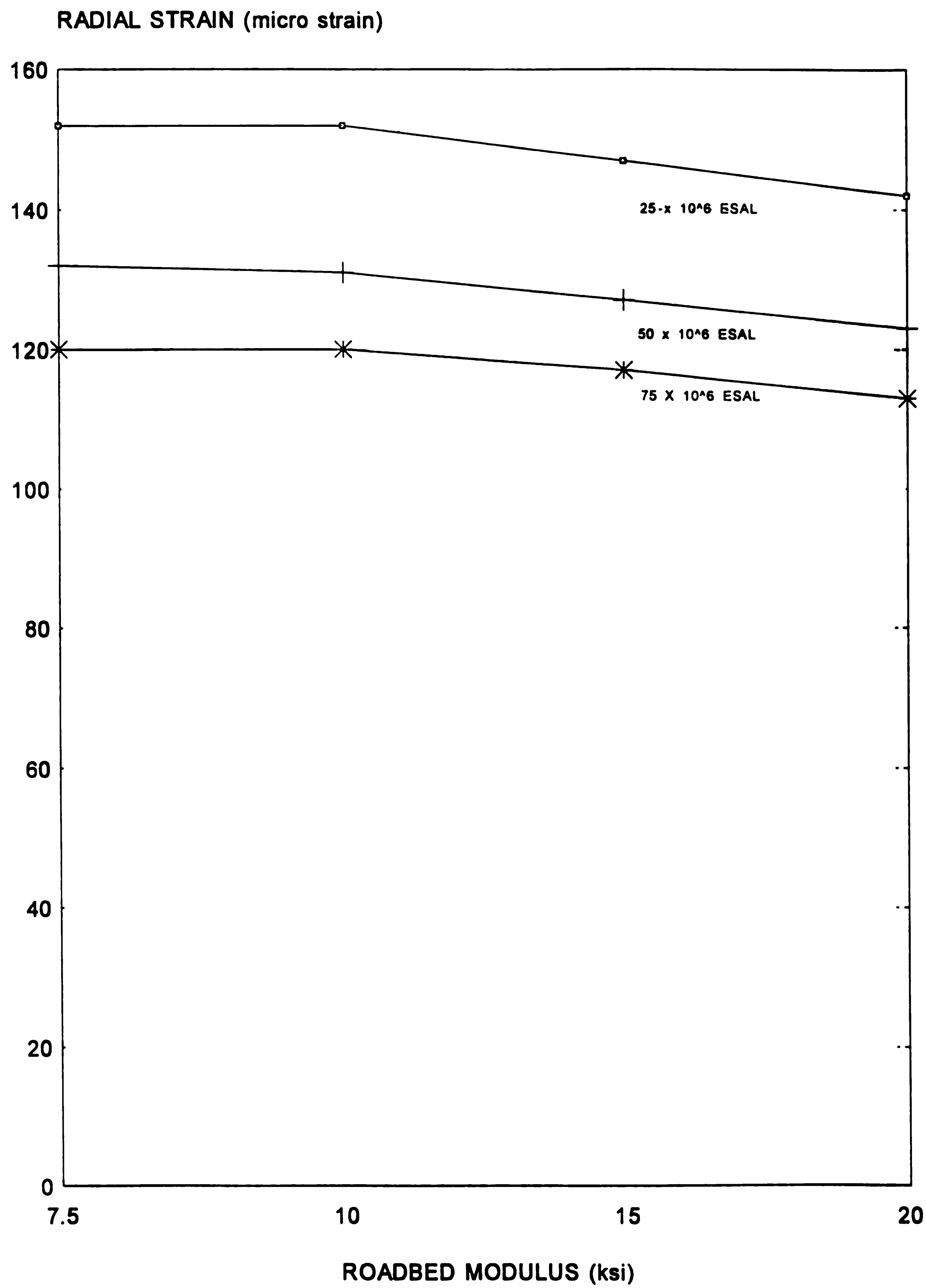

Figure 6.2: Effect of roadbed soil on radial tensile strain at bottom of AC layerfor different levels of18 kip ESAL.

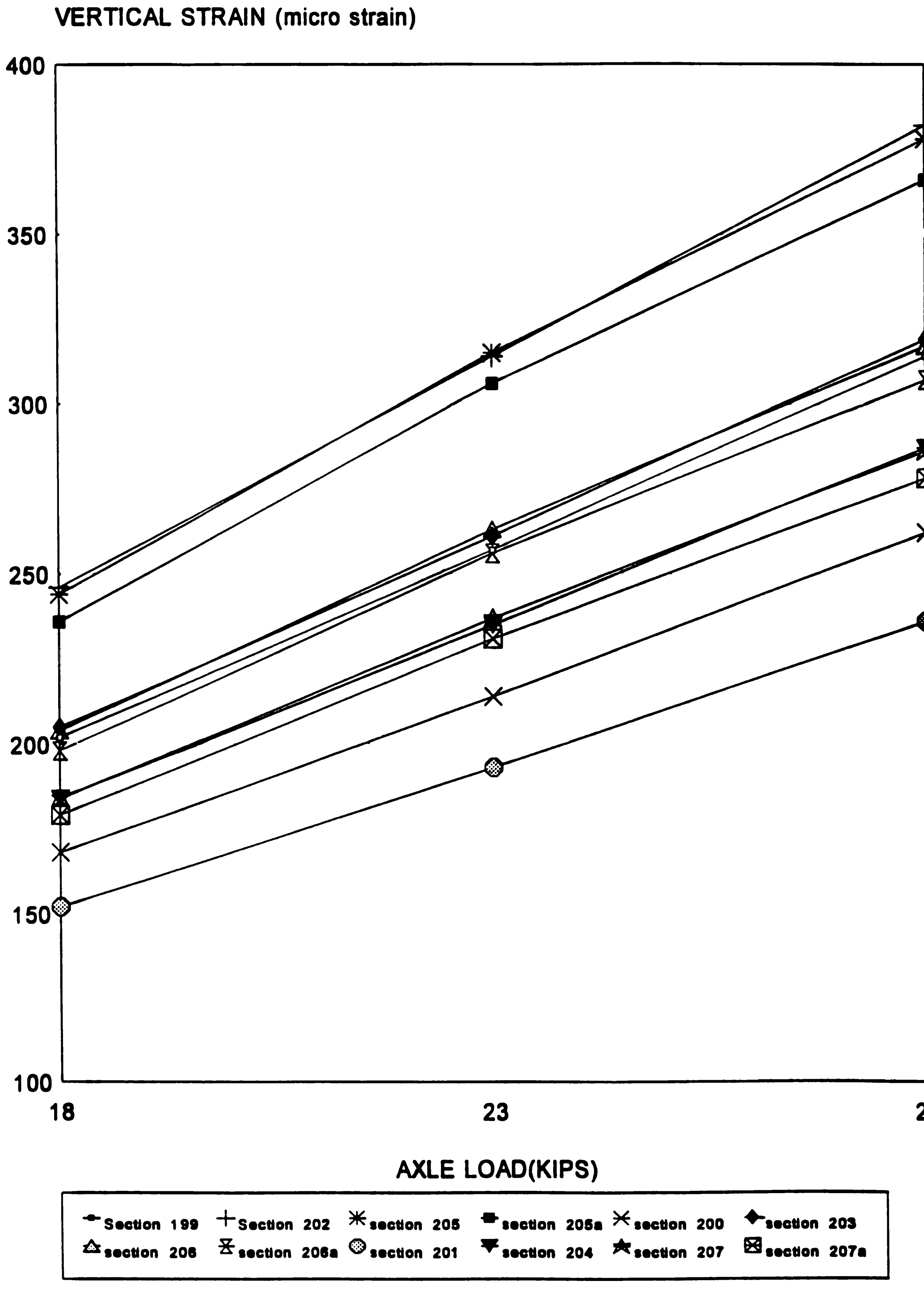

Figure 6.3: Effect of axle load on vertical compressive strain at top of roadbed for the indicated pavement sections

6.3 PREDICTED FATIGUE AND RUT PERFORMANCE OF THE AASHTO DESIGNED PAVEMENT SECTIONS

The fatigue and rut lives of each of the AASTHO designed pavement sections with respect to various fatigue and rut models are listed in Table 6.3 through 6.5 and 6.6 through 6.8 respectively. Tables 6.9 and 6.10 present a summary of the fatigue and rut lives respectively. Figures 6.4 through 6.12 present the pavement lives relative to roughness, fatigue and rut for pavement sections 199, 200 and 201. Examination of the figures indicate that:-

1. The fatigue lives of the AASHTO designed pavement sections predicted by the various fatigue models are shorter than the AASHTO design life except for sections 206 and 207, for which the fatigue life predicted by the MICH-PAVE model is greater than the AASHTO design life (see Tables 6.9 and 6.10 and Figures 6.4 through 6.6). This implies that the fatigue life should control the design of these pavements rather than the roughness as predicted by the AASHTO model.

2. The fatigue and rut lives of the AASHTO designed pavement sections decrease with increases in axle load and tire pressure (see Tables 6.9 and 6.10 and Figures 6.7 through 6.12). The implication of this is that the design of pavements that expected to carry high axle loads (as in Pakistan) must be based on fatigue and rut models rather

Table 6.3: The fatigue life (Million repetitions) of AASHTO designed pavement sections of Figure 3.2 Axle load = 18-Kip, Tire pressure = 80 psi.

AASHTO Design ESALs $*10^6$	Cell No.	Radial Tensile Strain, bottom of AC Layer (μstrain)	Asphalt Institute Model	Monsmith model	Michpave Model	NAASRA Model
			Fatigue Life	Fatigue Life	Fatigue Life	Fatigue Life
25	199	152	4.49	0.23	4.09	7.11
	202	152	4.49	0.23	5.87	7.11
	205a	147	5.01	0.26	11.09	8.40
	205	142	5.62	0.29	24.6	9.99
50	200	132	7.15	0.37	8.61	14.39
	203	131	7.33	0.38	12.62	14.95
	206a	127	8.12	0.42	23.79	17.45
	206	123	9.02	0.47	52.36	20.48
75	201	120	9.78	0.51	13.74	23.17
	204	120	9.78	0.51	20.28	23.17
	207a	117	10.63	0.56	38.47	26.30
	207	113	11.92	0.63	84.36	31.30

Table 6.4: The fatigue life (Million repetitions) of AASHTO designed pavement sections of Figure 3.2 Axle load = 23-kip, Tire pressure = 120 psi.

AASHTO Design ESALs $*10^6$	Cell No.	Radial Tensile Strain, bottom of AC Layer (μ strain)	Asphalt Institute Model	Monismith model	Michpave Model	NAASRA Model
			Fatigue life	Fatigue Life	Fatigue Life	Fatigue Life
25	199	204	1.71	0.083	2.21	1.63
	202	203	1.74	0.085	3.24	1.67
	205a	198	1.88	0.092	6.18	1.90
	205	191	2.12	0.104	13.62	2.27
50	200	175	2.83	0.141	4.60	3.51
	203	174	2.88	0.144	6.88	3.62
	206a	170	3.11	0.156	13.18	4.06
	206	164	3.50	0.176	28.90	4.86
75	01	160	3.80	0.191	7.28	5.50
	204	159	3.88	0.196	10.97	5.67
	207a	155	4.21	0.213	21.16	6.44
	207	150	4.69	0.239	46.37	7.59

Table 6.5: The fatigue life (Million ESALs) of AASHTO designed pavement sections of Figure 3.2 Axle load = 28-kip, Tire pressure = 120 psi.

AASHTO Design ESALs *10^6	Cell No.	Radial Tensile Strain, bottom of AC Layer (μstrain)	Asphalt Institute Model	Monsmith model	Michpave Model	NAASRA Model
			Fatigue Life	Fatigue Life	Fatigue Life	Fatigue Life
25	199	234	1.09	0.052	1.20	0.82
	202	233	1.10	0.052	1.73	0.84
	205	227	1.20	0.057	3.26	0.95
	205a	218	1.37	0.066	7.25	1.17
50	200	203	1.73	0.084	2.56	1.67
	203	202	1.76	0.086	3.73	1.71
	206	196	1.95	0.095	7.02	1.99
	206a	189	2.19	0.11	15.46	2.39
75	201	186	2.31	0.11	4.10	2.59
	204	185	2.35	0.12	6.01	2.66
	207	180	2.58	0.13	11.36	3.05
	207a	174	2.88	0.14	24.93	3.61

Table 6.6: Rut life (Million repetitions) of AASHTO designed pavement sections of Figure 3.2
Axle Load = 18-kip, Tire Pressure = 80 psi.

AASHTO Design ESALs $*10^6$	Cell NO.	Vertical compressive strain, top of roadbed (μstrain)	Asphalt Institute Model	TRRL Model	ERES Model
			Rut Life	Rut Life	Rut Life
25	199	202	49.21	24.29	47.43
	202	246	20.35	11.15	19.62
	205a	244	21.11	11.51	20.36
	205	236	24.51	13.14	23.64
50	200	168	112.37	50.30	110.00
	203	205	46.06	22.92	44.40
	206a	204	47.08	23.36	45.38
	206	198	53.82	26.29	51.87
75	201	152	175.95	74.70	170.00
	204	184	74.76	35.12	72.03
	207a	184	74.76	35.12	72.03
	207	179	84.58	39.16	81.49

Table 6.7: Rut life (Million repetitions) of AASHTO designed pavement sections of Figure 3.2

Axle load = 23-kips, Tire pressure = 120 psi.

AASHTO Design ESALs $*10^6$	Cell No.	Vertical compressive strain, top of roadbed (μstrain)	Asphalt Institute Model	TRRL Model	ERES Model
			Rut Life	Rut Life	Rut Life
25	199	257	16.73	9.38	16.14
	202	314	6.82	4.25	6.58
	205a	315	6.72	4.20	6.49
	205	306	7.65	4.71	7.39
50	200	214	38.00	19.33	36.63
	203	261	15.61	8.83	15.06
	206a	263	15.09	8.56	14.55
	206	256	17.03	9.53	16.42
75	201	193	60.36	29.08	58.17
	204	235	24.98	13.36	24.09
	207a	237	24.05	12.92	23.19
	207	231	26.98	14.30	26.02

Table 6.8: Rut life (Million ESALs) of AASHTO designed pavement sections of Figure 3.2

Axle load = 28-kip, Tire pressure = 120 psi.

AASHTO Design ESALs $*10^6$	Cell No.	Vertical compressive strain, top of roadbed (μstrain)	Asphalt Institute Model	TRRL Model	ERES Model
			Rut Life	Rut Life	Rut Life
25	199	314	6.82	4.25	6.58
	202	382	2.83	1.96	2.74
	205a	378	2.97	2.04	2.87
	205	366	3.43	2.32	3.31
50	200	262	15.35	8.70	14.80
	203	319	6.35	4.00	6.13
	206a	317	6.54	4.10	6.31
	206	307	7.55	4.65	7.28
75	201	236	24.51	13.14	23.63
	204	287	10.20	6.07	9.84
	207a	286	10.36	6.15	10.00
	207	278	11.77	6.88	11.35

Table 6.9: Summary of fatigue lives (Million repetitions) of pavement sections of Figure 3.2

AASHTO Design ESALs $*10^6$	Cell No.	Asphalt Institute Model-Fatigue Life for Axle Load of			Monismith Model-Fatigue Life for Axle Load of			Michpave Model-Fatigue Life for Axle Load of			NASARA Model-Fatigue Life for Axle Load of		
		18-kip	23-kip	28-kip	18-kip	23-kip	28-kip	18-kip	23-kip	28-kip	18-kip	23-kip	28-kip
25	199	4.49	1.70	1.09	0.23	0.083	0.052	4.09	2.21	1.20	7.11	1.63	0.82
	202	4.49	1.73	1.10	0.23	0.085	0.052	5.87	3.24	1.73	7.11	1.67	0.84
	205a	5.01	1.88	1.20	0.26	0.092	0.057	11.09	6.18	3.26	8.40	1.90	0.95
	205	5.62	2.12	1.37	0.29	0.104	0.066	24.60	13.62	7.25	9.99	2.27	1.17
50	200	7.15	2.83	1.73	0.37	0.141	0.084	8.61	4.60	2.56	14.39	3.51	1.67
	203	7.33	2.88	1.76	0.38	0.144	0.086	12.62	6.88	3.73	14.95	3.61	1.71
	206a	8.12	3.11	1.95	0.42	0.156	0.095	23.79	13.18	7.02	17.45	4.06	1.99
	206	9.02	3.50	2.19	0.47	0.176	0.110	52.36	28.90	15.46	20.48	4.86	2.39
75	201	9.78	3.80	2.31	0.51	0.191	0.110	13.74	7.28	4.10	23.17	5.50	2.59
	204	9.78	3.88	2.35	0.51	0.196	0.120	20.28	10.97	6.01	23.17	5.67	2.66
	207a	10.63	4.21	2.58	0.56	0.213	0.130	38.47	21.16	11.36	26.30	6.44	3.05
	207	11.92	4.69	2.88	0.56	0.239	0.140	84.36	46.37	24.93	31.30	7.59	3.61

Table 6.10: Summary of rut lives (Million repetitions) of the pavement sections of Figure 3.2

AASHTO Design ESALs $*10^6$	Cell No.	Asphalt Institute Model Rut Life for Axle Load of			TRRL Model Rut Life for Axle Load of			ERES Model Rut Life for Axle Load of		
		18-kip	23-kip	28-kip	18-kip	23-kip	28-kip	18-kip	23-kip	28-kip
25	199	49.21	16.73	6.82	24.29	9.38	4.25	47.43	16.14	6.58
	202	20.35	6.82	2.83	11.15	4.25	1.96	19.62	6.58	2.74
	205a	21.11	6.72	2.97	11.51	4.20	2.04	20.36	6.49	2.87
	205	24.51	7.65	3.43	13.14	4.71	2.32	23.64	7.39	3.31
50	200	112.37	38.00	15.35	50.30	19.33	8.70	110.00	36.63	14.80
	203	46.06	15.61	6.35	22.92	8.83	4.00	44.40	15.06	6.13
	206a	47.08	15.09	6.54	23.36	8.56	4.10	45.38	14.55	6.31
	206	53.82	17.03	7.55	26.29	9.53	4.65	51.87	16.42	7.28
75	201	175.95	60.36	24.51	74.70	29.08	13.14	170.00	58.17	23.63
	204	74.76	24.98	10.20	35.12	13.36	6.07	72.03	24.09	9.84
	207a	74.76	24.05	10.36	35.12	12.92	6.15	72.03	23.19	10.00
	207	84.58	26.98	11.77	39.16	14.30	6.88	81.49	26.02	11.35

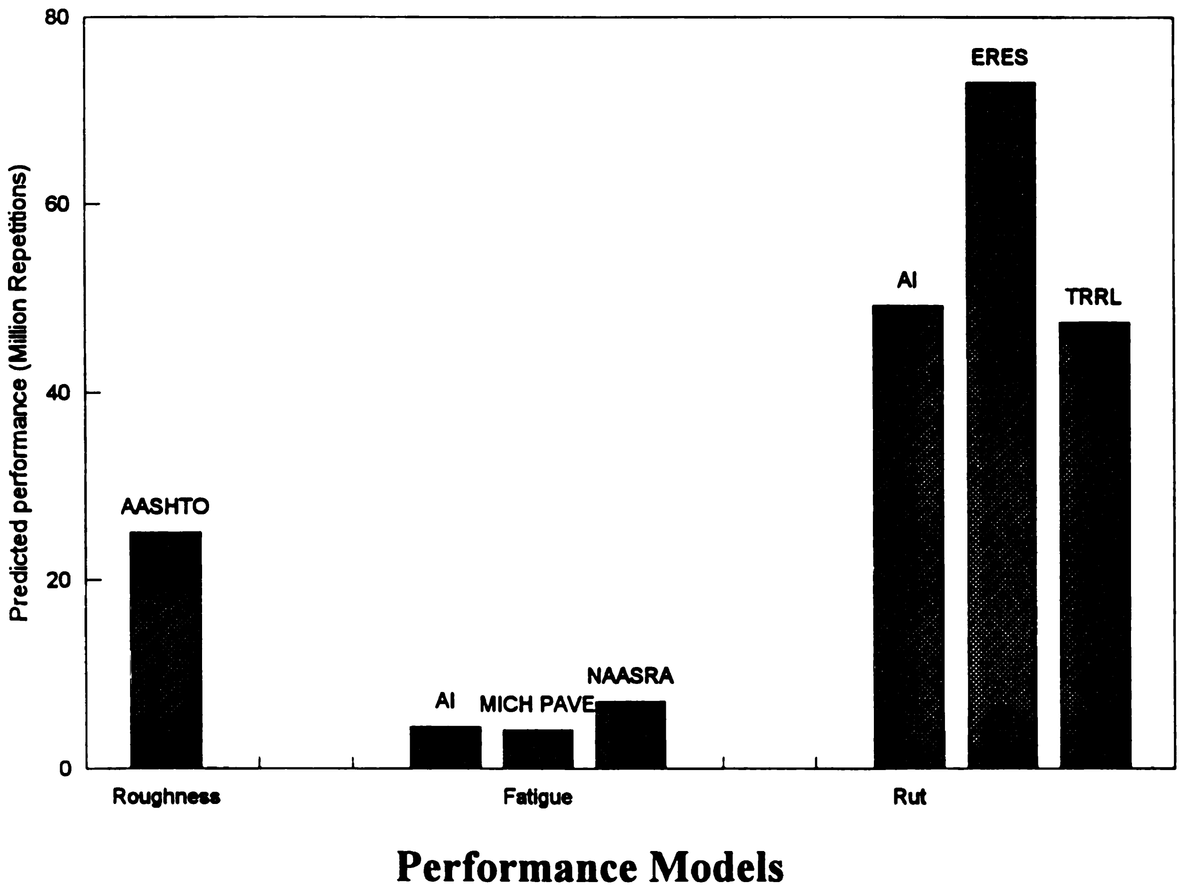

Figure 6.4: Comparison of predicted performances of pavement section 199 (18 - kip ESAL)

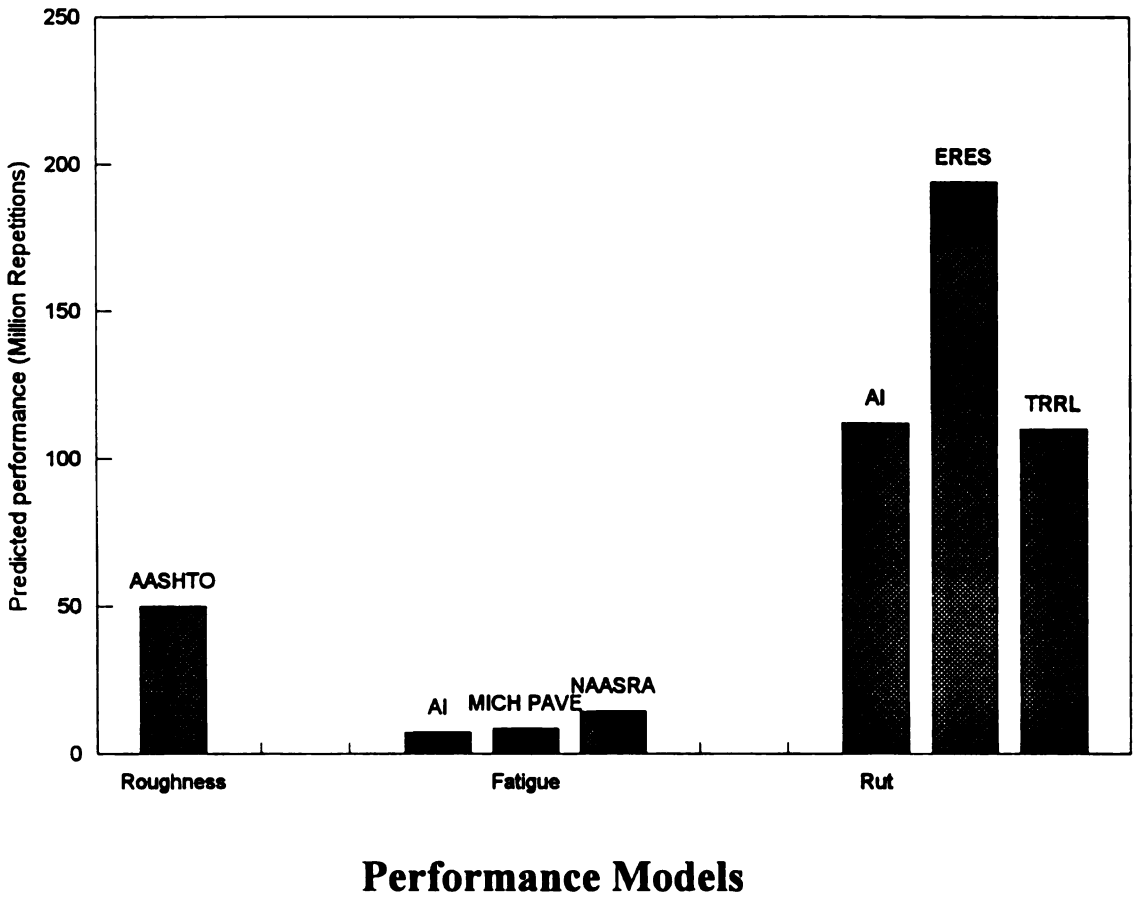

Figure 6.5: Comparison of predicted performances of pavement section 200 (18 - kip ESAL)

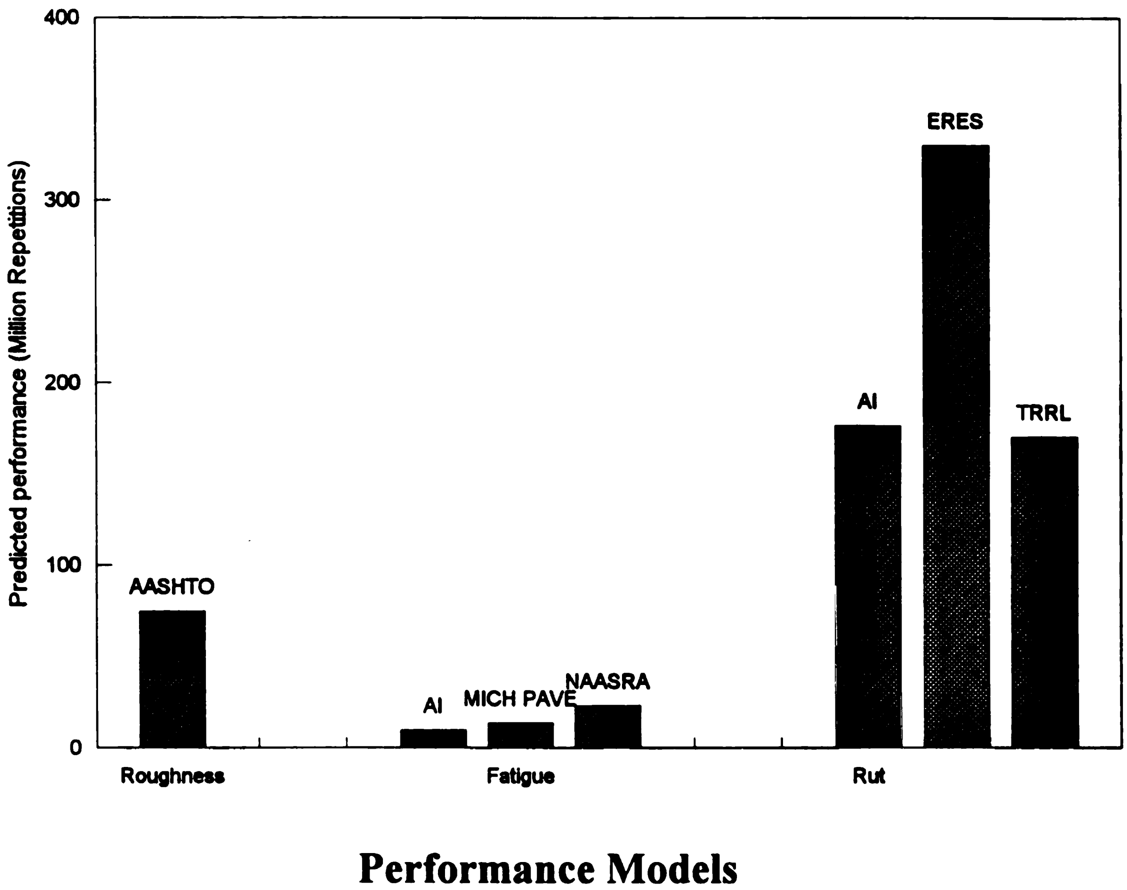

Figure 6.6: Comparison of predicted performances of pavement section 201(18 - kip ESAL)

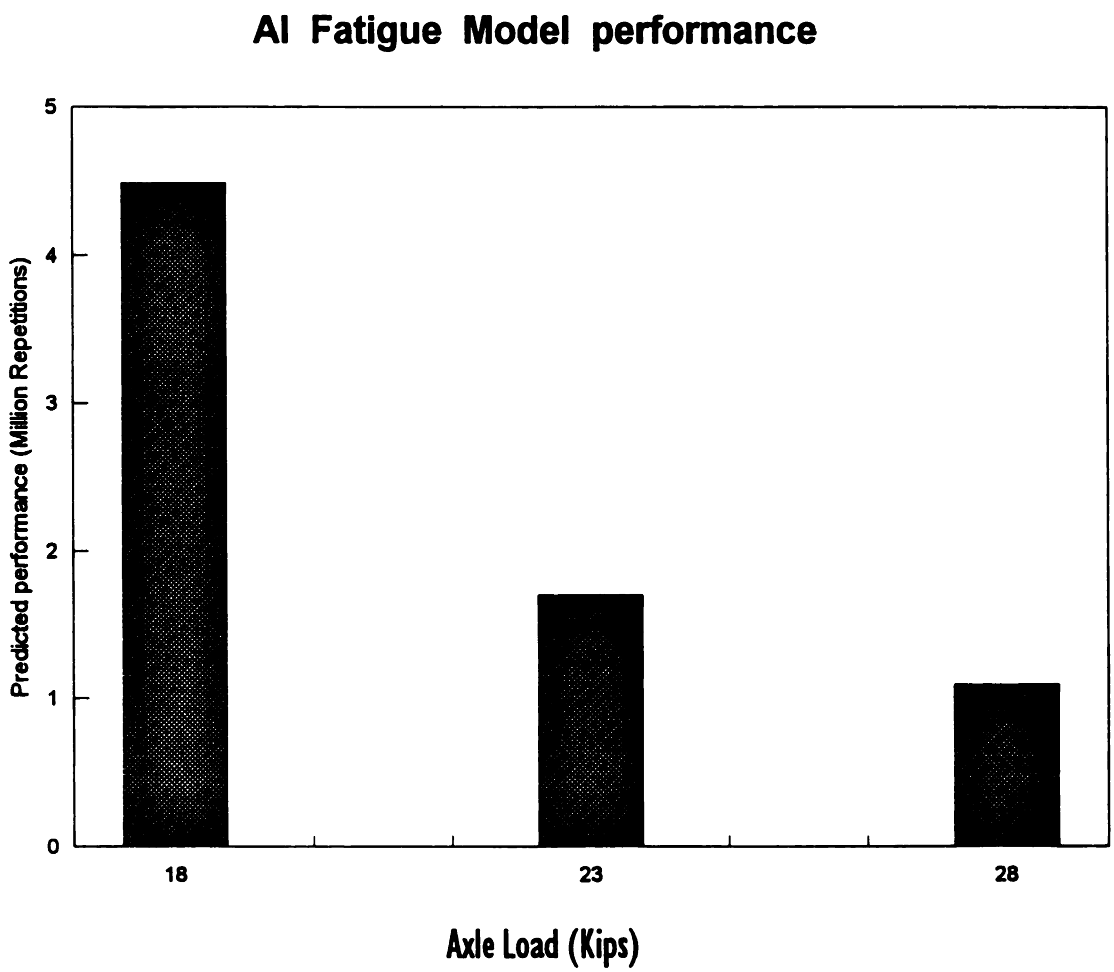

Figure 6.7: Effect of axle load on predicted fatigue performance of pavement section 199

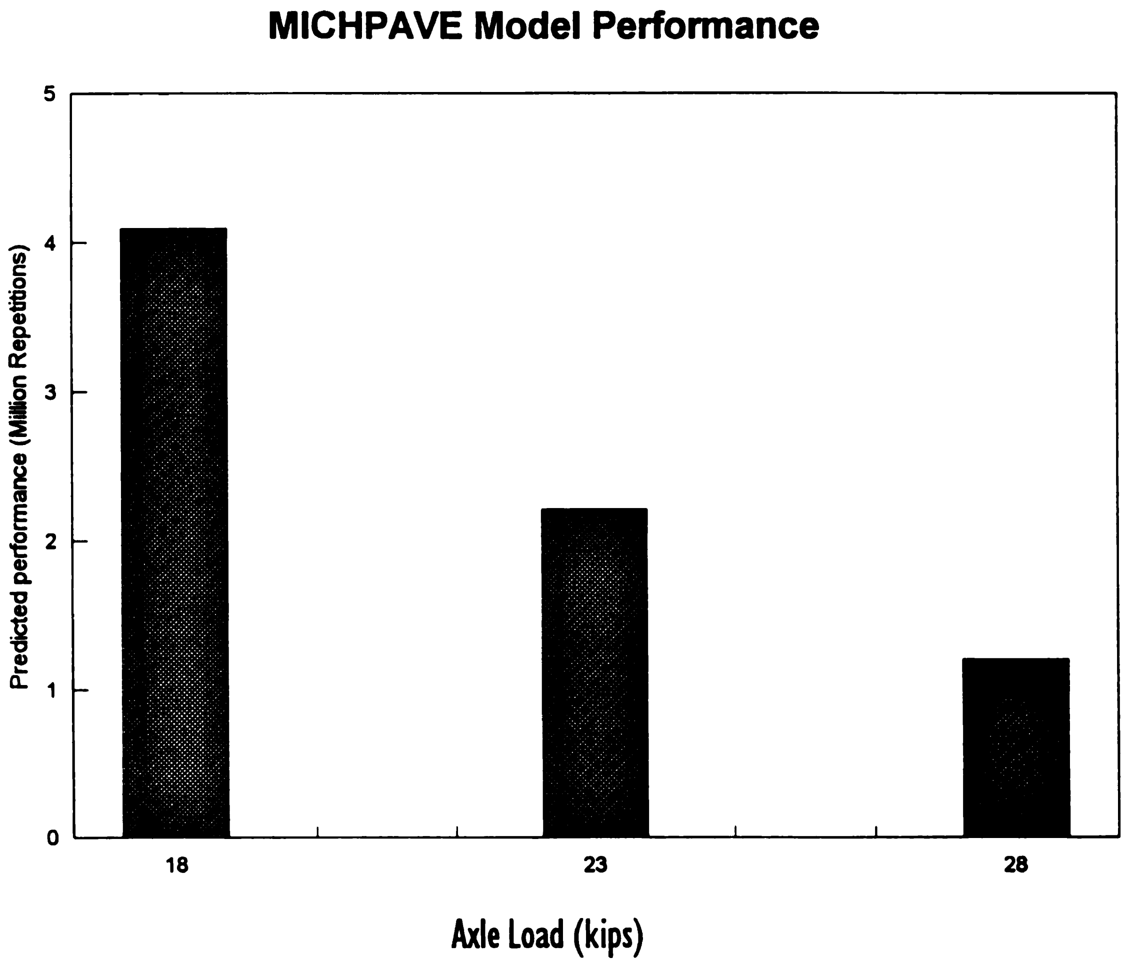

Figure 6-8: Effect of axle load on predicted fatigue performance of pavement section 199

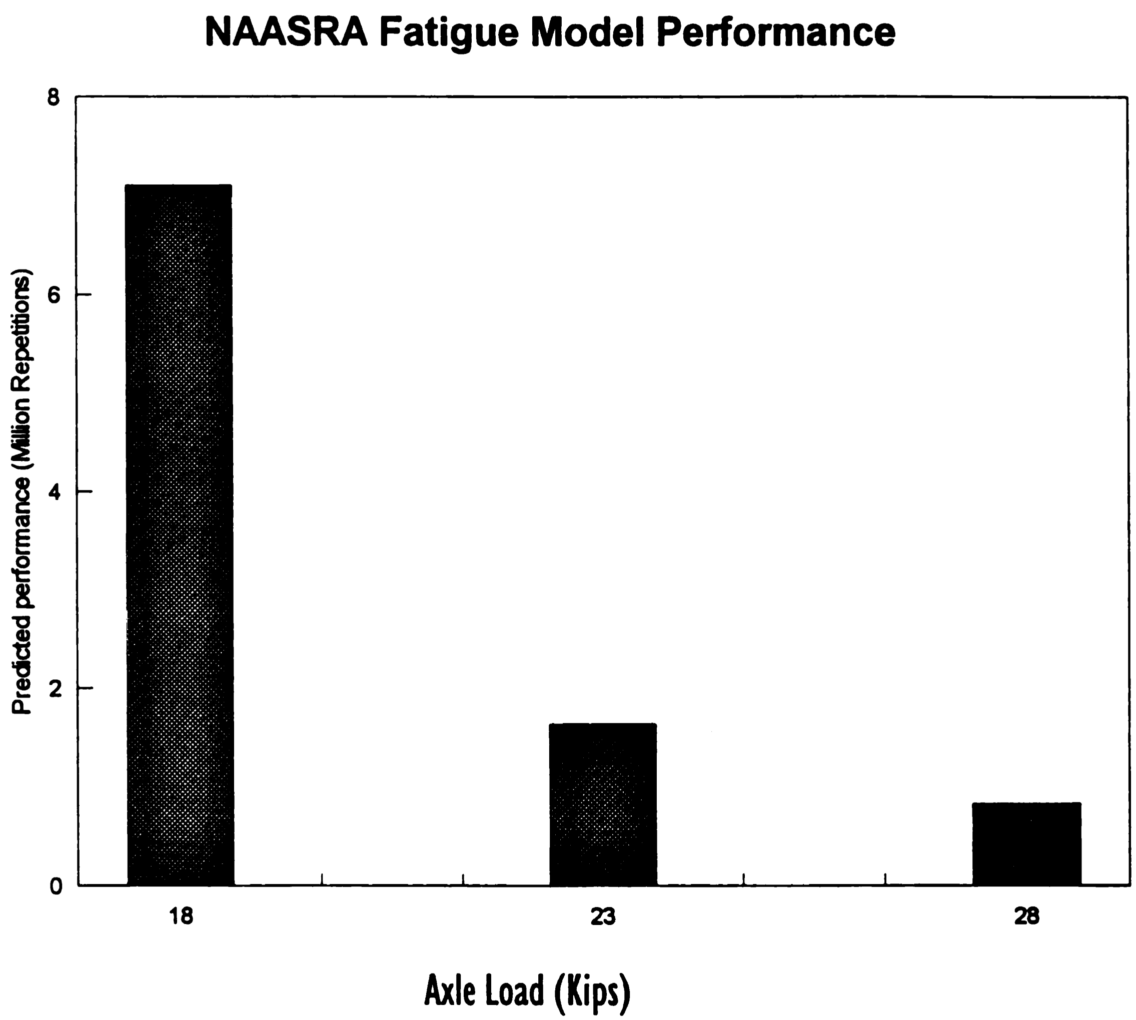

Figure 6.9: Effect of axle load on predicted fatigue performance of pavement section 199

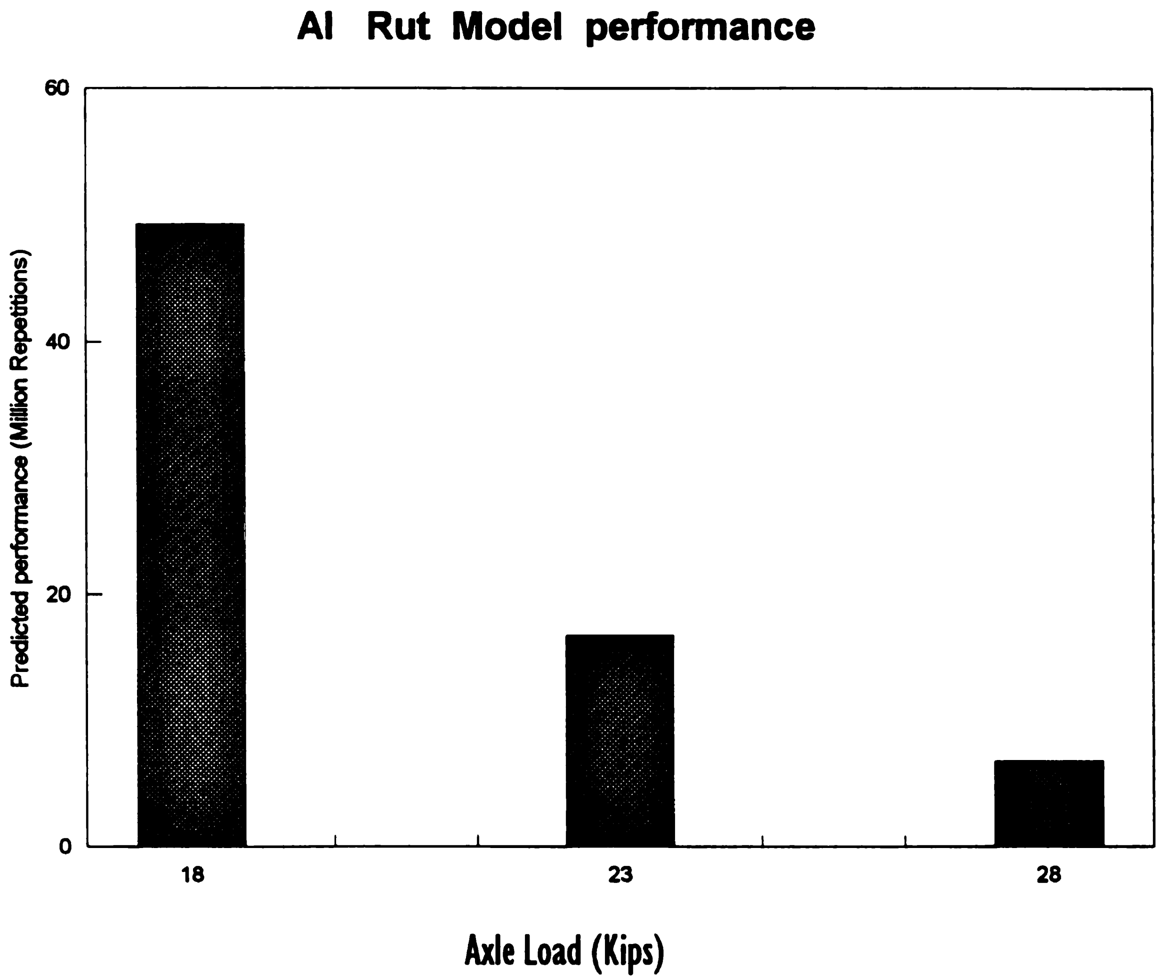

Figure 6.10: Effect of axle load on predicted rut performance of pavement section 199

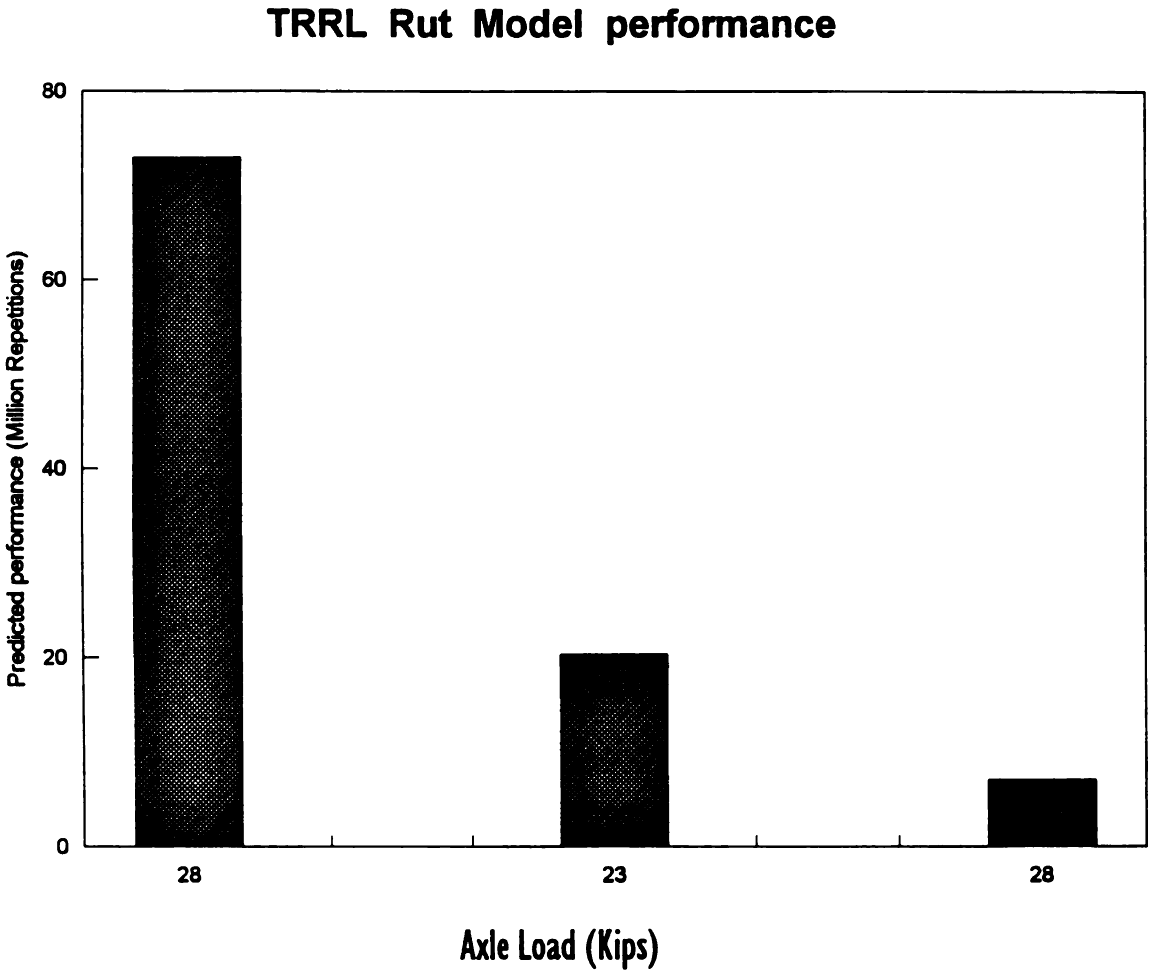

Figure 6.11: Effect of axle load on predicted rut performance of pavement section 199

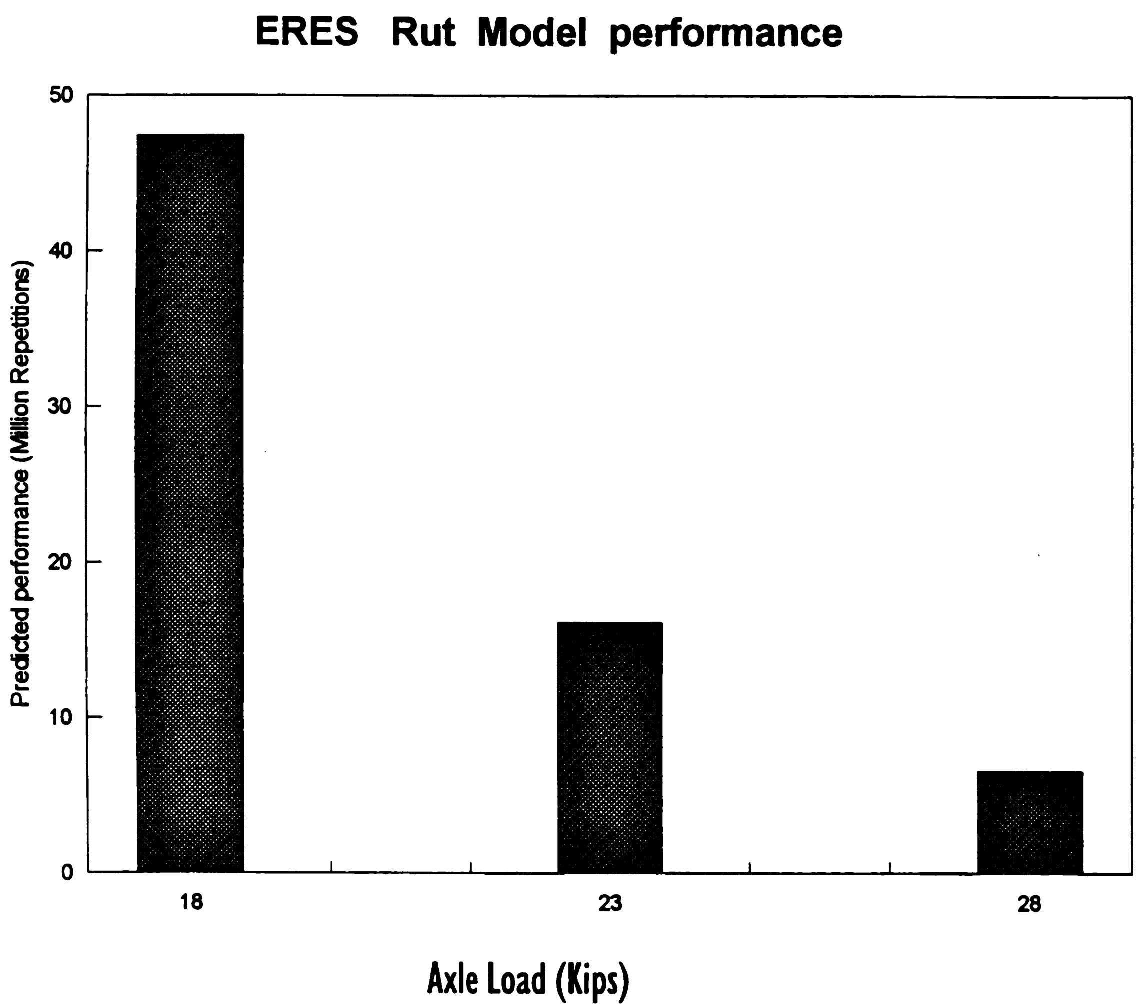

Figure 6.12: Effect of axle load on predicted rut performance of pavement section 199

than on roughness. Hence the AASHTO design procedure (which is roughness based model) is not applicable in Pakistan.

4. The different fatigue and rut performance models used in the study show large differences in the predicted fatigue and rut performance for any one pavement section (see Tables 6.9 and 6.10 and Figures 6.4 through 6.6). Given that those models were developed for pavements in different environmental regions and different pavement designs and construction practices, one can conclude that Pakistan must develop rut and fatigue models that are applicable to the axle loads found in Pakistan and to the environmental conditions.

CHAPTER 7

STUDY RESULTS - ENHANCEMENT OF FATIGUE/RUT PERFORMANCE OF THE AASHTO (86) BASED DESIGNS

7.1 GENERAL

It was stated in Chapter 6 that for the pavement sections of Figure 3.2 and in the range of material properties used, the predicted fatigue life (in terms of 18-kip ESAL) using various fatigue models, is much shorter than the Design ESALs used in AASHTO procedure. Since the AASHTO design procedure is based on pavement roughness, one can conclude that for the pavement sections of Figure 3.2, the fatigue life not roughness should control the pavement design process. Given the above scenario, the question becomes what material types should be used so that the fatigue life of the pavement is equal to or longer than the AASHTO Design ESALs, input in the procedure?

To answer the question, three trial designs were conducted. In the first trial, the granular base layer was simply replaced by an AC stabilized base material. The second trial consisted of eliminating the subbase layer and replacing the granular base layer by an asphalt treated layer. In the third trial, the values of the modulus of the base and subbase layer were increased (to be achieved through compaction). In these trials, the thicknesses obtained from the AASHTO Design Procedure, listed in Table 6.1 (without changing the base/subbase modulus) were used. The results of the analysis are discussed/presented below.

7.2 TRIAL 1, REPLACING GRANULAR BASE WITH AN AC STABILIZED BASE (layer modulus equal to or greater than 250 ksi)

In this trial, the granular base layer (Layer modulus 30 ksi) of each pavement section of Figure 3.2 was replaced by an AC stabilized base layer while keeping the same thicknesses. Mechanistic analysis was then conducted, and the fatigue life (in terms of 18-kip ESAL) and the number of ESALs to 0.5 inch rut were then computed using various prediction models. Table 7.1, Table 7.3 and Table 7.5 present the original and enhanced fatigue lives while the original and enhanced rut lives are listed in Table 7.2, Table 7.4 and Table 7.6. Figure 7.1, Figure 7.3 and Figure 7.5 present the comparison of the original and enhanced fatigue lives whereas Figure 7.2, Figure 7.4 and Figure 7.6 depict the comparison of the original and enhanced rut lives for pavement section 199 (Monismith model exhibits very low original and enhanced fatigue performance therefore it has not been discussed and shown in the Figures). From the examination of the results in this trial following is observed:

1. For the combination of 18 kip axle load and 80 psi tire pressure, to exhibit fatigue performance equal to or greater than the AASHTO input ESALs following is seen:

   a. The elastic modulus of the AC stabilized base (for the pavement sections considered in this study) needs to be enhanced in the range of 250 ksi to 300 ksi. This range of base modulus satisfies all the fatigue criterion except Monismith criterion (see Table 7.1).

b. The magnitude of the enhancement varies with the type of fatigue/rut prediction model. In the range of AC stabilized base modulus (250 ksi to 300 ksi) used for this trial, Asphalt Institute model exhibit fatigue life which is almost equal to AASHTO input ESALs whereas MICHPAVE and NAASRA fatigue models exhibit fatigue life much greater than the AASHTO input ESALs (see Table 7.1). Figure 7.1 present the comparison of the enhanced fatigue lives predicted by various fatigue models for pavement section 199.

c. The results of enhanced fatigue lives exhibited due to various fatigue criterion indicate that the sections where there is no subbase used, require relatively less increase in the base modulus to achieve fatigue life equal to or greater than the sections where some subbase thickness is used. This reduction in base modulus is partly attributable to the increased roadbed modulus (see Tables 7.1 and Tables 7.2).

d. The rut life exhibited by all the rut

Table 7.1: Fatigue life (Million repetitions) of AASHTO designed sections of Figure 3.2 (Granular Base Replaced by Asphalt stabilized Base) with respect to various fatigue models. Axle load = 18 kips, Tire pressure = 80 psi.

AASHTO Design ESALs $*10^6$	Cell No.	Base M_R (Ksi)	Radial tensile strain, bottom of AC Layer (μstrain)	Asphalt Institute Model		Monsmith Model		Michpave Model		NASRA Model	
				Enhanced Fatigue Life	Original Fatigue Life	Enhanced Fatigue Life	Original Fatigue Life	Enhanced Fatigue Life	Original Fatigue Life	Enhanced Fatigue Life	Original Fatigue Life
25	199	250	90.6	24.66	4.49	1.34	0.23	95.1	4.09	94.46	7.11
	202	250	89.5	25.67	4.49	1.38	0.23	182.8	5.87	100.41	7.11
	205a	250	85.4	29.95	5.01	1.64	0.26	380.1	11.09	126.95	8.40
	205	250	79.0	38.70	5.62	2.14	0.29	564.7	24.60	187.4	9.99
50	200	270	73.7	48.63	7.15	2.69	0.37	214.3	8.61	265.20	14.39
	203	275	72.7	50.87	7.33	2.82	0.38	438.1	12.62	283.95	14.95
	206a	250	72.6	51.10	8.12	2.82	0.42	1005	23.79	285.91	17.45
	206	250	67.3	65.57	9.02	3.70	0.47	1416	52.36	417.67	20.48
75	201	300	63.4	75.80	9.78	4.26	0.51	397.3	13.74	520.57	23.17
	204	300	63.4	79.80	9.78	4.57	0.51	795.1	20.28	562.94	23.17
	207a	275	63.3	80.22	10.63	4.57	0.56	1892	38.47	567.41	26.30
	207	250	61.3	89.15	11.92	5.09	0.63	2934	84.36	666.20	31.30

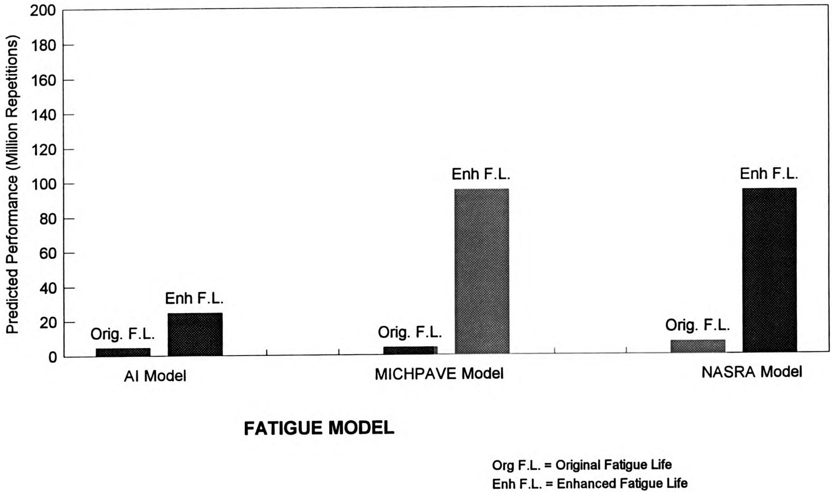

Figure 7.1: Comparison of original and enhanced fatigue life of pavement section 199. Axle load = 18 kip, Tire pressure = 80 psi, Base Type = Asphalt stab.

performance criterion used in this study namely Asphalt Institute, TRRL and ERES is much greater than the AASHTO input ESALs (see Table 7.2). Figure 7.2 present the comparison of the enhanced rut lives predicted by various rut models for pavement section 199.

2. For combination of 23 kip axle load and tire pressure of 120 psi to exhibit the fatigue performance equal to or greater than the AASHTO input ESALs following is seen:

   a. A higher increase in the elastic moudli of the AC stabilize base layer is required. The increase required in the elastic moudli of the base is in the range of 335 ksi to 450 ksi (see Table 7.3).

   b. Within this range of elastic moudli i.e., 335 ksi to 450 ksi, the magnitude of enhancement varies with the type of fatigue prediction model. Asphalt Institute model exhibit the fatigue life almost equal to or greater than the AASHTO input ESALs whereas MICHPAVE and NAASRA fatigue models exhibit fatigue life much greater than the AASHTO input ESALs (see Table 7.3). Figure 7.3 present the comparison of the enhanced fatigue life predicted by

Table 7.2: Rut life (Million repetitions) of AASHTO designed sections of Figure 3.1 (Granular Base Replaced with Asphalt Stabilized Base) with respect to various rut models. Axle load = 18-kip, Tire Pressure = 80 psi.

AASHTO Design ESALs $*10^6$	Cell No.	Base M_R (Ksi)	Vertical compressive strain, top of roadbed (μstrain)	Asphalt Institute Model		TRRL Model		ERES Model	
				Enhanced Rut Life	Original Rut Life	Enhanced Rut Life	Original Rut Life	Enhanced Rut life	Original Rut life
25	199	250	130	354.47	49.21	758.53	72.97	340	47.43
	202	250	157	152.20	20.35	278.35	25.61	150	19.62
	205a	250	100	1148.03	21.11	3056.67	26.72	1104	20.36
	205	250	95.1	1438.14	24.51	3991.63	31.94	1382	23.64
50	200	270	108	813.41	112.37	2030.91	194.23	780	110.00
	203	275	129	366.95	46.06	790.29	67.49	350	44.40
	206a	250	85.3	2340.99	47.08	7113.00	69.24	2300	45.38
	206	250	81.0	2951.47	53.82	9362.36	81.17	2836	51.87
75	201	300	95.0	1444.94	175.95	4014.08	330.60	1400	170.00
	204	300	114	638.44	74.76	1523.93	119.81	610	72.03
	207a	275	73.8	4478.76	74.76	15351.30	119.81	4300	72.03
	207	250	73.8	4478.78	84.58	15351.30	138.71	4304	81.49

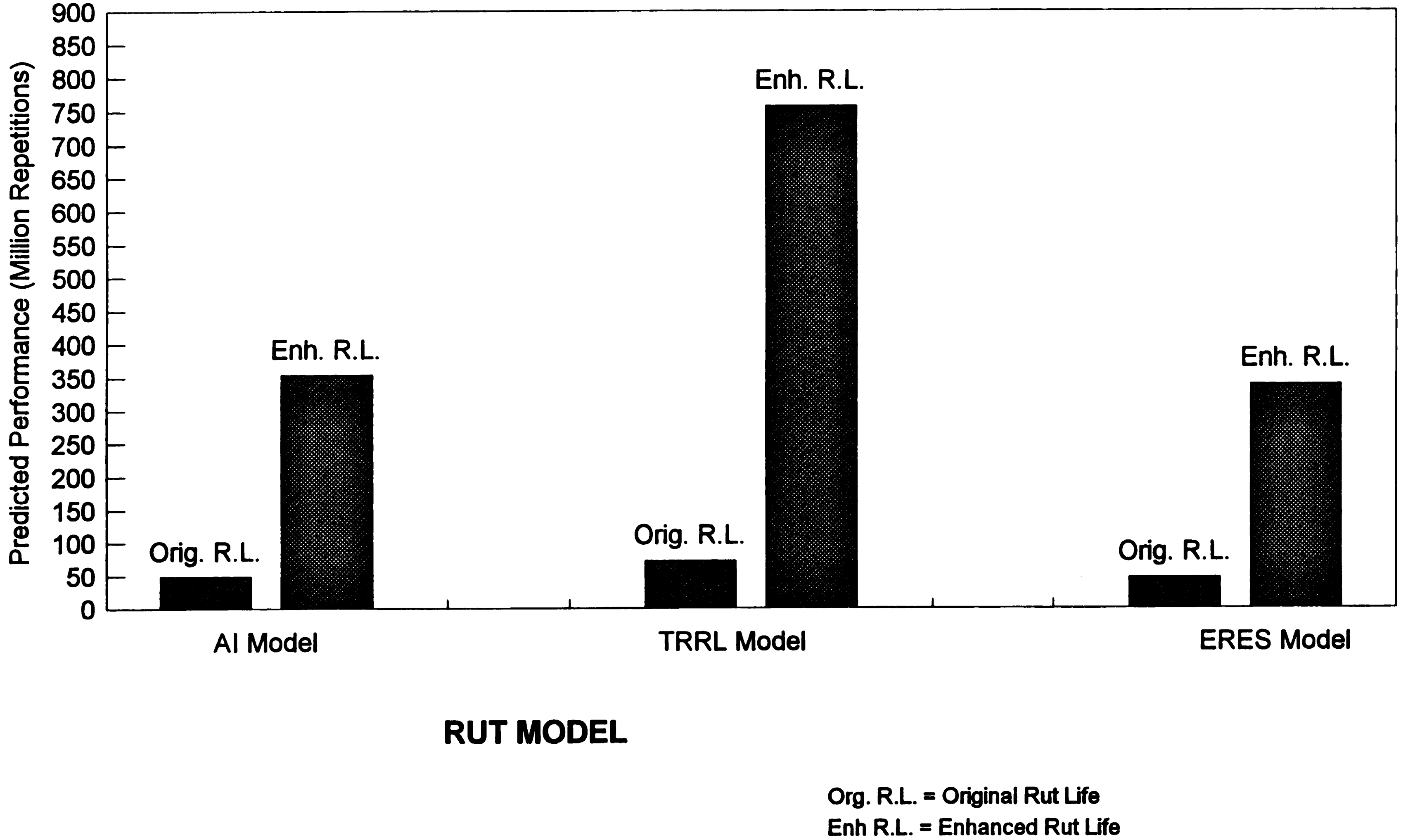

Figure 7.2: Comparison of original and enhanced rut life of pavement section 199. Axle load = 18 kip, Tire pressure = 80 psi, Base Type = Asphalt stab.

Table 7.3: Fatigue life (Million repetitions) of AASHTO designed sections of Figure 3.2 (Granular Base Replaced with Asphalt Stabilized Base) with respect to various fatigue models. Axle load = 23 kips, Tire pressure = 120 psi.

AASHTO Design ESALs $*10^6$	Cell No.	Base M_R (Ksi)	Radial tensile strain, bottom of AC Layer (μstrain)	Asphalt Institute Model		Monsmith Model		Michpave Model		NASRA Model	
				Enhanced Fatigue Life	Original Fatigue Life	Enhanced Fatigue Life	Original Fatigue Life	Enhanced Fatigue Life	Original Fatigue Life	Enhanced Fatigue Life	Original Fatigue life
25	199	435	89.4	25.76	1.71	1.41	0.083	169.6	2.21	100.98	1.63
	202	425	89.1	26.05	1.74	1.41	0.085	327	3.24	102.69	1.67
	205a	385	89.9	25.29	1.88	1.38	0.092	755.5	6.18	98.20	1.89
	205	335	90.1	25.11	2.12	1.38	0.104	1239	13.62	97.11	2.27
50	200	450	74.7	46.52	2.83	2.57	0.141	331.5	4.60	247.92	3.51
	203	450	73.4	49.29	2.88	2.86	0.144	688.7	6.88	270.66	3.61
	206a	425	72.5	51.33	3.11	2.88	0.156	1810	13.18	287.89	4.06
	206	370	73.0	50.18	3.50	2.82	0.176	2995	28.90	278.16	4.86
75	201	450	68.1	63.07	3.80	3.55	0.191	479.1	7.28	393.71	5.50
	204	450	66.8	67.20	3.88	3.80	0.16	1001	10.97	433.54	5.67
	207a	440	64.7	74.65	4.21	4.26	0.213	2897	21.16	508.62	6.44
	207	410	63.2	80.64	4.69	4.57	0.239	5686	46.37	571.91	7.59

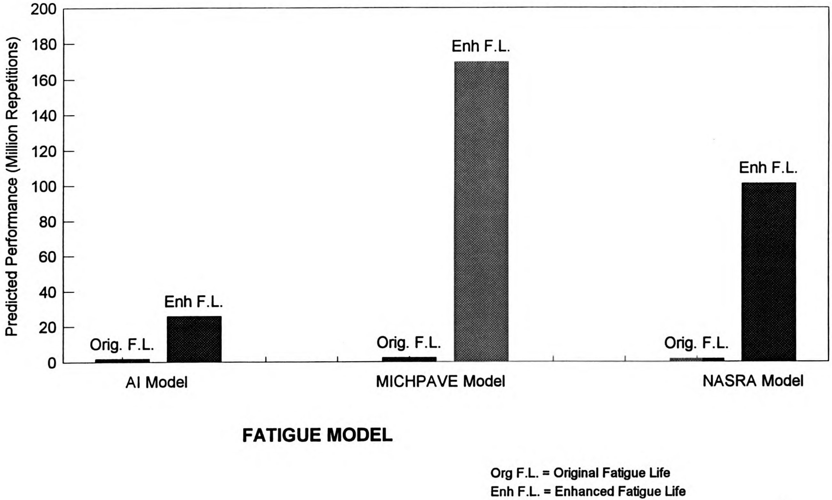

Figure 7.3: Comparison of original and enhanced fatigue life of pavement section 199. Axle load = 23 kip, Tire pressure = 120 psi, Base type = Asphalt stab.

various fatigue models for pavement section 199.

c. For this combination of load and tire pressure, the rut life exhibited by all the rut criterion used in this study namely Asphalt Institute, TRRL and ERES is much greater than the AASHTO input ESALs (see Table 7.4). Figure 7.4 presents the comparison of the enhanced rut lives predicted by various rut models for pavement section 199.

3. Combination of 28 kip axle load and 120 psi tire pressure requires further increase in the moduli of the AC stabilized base layer. For this combination of axle load and tire pressure, the elastic moduli of the base was increased to maximum limit of 450 ksi (Please remember this is the elastic moduli used for the AC layer in this study). For this limit of elastic moduli following is seen:

a. Asphalt Institute model exhibits the magnitude of enhanced fatigue life shorter (39% to 54% shorter) than AASHTO input ESALs whereas the MICHPAVE and NAASRA fatigue criterion exhibits the magnitude of fatigue life almost double than the AASHTO input ESALs (see Table 7.5). Figure 7.5 present the comparison of the

Table 7.4: Rut life (Million repetitions) of AASHTO designed sections of Figure 3.2 (Granular Base Replaced with Asphalt Stabilized Base) with respect to various rut models. Axle load = 23-kips, Tire pressure = 120 psi.

AASHTO Design ESALs $*10^6$	Cell No.	Base M_R (Ksi)	Vertical compressive strain, top of roadbed (μstrain)	Asphalt Institute Model		TRRL Model		ERES Model	
				Enhanced Rut Life	Original Rut Life	Enhanced Rut Life	Original Rut Life	Enhanced Rut Life	Original Rut Life
25	199	435	141	246.35	16.73	492.69	20.30	240	16.14
	202	425	168	112.37	6.82	194.28	7.00	110	6.58
	205a	385	103	1005.87	6.72	2612.49	6.89	970	6.49
	205	335	106	884.46	7.65	2242.95	8.04	850	7.39
50	200	450	119	526.74	38.00	1213.16	53.67	510	36.63
	203	450	140	254.33	15.61	511.71	18.71	240	15.06
	206a	425	82.6	2703.84	15.09	8438.37	17.95	2600	14.55
	206	370	84.0	2507.72	17.03	7717.37	20.73	2400	16.42
75	201	450	109	780.514	60.36	1933.88	92.96	750	58.17
	204	450	128	379.97	24.98	823.66	32.66	370	24.09
	207a	440	73.7	4506.05	24.05	15462.23	31.22	4300	23.19
	207	410	73.3	4617.27	26.98	15915.71	35.79	4400	26.02

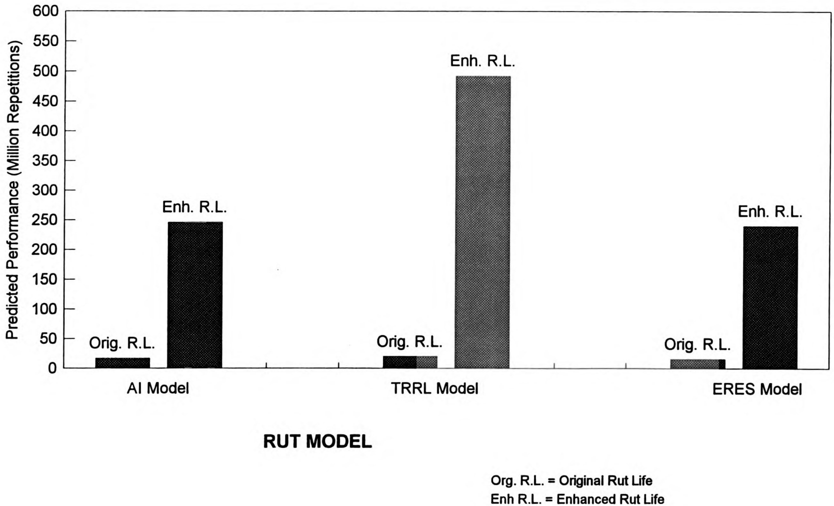

Figure 7.4: Comparison of original and enhanced rut life of pavement section 199. Axle load = 23 kip, Tire pressure = 120 psi, Base Type = Asphalt stab.

Table 7.5: Fatigue life (Million repetitions) of AASHTO designed sections of Figure 3.2 (Granular Base Replaced with Asphalt Stabilized Base) with respect to various fatigue models. Axle load = 28 kips, Tire pressure = 120 psi.

AASHTO Design ESALs $*10^6$	Cell No.	Base M_R (Ksi)	Radial tensile strain, bottom of AC Layer (μstrain)	Asphalt Institute Model		Monsmith Model		Michpave Model		NASRA Model	
				Enhanced Fatigue Life	Original Fatigue Life	Enhanced Fatigue Life	Original Fatigue Life	Enhanced Fatigue Life	Original Fatigue Life	Enhanced Fatigue Life	Original Fatigue Life
25	199	450	105	15.18	1.09	0.81	0.052	112.1	1.20	45.18	0.82
	202	450	104	16.66	1.10	0.83	0.052	224.7	1.73	47.40	0.84
	205a	450	99.4	18.18	1.20	0.98	0.057	654.9	3.26	59.43	0.95
	205	450	93.1	22.54	1.37	1.23	0.066	1511	7.25	82.44	1.17
50	200	450	89.8	25.39	1.73	1.38	0.084	206.4	2.56	98.20	1.67
	203	450	88.3	26.83	1.76	1.44	0.086	420.2	3.73	107.42	1.71
	206a	450	84.6	30.89	1.95	1.7	0.095	1241	7.02	133.06	1.99
	206	450	79.6	37.75	2.19	2.09	0.110	2866	15.46	180.44	2.39
75	201	450	81.9	34.37	2.31	1.90	0.110	302.2	4.10	156.49	2.59
	204	450	80.5	36.38	2.35	2.00	0.120	619.6	6.01	170.58	2.66
	207a	450	77.1	41.93	2.58	2.34	0.130	1845	11.36	211.66	3.05
	207	450	72.6	51.10	2.88	2.82	0.140	4266	24.93	285.91	3.61

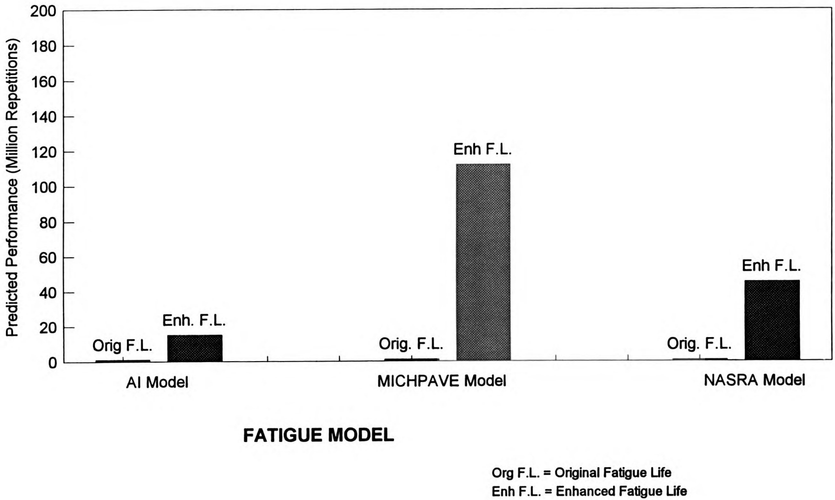

Figure 7.5: Comparison of original and enhanced fatigue performance of pavement section 199. Axle load = 28 kip, Tire pressure = 120 psi, Base type = Asphalt stab.

enhanced fatigue lives predicted by various fatigue models for pavement section 199.

b. The magnitude of enhanced rut life exhibited by all the rut criterion used in this study namely Asphalt Institute, TRRL and ERES is much greater than the AASHTO design life (see Table 7.6). Figure 7.6 present the comparison of the enhanced rut lives predicted by various rut models for pavement section 199.

4. For any axle load, the chances of failure of pavement sections (considered in this study) in fatigue are relatively more as compared to its failure in rut. For example, for combination of 28 kip axle load and 120 psi tire pressure for section 199, the fatigue life predicted by Asphalt Institute, MICHPAVE and NAASRA models is 15.18 112.10, 45.18 million repetitions respectively (see Figure 7.5) whereas the rut life predicted by AI, TRRL and ERES models is 246.35, 492.69 and 240 million repetitions respectively (see Figure 7.6). This shows that chances of section 199 failing in fatigue are more as compared to its failing in rut. This phenomena also applies to the other pavement sections considered in this study.

Table 7.6: Rut life (Million repetitions) of AASHTO designed sections of Figure 3.2 (Granular Base Replaced with Asphalt Stabilized Base) with respect to various rut models. Axle load = 28-kips, Tire pressure = 120 psi.

AASHTO Design ESALs $*10^6$	Cell No.	Base M_R (Ksi)	Vertical compressive strain, top of roadbed (μstrain)	Asphalt Institute Model		TRRL Model		ERES Model	
				Enhanced Rut Life	Original Rut Life	Enhanced Rut Life	Original Rut Life	Enhanced Rut life	Original rut life
25	199	450	169	109.42	6.82	188.23	7.00	110	6.58
	202	450	200	51.46	2.83	76.92	2.47	50	2.74
	205a	450	113	664.14	2.97	1596.94	2.61	640	2.87
	205	450	108	813.41	3.43	2030.91	3.10	780	3.31
50	200	450	144	224.17	15.35	440.56	18.34	220	14.80
	203	450	170	106.57	6.35	182.38	6.45	100	6.13
	206a	450	96.2	1365.92	6.54	3755.16	6.67	1300	6.31
	206	450	91.9	1676.48	7.55	4787.63	7.90	1600	7.28
75	201	450	131	342.51	24.51	728.27	31.94	330	23.63
	204	450	155	161.20	10.20	297.99	11.30	160	9.84
	207a	450	87.7	2067.34	10.36	6138.16	11.50	2000	10.00
	207	450	83.8	2534.65	11.77	7816.00	13.38	2400	11.35

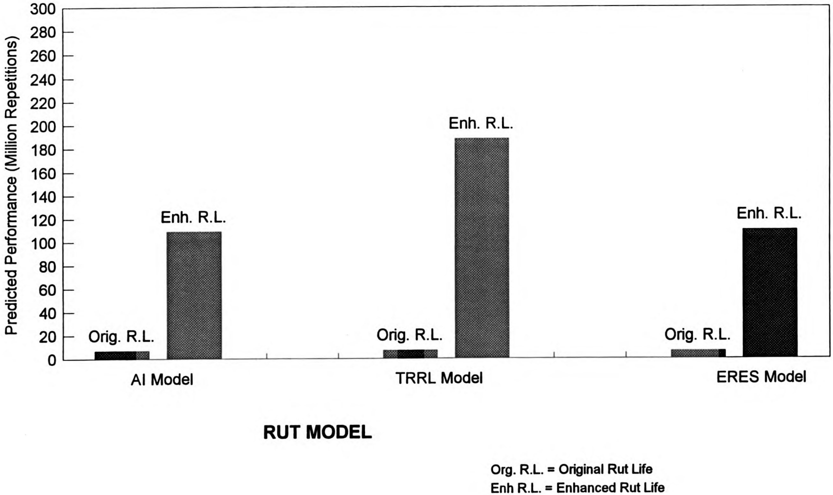

Figure 7.6: Comparison of original and enhanced rut life of pavement section 199. Axle load = 28 kip, Tire pressure = 120 psi, Base Type = Asphalt stab.

7.3 TRIAL 2, ELIMINATING SUBBASE AND REPLACING GRANULAR BASE WITH ASPHALT TREATED BASE (Layer Modulus Less than or equal to 200 Ksi).

In this trial, the subbase was eliminated and granular base layer of each pavement section of Figure 3.2 was replaced by an Asphalt Treated base (while keeping the same thicknesses). Mechanistic analysis was than conducted, and the fatigue life (in terms of 18 Kip ESAL) and the number of ESALs to 0.5 inch rut were then computed using various prediction models. Table 7.7, Table 7.9 and Table 7.11 present the original and enhanced fatigue lives and Table 7.8, Table 7.10 and Table 7.12 present the original and enhanced rut lives. Figure 7.7, Figure 7.9 and Figure 7.11 present the comparison of the original and enhanced fatigues lives whereas Figure 7.8, Figure 7.10 and Figure 7.12 present the comparison of the original and enhanced rut lives for pavement section 199 (Monismith model exhibits very low original and enhanced fatigue performance therefore it has not been discussed and shown in Figures). From the examination of the results in this trial following is observed:-

1. For the combination of 18-kip axle load and 80 psi tire pressure, elimination of the subbase layer and enhancement of granular base to asphalt treated base, following is seen:
   a. To exhibit fatigue life equal to or greater than the AASHTO input ESALs the layer moduli

of the asphalt treated base needs to be increased in the range of 110 ksi to 160 ksi (see Table 7.7).

b. The magnitude of enhancement varies with the type of fatigue/rut prediction models. This result is similar to what was predicted in Trial 1. Asphalt Institute model exhibits the magnitude of enhanced fatigue life almost equal to or slightly greater than the AASHTO input ESALs whereas the MICHPAVE and NAASRA fatigue models exhibit the magnitude of fatigue lives much greater than the AASHTO input ESALs except for section 199 in which the fatigue life predicted by MICHPAVE model is slightly shorter than the AASHTO input ESALs (see Table 7.7). Figure 7.7 presents the comparison of the enhanced fatigue lives predicted by various fatigue models for pavement section 199.

c. At this load and tire pressure, the magnitude of enhanced rut life exhibited by all the rut criterion namely Asphalt Institute, TRRL and ERES is much greater than the AASHTO design life (see Table 7.8). Figure 7.8 present the comparison of the enhanced rut lives predicted by various rut models for pavement section 199.

Table 7.7: Fatigue life (Million repetitions) of AASHTO designed sections of Figure 3.2 (Subbase eliminated and granular base replaced with asphalt treated base) with respect to various fatigue models. Axle load = 18-kip, Tire pressure = 80 psi.

AASHTO Design ESALs $*10^6$	Cell No.	Base M_R (Ksi)	Radial tensile strain, bottom of AC Layer (μstrain)	Asphalt Institute Model		Monsmith Model		Michpave Model		NASRA Model	
				Enhanced Fatigue Life	Original Fatigue Life	Enhanced Fatigue Life	Original Fatigue Life	Enhanced Fatigue Life	Original Fatigue Life	Enhanced Fatigue Life	Original Fatigue Life
25	199	130	90.9	24.39	4.49	1.32	0.23	20.98	4.09	92.92	7.11
	202	130	88.5	26.63	4.49	1.45	0.23	43.28	5.87	106.22	7.11
	205	120	88.9	26.24	5.01	1.43	0.26	108.6	11.09	103.85	8.40
	205a	110	90.2	25.02	5.62	1.36	0.29	210.7	24.60	96.58	9.99
50	200	150	73.1	49.96	7.15	2.79	0.37	55.94	8.61	276.26	14.39
	203	150	71.4	53.98	7.33	3.02	0.38	116.6	12.62	310.75	14.95
	206	140	72.8	52.99	8.12	2.96	0.42	299.7	23.79	302.20	17.45
	206a	130	72.8	50.64	9.02	2.83	0.47	592.2	52.36	282.00	20.48
75	201	160	65.0	73.52	9.78	4.17	0.51	97.4	13.74	496.99	23.17
	204	160	63.5	79.39	9.78	4.51	0.51	204.5	20.28	558.53	23.17
	207	150	63.9	77.77	10.63	4.42	0.56	533.6	38.47	541.26	26.30
	207a	140	64.7	74.65	11.92	4.23	0.63	1064.0	84.36	508.62	31.30

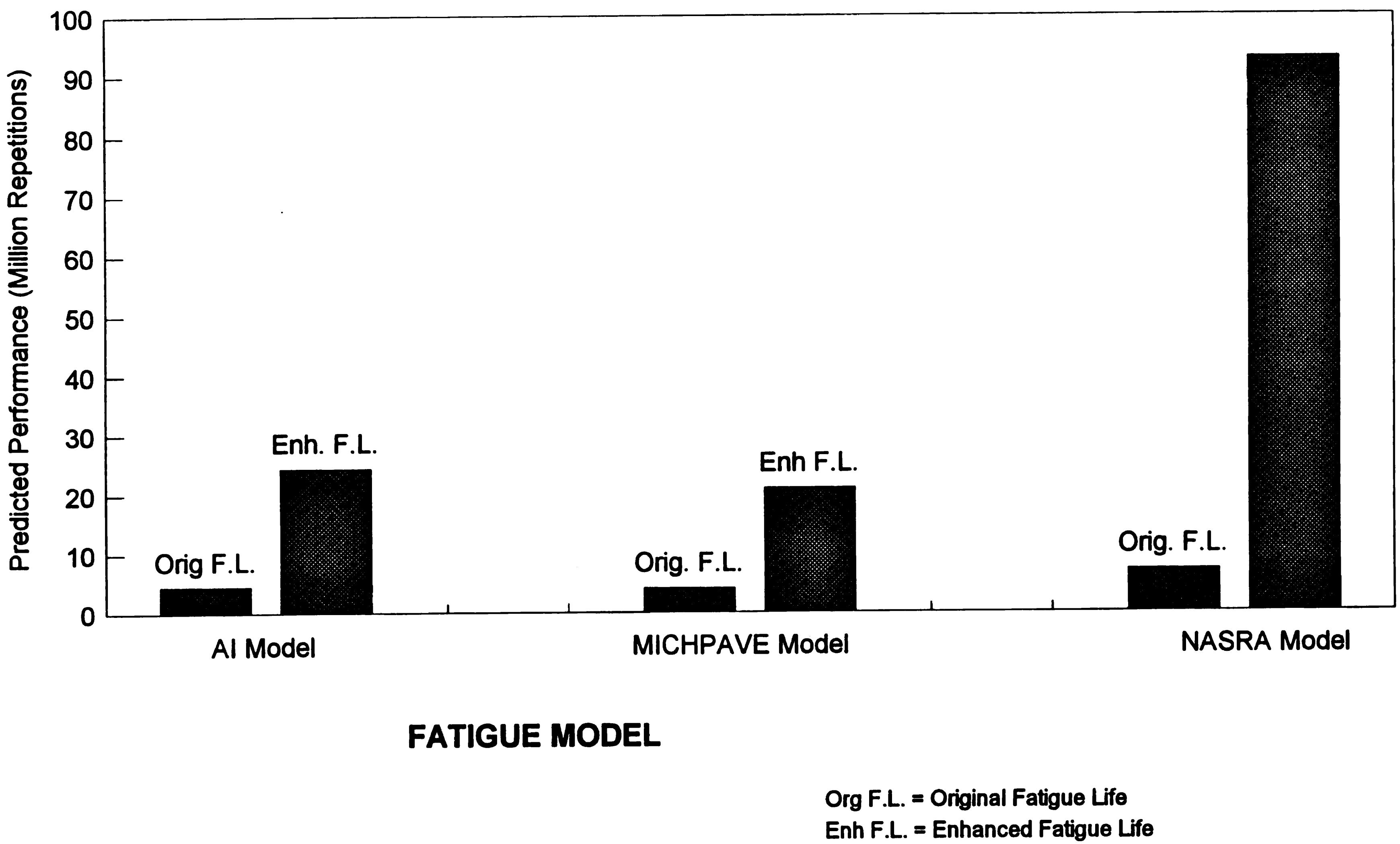

Figure 7.7: Comparison of original and enhanced fatigue life of pavement section 199. Axle load = 18 kip, Tire pressure = 80 psi, Base type = Asphalt treated

Table 7.8: Rut life (Million repetitions) of AASHTO designed sections of Figure 3.2 (Subbase Eliminated and Granular Base Replaced with Asphalt Treated Base) with respect to various rut models. Axle load = 18-kip, Tire pressure = 80 psi.

AASHTO Design ESALs $*10^6$	Cell No.	Base M_R (Ksi)	Vertical compressive strain, top of roadbed (μstrain)	Asphalt Institute Model		TRRL Model		ERES Model	
				Enhanced Rut Life	Original Rut Life	Enhanced Rut Life	Original Rut Life	Enhanced Rut life	Original Rut Life
25	199	200	126	407.75	49.21	895.51	72.97	390	47.43
	202	200	121	488.85	20.35	1110.40	25.61	470	19.36
	205a	200	112	691.12	21.11	1674.16	26.72	660	20.36
	205	180	112	691.12	24.51	1674.16	31.94	660	23.64
50	200	200	107	848.03	112.37	2133.85	194.23	820	110.00
	203	200	102	1050.80	46.06	2751.45	67.49	1000	44.40
	206a	200	95.4	1417.99	47.08	2925.49	69.24	1400	45.38
	206	200	90.4	1804.75	53.82	5224.85	81.17	1700	51.87
75	201	200	96.8	1328.40	175.95	3633.85	330.60	1300	170.00
	204	200	92.6	1620.44	74.76	1760.05	119.81	1600	72.03
	207a	200	86.6	2187.61	74.76	6563.80	119.81	2010	72.03
	207	200	82.3	2748.27	84.58	8603.09	138.71	2600	81.49

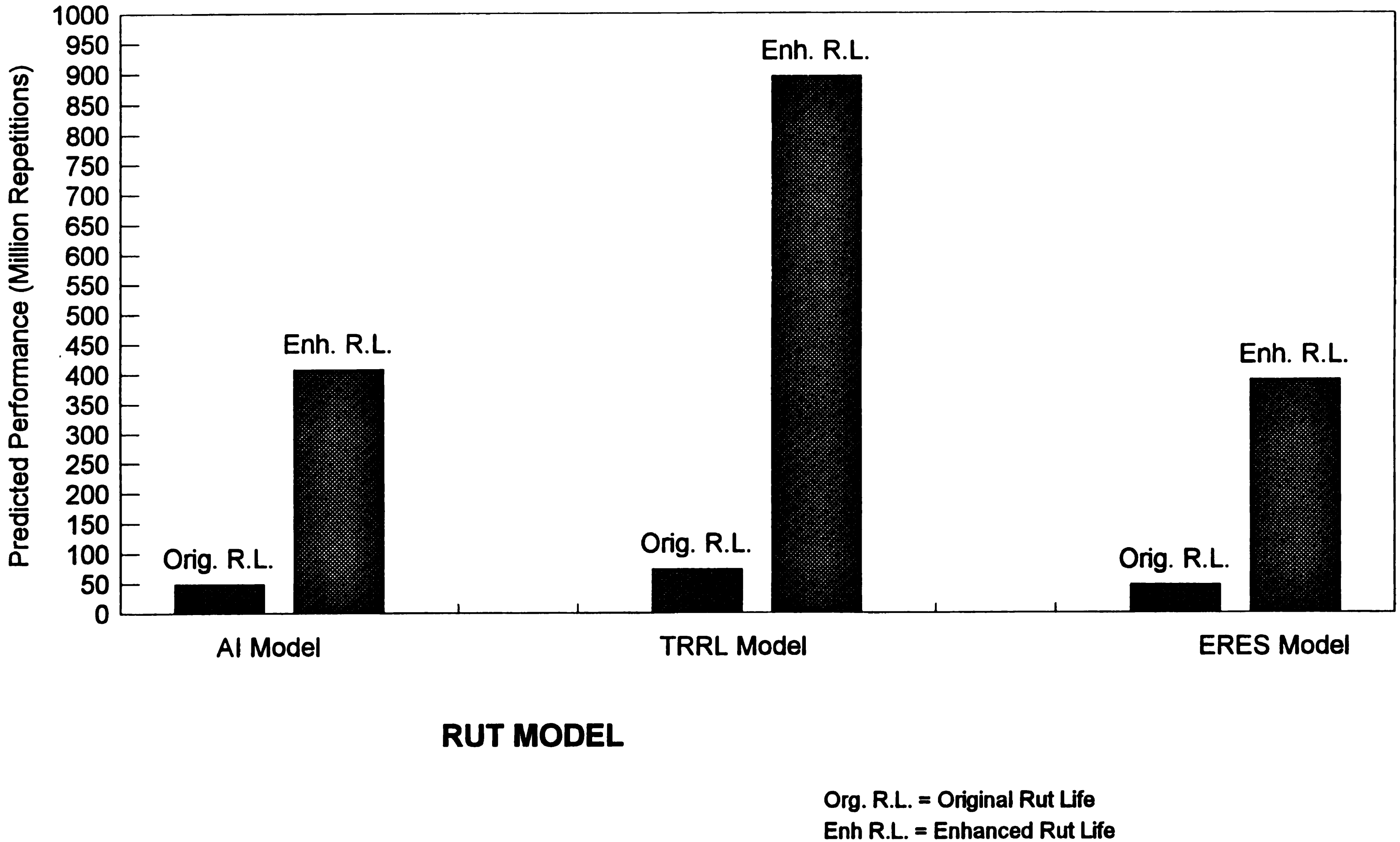

Figure 7.8: Comparison of original and enhanced rut life of pavement section 199. Axle load = 18 kip, Tire pressure = 80 psi, Base Type = Asphalt treated.

2. For combination of 23 kip axle load and 120 psi tire pressure after elimination of subbase, the asphalt treated base modulus was increased to a maximum value of 200 ksi. From the examination of the results, it is observed that:

   a. The elimination of subbase and replacement of granular base with asphalt treated base enhances the magnitude of the fatigue life of the pavement sections considered in this study but it remains less than the AASHTO input ESALs with some of the fatigue criterion. For example, the enhanced fatigue life of all the pavement sections of this study with MICH-PAVE fatigue criterion is greater than the AASHTO input ESALs and this is true for some of the pavement sections with NAASRA fatigue criterion whereas the magnitude of the enhanced fatigue life with Asphalt Institute fatigue criterion remains shorter than the AASHTO input ESALs by 50% to 82% (see Table 7.9). Figure 7.9 present the comparison of the enhanced fatigue lives predicted by various fatigue models for pavement section 199.

   b. For this load and tire pressure, the magnitude of enhanced rut life exhibited by all the rut criterion namely Asphalt Institute, TRRL and ERES is much greater than the AASHTO input

Table 7.9: Fatigue life (Million repetitions) of AASHTO designed sections of Figure 3.2 (Subbase Eliminated and Granular Base Replaced with Asphalt Treated Base) with respect to various fatigue models. Axle load = 23 kips, Tyre pressure = 120 psi.

AASHTO Design ESALs $*10^6$	Cell No.	Base M_R (Ksi)	Radial tensile strain, bottom of AC Layer (μstrain)	Asphalt Institute Model		Monsmith Model		Michpave Model		NASRA Model	
				Enhanced Fatigue Life	Original Fatigue Life	Enhanced Fatigue life	Original Fatigue Life	Enhanced Fatigue life	Original Fatigue Life	Enhanced Fatigue life	Original Fatigue life
25	199	200	143	5.49	1.71	0.28	0.083	26.45	2.21	9.64	1.63
	202	200	135	6.64	1.73	0.34	0.085	55.73	3.24	12.86	1.67
	205a	200	122	9.26	1.88	0.48	0.092	166.00	6.18	21.34	1.90
	205	200	112	12.27	2.12	0.64	0.104	381.40	13.62	32.72	2.27
50	200	200	120	9.78	2.83	0.51	0.141	51.50	4.60	23.17	3.51
	203	200	113	11.92	2.88	0.63	0.144	109.40	6.88	31.30	3.61
	206a	200	103	16.17	3.11	0.87	0.156	327.90	13.18	49.74	4.06
	206	200	95.1	21.02	3.50	1.12	0.176	752.40	28.90	74.13	4.86
75	201	200	109	13.42	3.80	0.71	0.191	77.52	7.28	37.48	5.50
	204	200	103	16.17	3.88	0.87	0.196	165.50	10.97	49.74	5.67
	207a	200	93.4	22.31	4.21	1.20	0.213	499.20	21.16	81.13	6.44
	207	200	86.4	28.82	4.69	1.58	0.239	1147	46.37	119.77	7.59

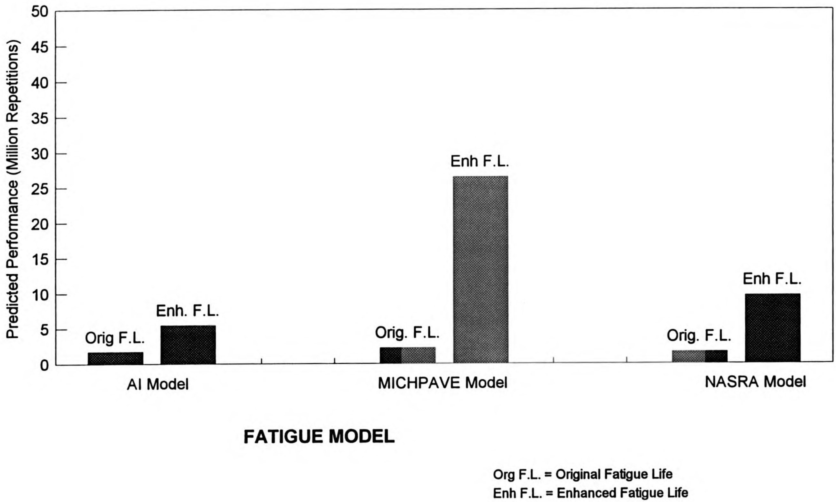

Figure 7.9: Comparison of original and enhanced fatigue life of pavement section 199. Axle load = 23 kip, Tire pressure = 120 psi, Base type = Asphalt treated

ESALs (see Table 7.10). Figure 7.10 present the comparison of the enhanced rut lives predicted by various rut models for pavement section 199.

3. For combination of 28 kip axle load and 120 psi tire pressure, the elimination of subbase and use of the highest value of the asphalt treated base modulus i.e., 200 ksi (please remember this is the highest value of asphalt treated base used for this study), the examination of the results indicates that:

   a. For the combination of 28-kip axle load and 120 psi tire pressure, the magnitude of the enhanced fatigue life is greater than the AASHTO input ESALs only with MICH-PAVE criterion except for pavement sections 199, 200, and 201 for which the fatigue life is less than the AASHTO input ESALs by about 40% (see Table 7.11). The magnitude of enhanced fatigue life exhibited by the other fatigue criterion namely Asphalt Institute and NAASRA is less than the AASHTO input EASLs by about 72% to 89% and 37% to 84% respectively. Figure 7.11 present the comparison of the enhanced fatigue lives predicted by various fatigue models for pavement section 199.

Table 7.10: Rut life (Million repetitions) of AASHTO designed sections of Figure 3.2 (Subbase Eliminated and Granular Base Replaced with Asphalt Treated Base) with respect to various rut models. Axle load = 23 kips, Tire pressure =12 psi.

AASHTO Design ESALs $*10^6$	Cell No.	Base M_R (Ksi)	Vertical compressive strain, top of roadbed (μstrain)	Asphalt Institute Model		TRRL Model		ERES Model	
				Enhanced Rut Life	Original Rut Life	Enhanced Rut Life	Original Rut Life	Enhanced Rut Life	Oroginal Rut Life
25	199	200	163	128.66	16.73	228.06	20.30	120	16.14
	202	200	156	156.62	6.82	287.95	7.00	150	6.58
	205a	200	146	210.74	6.72	409.45	6.89	200	6.49
	205	200	138	271.26	7.65	552.32	8.04	260	7.39
50	200	200	173	280.25	38.00	574.08	53.67	270	36.63
	203	200	131	342.51	15.61	728.27	18.71	330	15.06
	206a	200	123	454.23	15.09	1017.80	17.95	440	14.55
	206	200	117	568.30	17.03	1327.54	20.73	550	16.42
75	201	200	124	438.04	60.36	974.924	92.96	420	58.17
	204	200	119	526.74	24.98	1213.24	32.66	510	24.09
	207a	200	112	691.12	24.05	1674.16	31.22	660	23.19
	207	200	106	884.46	26.98	2242.95	35.79	850	26.02

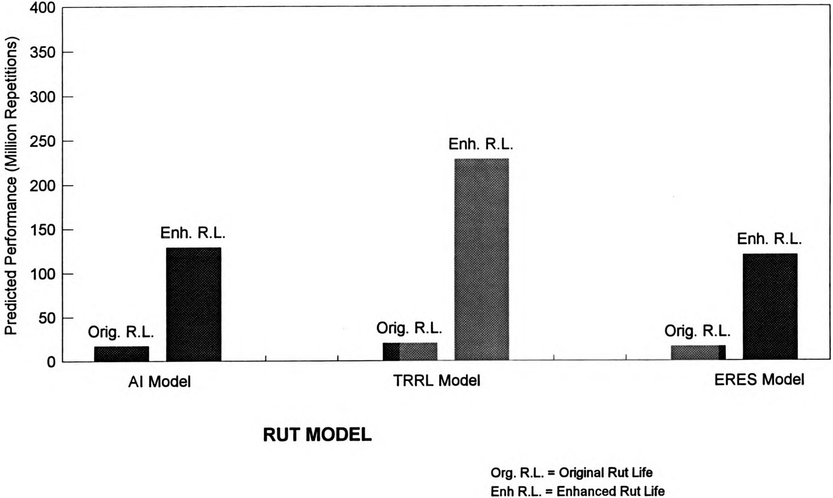

Figure 7.10: Comparison of original and enhanced rut life of pavement section 199. Axle load = 23 kip, Tire pressure = 120 psi, Base Type = Asphalt treated.

Table 7.11: Fatigue life (Million repetitions) of AASHTO designed sections of Figure3.2 (Subbase Eliminated and Granular Base Replaced with Asphalt Stabilized Base) with respect to various fatigue models. Axle load = 28 kips, Tire pressure = 120 psi.

AASHTO Design ESALs $*10^6$	Cell No.	Base M_R (Ksi)	Radial tensile strain, bottom of AC Layer (μstrain)	Asphalt Institute Model		Monsmith Model		Michpave Model		NASRA Model	
				Enhanced Fatigue Life	Original Fatigue life	Enhanced Fatigue life	Original Fatigue Life	Enhanced Fatigue life	Original Fatigue Life	Enhanced Fatigue Life	Original Fatigue Life
25	199	200	172	2.99	1.09	0.15	0.052	14.78	1.20	3.83	0.82
	202	200	162	3.64	1.10	0.18	0.052	30.80	1.73	5.17	0.84
	205a	200	146	5.13	1.20	0.26	0.057	91.10	3.26	8.69	0.95
	205	200	134	6.80	1.37	0.35	0.066	209.70	7.25	13.35	1.17
50	200	200	145	5.25	1.73	0.27	0.084	29.60	2.56	9.00	1.67
	203	200	137	6.32	1.76	0.32	0.086	62.06	3.73	11.95	1.71
	206a	200	124	8.78	1.95	0.46	0.095	183.90	7.02	19.67	1.99
	206	200	114	11.58	2.19	0.6	0.110	421.00	15.46	29.95	2.39
75	201	200	132	7.15	2.31	0.37	0.110	45.40	4.10	14.39	2.59
	204	200	124	8.78	2.35	0.46	0.120	95.59	6.01	19.67	2.66
	207a	200	113	11.92	2.58	0.63	0.130	284.00	11.36	31.30	3.05
	207	200	104	15.66	2.88	0.83	0.140	649.70	24.93	47.40	3.61

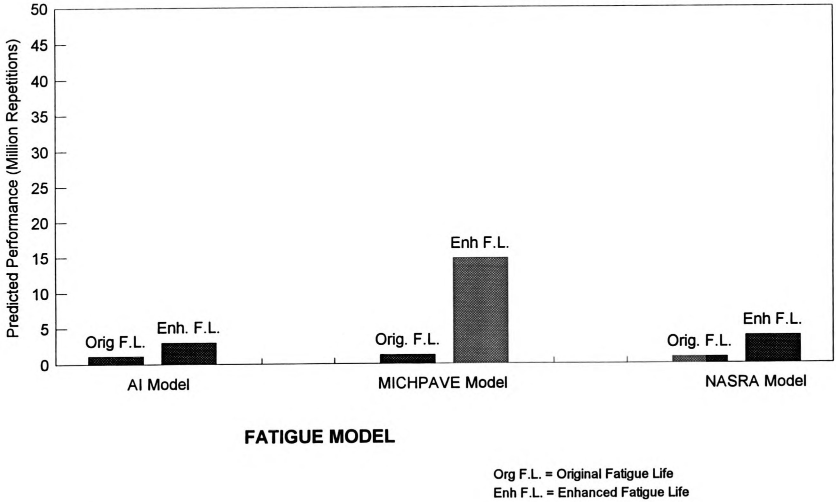

Figure 7.11: Comparison of original and enhanced fatigue life of pavement section 199. Axle load = 28 kip, Tire pressure = 120 psi, Base type = Asphalt treated

b. For this load and tire pressure, the magnitude of enhanced rut life exhibited by all the rut criterion namely Asphalt Institute, TRRL and ERES is much greater than the AASHTO input ESALs (see Table 7.12). Figure 7.12 present the comparison of the enhanced rut lives predicted by various rut models for pavement section 199.

4. For the combination of standard axle load of 18 Kip and 80 Psi tire pressure, the results (presented for fatigue life in Table 7.1 and Table 7.7 and for rut life in Table 7.2 and Table 7.8) indicate that the replacement of granular base with asphalt stabilized base (M_R base equal to or greater than 250 ksi) and the elimination of subbase and replacement of granular base with asphalt treated base (M_R base less than or equal to 200 Ksi) exhibits the magnitude of enhanced fatigue/rut life equal to or greater than the AASHTO input ESALs in both cases. This mean that for a standard axle load of 18 kip and tire pressure of 80 psi, the use of asphalt treated base when no subbase is used may give economical pavement sections for obvious reasons.

Table 7.12: Rut life (Million repetitions) of AASHTO designed sections of Figure 3.2 (Subbase Eliminated and Granular Base Replaced with Asphalt Treated Base) with respect to various rut models. Axle load = 28 kips, Tire pressure =120 psi.

AASHTO Design ESALs $*10^6$	Cell No.	Base M_R (Ksi)	Vertical compressive strain, top of roadbed (μstrain)	Asphalt Institute Model		TRRL Model		ERES Model	
				Enhanced Rut Life	Original Rut Life	Enhanced Rut Life	Original Rut Life	Enhanced Rut Life	Original Rut Life
25	199	200	196	56.33	6.82	85.64	7.00	54	6.58
	202	200	187	69.53	2.83	109.97	2.47	67	2.74
	205a	200	174	96.02	2.97	161.20	2.61	92	2.87
	205	200	165	121.82	3.43	213.79	3.10	120	3.31
50	200	200	166	118.57	15.35	207.00	18.34	110	14.80
	203	200	158	147.93	6.35	269.10	6.45	140	6.13
	206a	200	148	198.28	6.54	380.86	6.67	190	6.31
	206	200	140	254.33	7.55	511.71	7.90	240	7.28
75	201	200	150	186.71	24.51	354.68	31.94	180	23.63
	204	200	144	224.17	10.20	440.56	11.30	220	9.84
	207a	200	134	309.47	10.36	645.72	11.50	300	10.00
	207	200	128	379.97	11.77	823.66	13.38	370	11.35

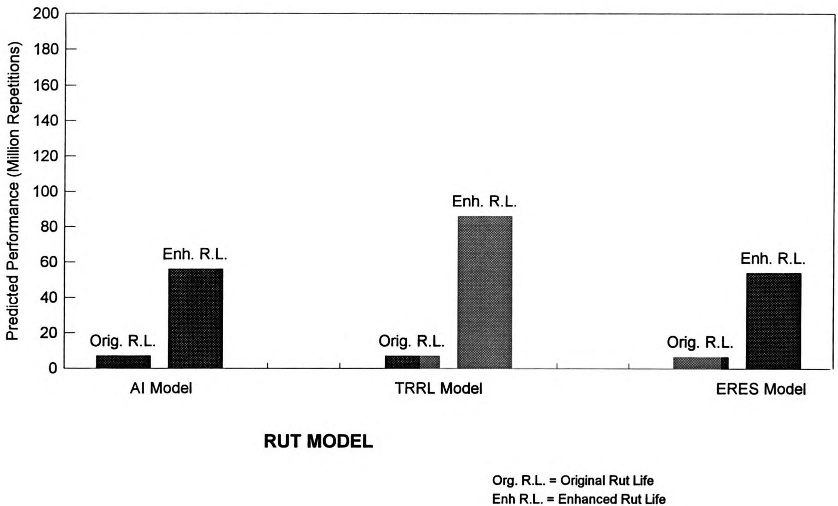

Figure 7.12: Comparison of original and enhanced rut life of pavement section 199. Axle load = 28 kip, Tire pressure = 120 psi, Base Type = Asphalt treated.

7.4 TRIAL 3, INCREASING LAYER MODULI (through compaction) OF THE GRANULAR BASE AND SUBBASE LAYER

In this trial the layer moduli of granular base and subbase layer of each pavement section of Figure 3.2 was increased upto a value of 75 Ksi and 40 Ksi respectively, mechanistic analysis was then conducted, the fatigue life (in terms of 18 Kip ESAL) and the number of ESAL to 0.5 inch rut were then computed using various prediction models as was done in Trial 1 and Trial 2 of the study. The original and enhanced fatigue lives are listed in Table 7.13, Table 7.15 and Table 7.17. The original and enhanced rut lives are listed in Table 7.14, Table 7.16 and Table 7.18. Figure 7.13, Figure 7.15 and Figure 7.17 present the comparison of original and enhanced fatigue lives. Figure 7.14, Figure 7.16 and Figure 7.18 present the comparison of original and enhanced rut lives for pavement section 199 (Monismith model exhibit very low original and enhanced fatigue performances, therefore it has not been discussed and shown in the Figures). Examination of the results in this trial indicate that :

1. For the combination of 18-kip axle load and 80 psi tire pressure, by increasing the layer moduli (through compaction) of the granular base and subbase layer following is seen:

   a. The magnitude of the fatigue and rut lives of pavement sections is enhanced. The enhancement varies with the type of fatigue and rut prediction model. This result is similar to the results observed in Trial 1 and Trial 2. The Enhanced fatigue life exhibited by MICHPAVE and NAASRA fatigue models is equal to or greater than the AASHTO input ESALs whereas Asphalt Institute model exhibit enhanced fatigue life which is almost half of the AASHTO input ESALs (see Table 7.13). Figure 7.13 present the comparison of the enhanced fatigue lives predicted by various fatigue models for pavement section 199.

b. The magnitude of enhanced rut life exhibited by all the rut criterion used in this study namely Asphalt Institute, TRRL and ERES is much higher than the AASHTO input ESALs (see Table 7.14). Figure 7.14 present the comparison of the enhanced rut lives predicted by various rut models for pavement section 199.

2. For the combination of 23-kip axle load and 120 psi tire pressure, by increasing the layer moduli (through compaction) of the granular base and subbase layer following is seen:

   a. The magnitude of enhanced fatigue life exhibited by MICHPAVE fatigue criterion is equal to or greater than the AASHTO input ESALs for only half of the pavement sections

Table 7.13: Fatigue life (Million repetitions) of AASHTO designed sections of Figure 3.2 (Granular Base and subbase but with Increased Modulus) with respect to various fatigue models. Axle load = 18 kips, Tire pressure = 80 psi.

AASHTO Design ESALs $*10^6$	Cell No.	Base M_R Ksi	Sub-base M_R (ksi)	Radial strain, bottom of AC Layer (μstrain)	Asphalt Institute Model		Monsmith Model		Michpave Model		NASRA Model	
					Enhanced Fatigue Life	Original Fatigue Life	Enhanced Fatigue Life	Original Fatigue Life	Enhanced Fatigue Life	Original Fatigue life	enhanced fatigue Life	Original Fatigue life
25	199	75	40	104	15.66	4.49	0.83	0.23	23.06	4.09	47.40	7.11
	202	75	40	107	14.26	4.49	0.76	0.23	30.80	5.87	41.11	7.11
	205a	75	-	111	12.64	5.01	0.66	0.26	46.30	11.09	34.22	8.40
	205	75	-	107	14.26	5.62	0.76	0.29	105.60	24.60	41.11	9.99
50	200	75	40	91.2	24.13	7.15	1.32	0.37	45.40	8.61	91.40	14.39
	203	75	40	93.5	22.23	7.33	1.20	0.38	62.80	12.62	80.70	14.95
	206a	75	-	97.4	19.43	8.12	1.04	0.42	96.90	23.79	65.78	17.45
	206	75	-	94.1	21.77	9.02	1.17	0.47	219.20	52.36	78.16	20.48
75	201	75	40	84.2	31.38	9.78	1.70	0.51	69.60	13.74	136.25	23.17
	204	75	40	86.3	28.93	9.78	1.58	0.51	97.60	20.28	120.46	23.17
	207a	75	-	89.8	25.39	10.63	1.38	0.56	153.80	38.47	98.75	26.30
	207	75	-	86.8	28.39	11.92	1.55	0.63	346.80	84.36	117.03	31.30

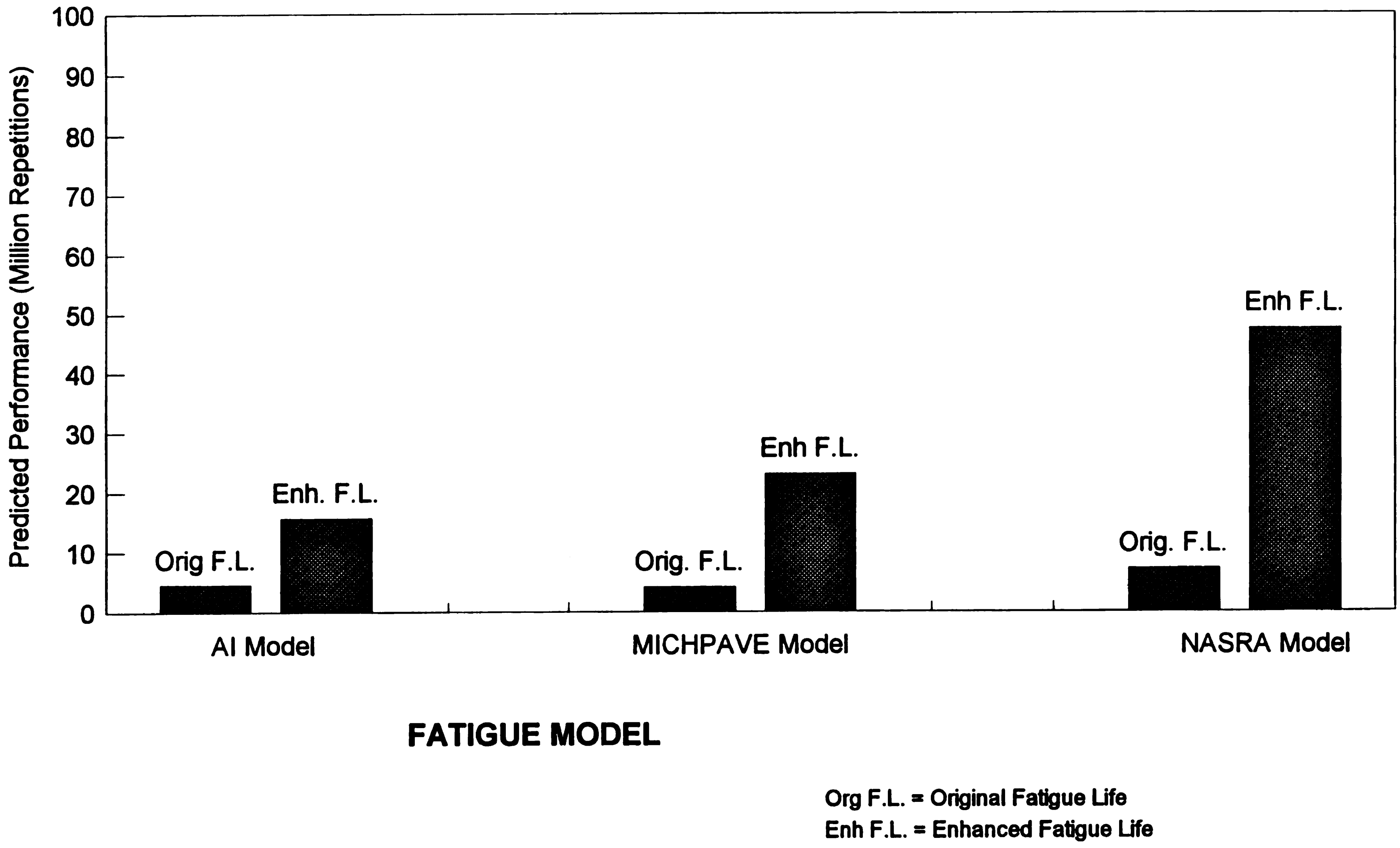

Figure 7.13: Comparison of original and enhanced fatigue life of pavement section 199. Axle load = 18 kip, Tire pressure = 80 psi, Base type = Enhanced Granular

Table 7.14: Rut life (Million repetitions) of AASHTO designed sections of Figure 3.2 (Granular Base and Subbase but with Increased modulus values) with respect to various rut models. Axle load = 18 kips, Tire pressure = 80 psi.

AASHTO Design ESALs $*10^6$	Cell No.	Base M_R (Ksi)	Subbase M_R (ksi)	Vertical compressive strain, top of roadbed (μstrain)	Asphalt Institute Model		TRRL Model		ERES Model	
					Enhanced Rut Life	Original Rut Life	Enhanced Rut Life	Original Rut Life	Enhanced Rut Life	Original Rut Life
25	199	75	40	122	471.15	49.21	1062.92	72.97	450	47.43
	202	75	40	152	175.95	20.35	330.60	25.61	170	19.62
	205a	75	-	173	98.54	21.11	166.22	26.72	95	20.36
	205	75	-	163	128.66	24.51	228.07	31.94	120	23.64
50	200	75	40	103	1005.87	112.37	2612.49	194.23	970	110.00
	203	75	40	128	379.97	46.06	823.66	67.49	370	44.40
	206a	75	-	146	210.74	47.08	409.45	69.49	200	45.38
	206	75	-	138	271.26	53.82	552.32	81.17	260	51.87
75	201	75	40	93.5	1551.72	175.95	4368.14	330.60	1500	170.00
	204	75	40	116	590.58	74.76	1389.45	119.81	570	72.03
	207a	75	-	132	331.04	74.76	699.42	119.81	320	72.03
	207	75	-	125	422.56	84.58	934.22	138.71	410	81.49

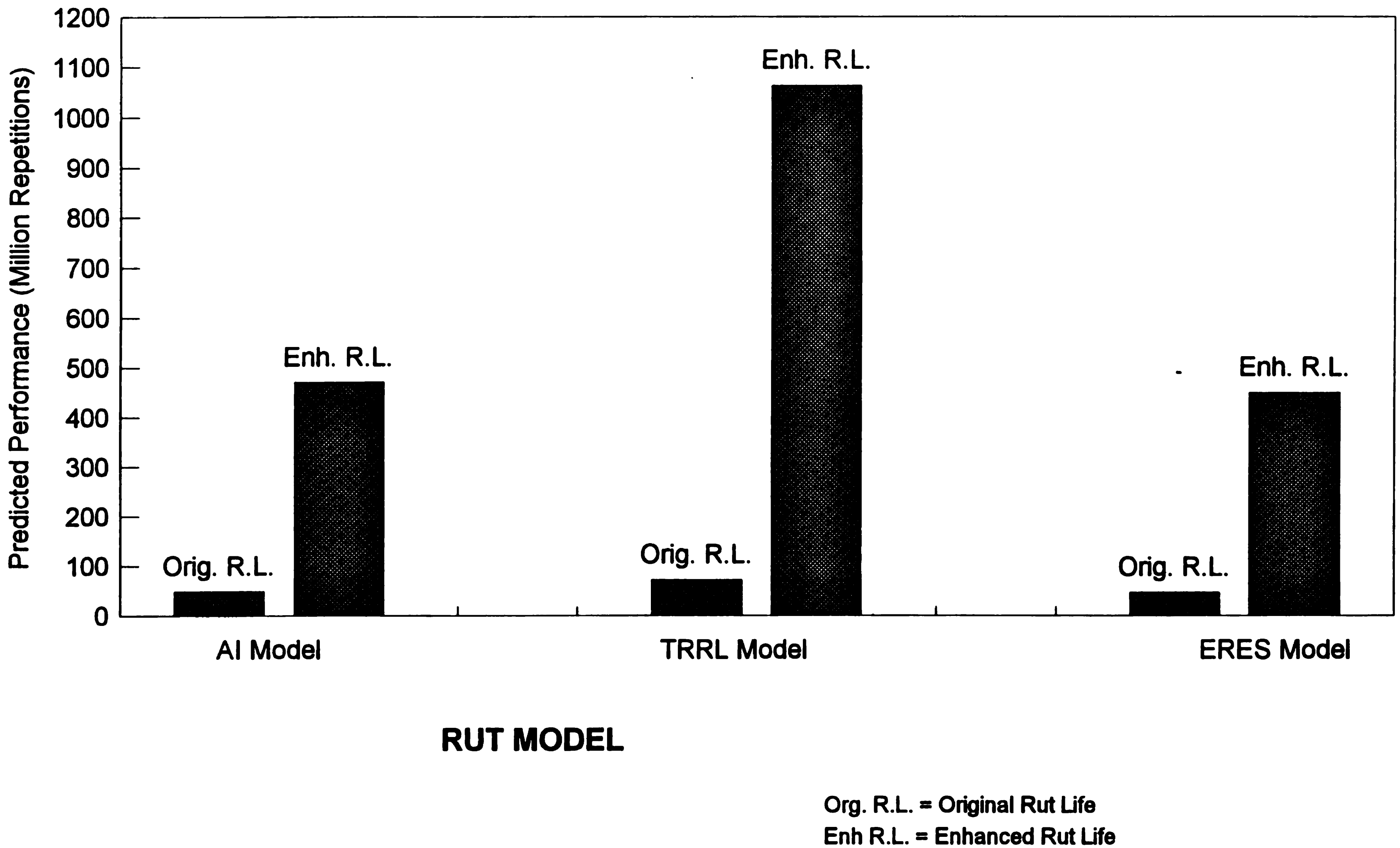

Figure 7.14: Comparison of original and enhanced rut life of pavement section 199. Axle load = 18 kip, Tire pressure = 80 psi, Base Type = Enhanced granular.

(i.e, pavement section numbers 205, 205a, 206, 206a, 207, and 207a). Please note that these are those pavement sections in which no subbase has been used. The magnitude of enhanced fatigue life exhibited by other fatigue criterion for all pavement sections considered in this study remains less than the AASHTO input ESALs. In Asphalt Institute model the magnitude of enhanced fatigue life is shorter than the AASHTO input ESALs by about 80% to 82%. In NAASRA fatigue model the magnitude of enhanced fatigue life is shorter than the AASHTO input ESALs by about 68% to 70% (see Table 7.15). Figure 7.15 present the comparison of the enhanced fatigue lives predicted by various fatigue models for pavement section 199.

b. The magnitude of enhanced rut life exhibited by all the rut criterion (considered in this study) is equal to or greater than the AASHTO input ESALs (see Table 7.16). Figure 7.16 present the comparison of the enhanced rut lives predicted by various rut models for pavement section 199.

3. For the combination of 28-kip axle load and tire pressure of 120 psi, by increasing the layer moduli

Table 7.15: Fatigue life (Million repetitions) of AASHTO designed sections of Figure 3.2 (Granular Base and subbase but with Increased Modulus) with respect to various fatigue models. Axle load = 23 kips, Tire pressure = 120 psi.

AASHTO Design ESALs $*10^6$	Cell No.	Base M_R Ksi	Sub-base M_R (ksi)	Radial strain, bottom of AC Layer (μstrain)	Asphalt Institute Model		Monsmith Model		Michpave Model		NASRA Model	
					Enhanced Fatigue Life	Original Fatigue Life	Enhanced Fatigue Life	Original Fatigue Life	Enhanced Fatigue Life	Original Fatigue life	Enhanced Fatigue Life	Original Fatigue life
25	199	75	40	140	5.89	1.71	0.30	0.083	11.85	2.21	10.72	1.63
	202	75	40	144	5.37	1.73	0.27	0.085	16.41	3.24	9.31	1.67
	205a	75	-	150	4.69	1.88	0.24	0.092	25.57	6.18	7.59	1.90
	205	75	-	145	5.25	2.12	0.27	0.104	57.95	13.62	9.00	2.27
50	200	75	40	122	9.26	2.83	0.48	0.141	23.16	4.60	21.34	3.51
	203	75	40	125	8.55	2.88	0.45	0.144	33.07	6.88	18.90	3.61
	206a	75	-	130	7.52	3.11	0.39	0.156	52.96	13.18	15.53	4.06
	206	75	-	126	8.33	3.50	0.44	0.176	119.50	28.90	18.16	4.86
75	201	75	40	112	12.27	3.80	0.64	0.191	35.24	7.28	32.72	5.50
	204	75	40	115	11.25	3.88	0.59	0.196	50.92	10.97	28.67	5.67
	207a	75	-	120	9.78	4.21	0.51	0.213	83.31	21.16	23.17	6.44
	207	75	-	116	10.93	4.69	0.57	0.239	187.90	46.37	27.46	7.59

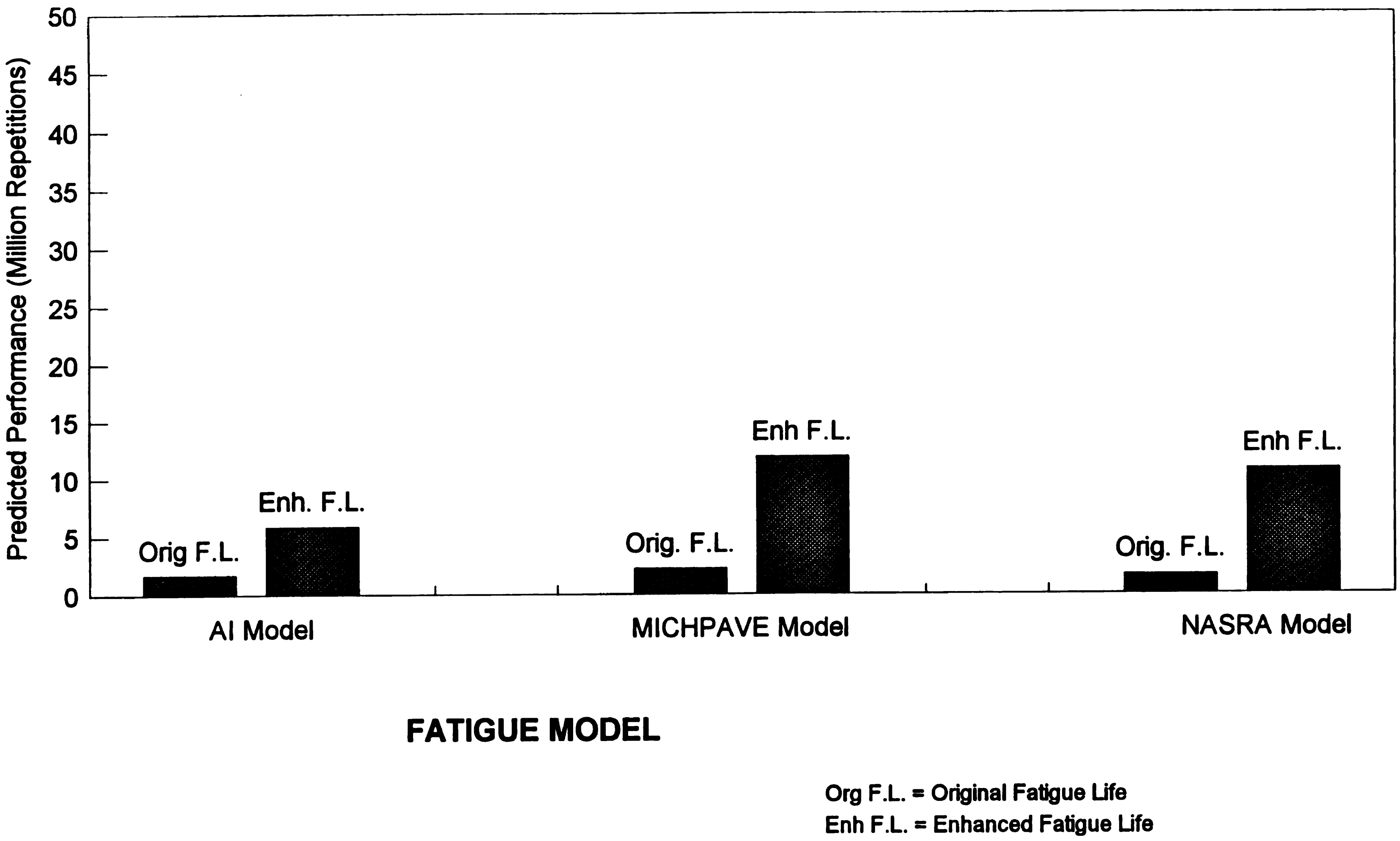

Figure 7.15: Comparison of original and enhanced fatigue life of pavement section 199. Axle load = 23 kip, Tire pressure = 120 psi, Base type = Enhanced Granular

Table 7.16: Rut life (Million repetitions) of AASHTO designed sections of Figure 3.2 (Granular Base and Subbase but with Increased modulus values) with respect to various rut models. Axle load = 23 kips, Tire pressure = 120 psi.

AASHTO Design ESALs $*10^6$	Cell No.	Base M_R (Ksi)	Subbase M_R (Ksi)	Vertical compressive strain, top of roadbed (μstrain)	Asphalt Institute Model		TRRL Model		ERES Model	
					Enhanced Rut Life	Original Rut Life	Enhanced Rut Life	Original Rut Life	Enhanced Rut Life	Original Rut Life
25	199	75	40	156	156.62	16.73	287.96	20.30	150	16.14
	202	75	40	195	57.64	6.82	88.00	7.00	56	6.58
	205a	75	-	224	30.97	6.72	42.15	6.89	30	6.49
	205	75	-	212	39.63	7.65	56.15	8.04	38	7.39
50	200	75	40	132	331.04	38.00	699.42	53.67	320	36.63
	203	75	40	163	128.66	15.61	228.07	18.71	120	15.06
	206a	75	-	188	67.89	15.09	106.88	17.95	65	14.55
	206	75	-	178	86.73	17.03	142.87	20.73	84	16.42
75	201	75	40	120	507.36	60.36	1160.46	92.96	490	58.17
	204	75	40	148	198.28	24.98	380.92	32.66	190	24.09
	207a	75	-	170	106.57	24.05	182.38	31.22	100	23.19
	207	75	-	161	135.98	26.98	243.51	35.79	130	26.02

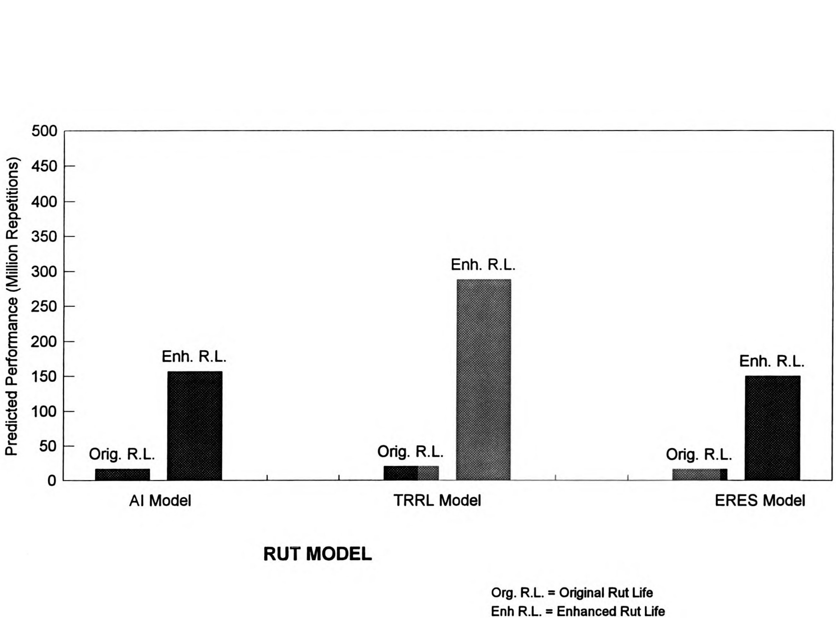

Figure 7.16: Comparison of original and enhanced rut life of pavement section 199. Axle load = 23 kip, Tire pressure = 120 psi, Base Type = Enhanced granular.

(through compaction) of the granular base and subbase layer following is seen:

a. The magnitude of enhanced fatigue life exhibited by MICHPAVE fatigue criterion is equal to or greater than the AASHTO input ESALs only for three of the pavement sections considered in this study (i.e, pavement section number 205a, 206a, 207a) (see Table 7.17). Please note that these are those pavement sections which has stronger roadbed soils (M_R 20 Ksi). The magnitude of enhanced fatigue life exhibited by all other fatigue criterion for all the pavement sections of this study remains much shorter than the AASHTO input ESALs. Figure 7.17 presents the comparison of the enhanced fatigue lives for pavement section 199.

b. The magnitude of enhanced rut life exhibited by Asphalt Institute and ERES rut criterion is higher than the AASHTO input ESALs only for half of the pavement sections (i.e, pavement section 199, 200, 201, 202,203 and 204)(See Table 7.18). Please remember that these are those pavement sections in which some thickness of subbase has been used. The magnitude of enhanced rut life exhibited by TRRL rut criterion is equal to or higher than

Table 7.17: Fatigue life (Million repetitions) of AASHTO designed sections of Figure 3.2 (Granular Base and subbase but with Increased Modulus) with respect to various fatigue models. Axle load = 28 kips, Tire pressure = 120 psi.

AASHTO Design ESALs $*10^6$	Cell No.	Base M_R Ksi	Sub-base M_R (ksi)	Radial strain, bottom of AC Layer (μstrain)	Asphalt Institute Model		Monsmith Model		Michpave Model		NASRA Model	
					Enhanced Fatigue Life	Original Fatigue Life	Enhanced Fatigue life	Original Fatigue life	Enhanced Fatigue life	Original Fatigue life	Enhanced Fatigue life	Original Fatigue life
25	199	75	40	159	3.88	1.09	0.19	0.052	6.86	1.20	5.67	0.82
	202	75	40	164	3.50	1.10	0.17	0.052	9.13	1.73	4.86	0.84
	205a	75	-	171	3.05	1.20	0.15	0.057	13.64	3.26	3.94	0.95
	205	75	-	165	3.43	1.37	0.17	0.066	31.15	7.25	4.72	1.17
50	200	75	40	140	5.89	1.73	0.30	0.084	13.64	2.56	10.72	1.67
	203	75	40	144	5.37	1.76	0.27	0.086	18.73	3.73	9.31	1.71
	206a	75	-	150	4.69	1.95	0.24	0.095	28.67	7.02	7.59	1.99
	206	75	-	145	5.25	2.19	0.27	0.110	64.85	15.46	9.00	2.39
75	201	75	40	130	7.52	2.31	0.39	0.110	20.98	4.10	15.53	2.59
	204	75	40	133	6.97	2.35	0.36	0.120	29.18	6.01	13.86	2.66
	207a	75	-	138	6.18	2.58	0.32	0.130	45.50	11.36	11.52	3.05
	207	75	-	134	6.80	2.88	0.35	0.140	102.80	24.93	13.34	3.61

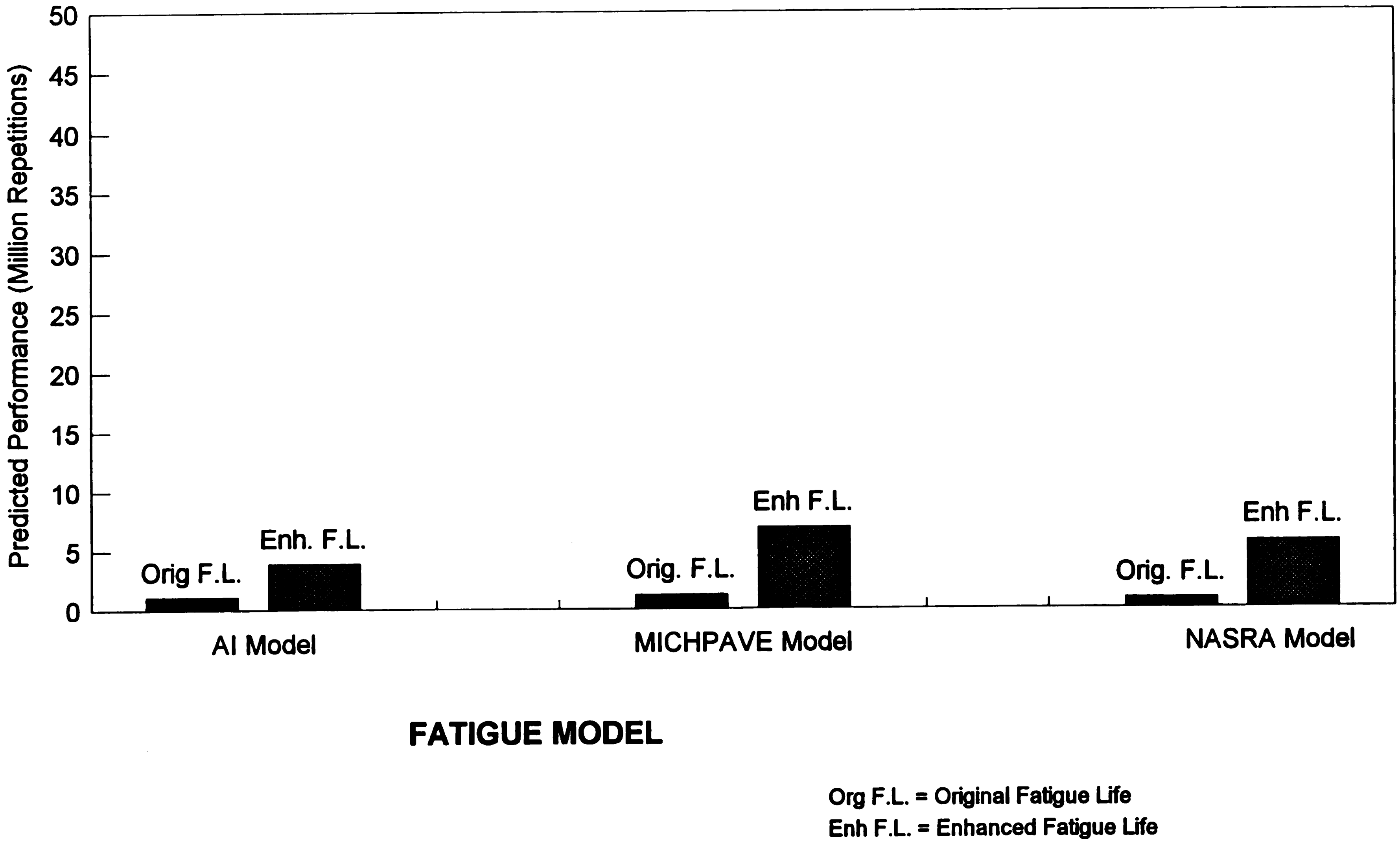

Figure 7.17: Comparison of original and enhanced fatigue life of pavement section 199. Axle load = 28 kip, Tire pressure = 120 psi, Base type = Enhanced Granular

the AASHTO input ESALs except for three pavement sections i. e., pavement section 205a and 206a and 207a for which it is slightly lower than the AASHTO input ESALs. Figure 7.18 presents the comparison of the enhanced fatigue lives for pavement section 199.

4. For combination of axle loads higher than 18 Kip and tire pressure of 80 psi (i.e 23 Kip axle load, 28 Kip axle load and 120 psi tire pressure) the enhancement in the magnitude of predicted fatigue life is shorter than the AASHTO input ESALs (see Table 7.15 and Table 7.17). Therefore for higher loads and tire pressures, the pavements designed by merely increasing the layer moduli (through compaction) of the granular base and subbase may not exhibit the performance equal to the AASHTO input ESALs and may fail in fatigue prematurely.

Table 7.18: Rut life (Million repetitions) of AASHTO designed sections of Figure 3.2 (Granular Base and Subbase but with Increased modulus values) with respect to various rut models. Axle load = 28 kips, Tire pressure = 120 psi.

AASHTO Design ESALs $*10^6$	Cell No.	Base M_R (Ksi)	Subbase M_R (Ksi)	Vertical compressive strain, top of roadbed (μstrain)	Asphalt Institute Model		TRRL Model		ERES Model	
					Enhanced Rut Life	Original Rut Life	Enhanced Rut Life	Original Rut Life	Enhanced Rut Life	Original Rut Life
25	199	75	40	190	64.75	6.82	101.04	7.00	62	6.58
	202	75	40	237	24.05	2.83	31.22	2.47	23	2.74
	205a	75	-	268	13.87	2.97	16.25	2.61	13	2.87
	205	75	-	253	17.95	3.43	22.06	3.10	17	3.31
50	200	75	40	160	139.83	15.35	251.75	18.34	130	14.80
	203	75	40	199	52.62	6.35	79.01	6.45	50	6.13
	206a	75	-	226	29.76	6.54	40.19	6.67	28	6.31
	206	75	-	214	38.00	7.55	53.71	7.90	36	7.28
75	201	75	40	145	217.33	24.51	424.68	31.94	210	23.63
	204	75	40	180	82.49	10.20	134.63	11.30	79	9.84
	207a	75	-	204	47.09	10.36	69.24	11.50	45	10.00
	207	75	-	194	58.98	11.77	90.47	13.38	56	11.35

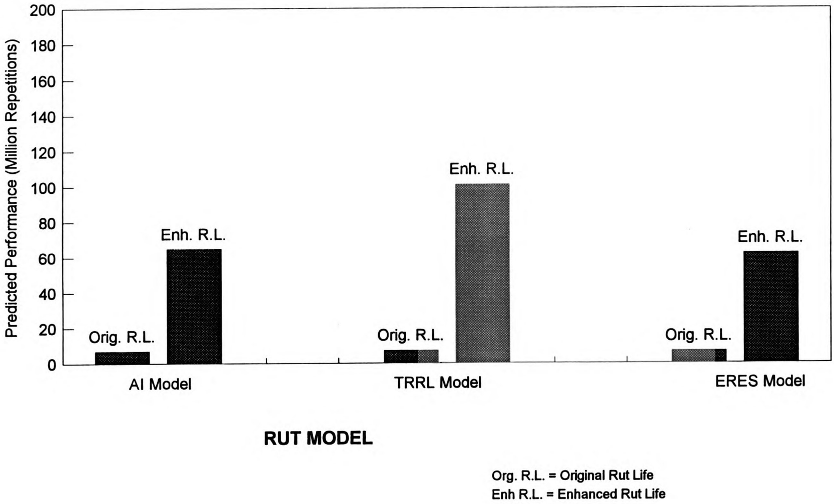

Figure 7.18: Comparison of original and enhanced rut life of pavement section 199. Axle load = 28 kip, Tire pressure = 120 psi, Base Type = Enhanced granular.

CHAPTER 8

CONCLUSIONS AND RECOMMENDATIONS

8.1 CONCLUSIONS

Based on the analysis of this study results, following conclusions are drawn:

1. Results of the SHRP study stand verified relative to the conditions in Pakistan except for the case of roadbed soil stiffer than the subbase/base. For this particular case the DNPS86 computer program does not produce same structural number for same traffic level and one type of roadbed soil (see Figure 5.7). However if the subbase/base softer than the roadbed is omitted from the program then it produces the same structural number for same traffic level and one type of roadbed soil (see Figure 5.6).

2. The AASHTO 86 design procedure produces underdesigned pavement sections for loading conditions in Pakistan with respect to various fatigue and rut models (see Table 6.9 and Table 6.10). Hence the AASHTO design procedure (which is roughness based model) is not applicable in Pakistan. Therefore, the design of pavements that are expected to carry high axle loads (as in Pakistan) must be based on fatigue and rut models rather than on roughness.

3. Pavement structures placed on stiffer roadbed soil are likely to experience less fatigue damage. This finding negates the observation from AASHTO design procedure that the variation in the roadbed soil strength affects only the subbase layer (see Figure 6.2).
4. The fatigue and rut performance decreases with increase of axle loads and tire pressure which is a normal phenomenon in Pakistan.

5. The Different fatigue and rut models used in the study show a very large difference in the fatigue and rut performance for any one pavement section. Similarly the enhanced predicted rut and fatigue performance for any one of the pavement sections also varies with the type of the fatigue/rut prediction model.

6. The results of the study indicate that for any axle load, the chances of failure of pavement sections (Considered in this study) in fatigue are relatively more as compared to its failure in rut.

7. Basing on the trials conducted in this study, it is concluded that to the conditions in Pakistan pavement bases need to be treated/stabilized and the fatigue life not the roughness should control the design process. For combination of higher axle loads and tire pressures (i.e 23 kip, 28 kip axle load and 120 psi tire pressure), the

pavements designed by merely increasing the layer moduli (through compaction) of the granular base and subbase may not exhibit the performance equal to the AASHTO input ESALS and may fail in fatigue prematurely.

8. For the combination of standard axle load of 18 Kip and 80 Psi tire pressure, the examination of results of Trial 1 (the replacement of granular base with asphalt stabilized base, M_R base > 250 Ksi) and Trial 2 (elimination of subbase and replacement of granular base with asphalt treated base, M_R base < 200 Ksi) indicate that the magnitude of enhanced fatigue/rut life exhibited (due to various fatigue/rut models used in this study)in both the trials is equal to or greater than the AASHTO input ESALS. This mean that for the combination of standard axle load of 18 Kip and tire pressure of 80 Psi, the use of asphalt treated base (M_R < 200 Ksi) alongwith elimination of subbase may be economical in Pakistan as compared to the use of asphalt stabilized base (M_R > 250 Ksi) along with some thickness of subbase.

8.2 RECOMMENDATIONS

1. The study indicates that the AASHTO design procedure cannot be adopted for conditions other than it was developed. Hence, it is recommended that the AASHTO design procedure should not be used as the only procedure

for design of pavements in Pakistan. The pavement designs be examined mechanistically for loading conditions of Pakistan.

2. None of the existing pavement performance models can be used for the existing environmental and material conditions in Pakistan. It is strongly recommended that fatigue and rut data be collected and the models be calibrated for conditions in Pakistan or local models be developed.

3. It is highly recommended that to control the heavy axle load conditions observed in Pakistan, the National Highway Authority in Pakistan should install weigh stations all along its road network and enforce the legal load limits.

REFERENCES

1. The Study on National Transport Plan in the Islamic Republic of Pakistan, Final Report, Volume II, Feburary 1995, JICA.

2. Training Block. Flexible Pavement Design. University of Michigan, U.S.A.

3. Thawat Watanatada, Clell G. Harral, William D. o. Paterson, Ashok M. Dhareshwar, Anil Bhandari,and Koji Tsunokania. The Highway Design and Maintenance Standards Model. Volume 1, Description of the HDM-iii Model. A World Bank Publication.

4. Zafar Iqbal Faruqi, "Axle Load Survey to Establish Latest Truck Factors for Pavement Design Between Taxila and Lahore on National Highway (N-5). A Thesis Work for M.sc. (Civil Engineering) in Military College of Engineering Risalpur, 1993.

5. E.J. Yoder and M. W. Witzak. Principles of Pavement Design. Second Edition. New York, Jhon Willey $Sons, 1975.72.

6. American Association of State Highway and Transportation officials. AASHTO Guide for Design of Pavement

structures. Washington D.C., 1986.

7. Per Ullidtz. Pavement Analysis. Elservier Science Publishers B.V., Amsterdam- Oxford- New york- Tokyo, 1987.

8. Road Note 29, A guide to the Structural Design of Pavements for New Roads. Third Edition, Road Research Laboratory, Department of Environment, Department of Transportation, London, 1977.

9. Yang H. Huang University of Kentucky. Pavement Analysis and Design. Published by Prentice - Hall, Inc. U.S.A. 1993.

10. Zafar Iqbal Raja. Pavement Design procedure for pakistan, an Article Published in Corps of Engineers Journal 1993, Published by Military College of Engineering Risalpur.

11. Gilbert Y. Baladi, and Francis X. Mckelvey Professors of Civil and Environmental Engineering, Michigan State University. Mechanistic Evaluation and Calibration of the AASHTO Design Equations and Mechanistic Analysis of the SHRP Asphalt Surfaced pavement Sections.Unpublished Data.

12. Ronald S. Harichandran, Ming-Shan Yeh, and Gilbert Y. Baladi. "MICHPAVE: A Nonlinear finite Element Program for Analysis of Flexible Pavements". Transportation Research Record no. 1286, Washington, D.C. 1990.

13. ELSYM5 INTERACTIVE MICROCOMPUTER VERSION, User's Manual for IBM-PC and Compatible Microcomputer, Report no. FHWA-TS-87-206, Final report december 1986, US Department of Transportation USA.

14. Summary of Traffic Data for National Highways (1994). National Transport Research Centre Ministry of Communication Islamabad.

15. Report 5, Highway Research Board Special Report 61E, "The ASSHO Road Test," 1962.

16. Bonquist, R., R., "Effects of tire pressure on flexible pavement response and performance," Draft Report, Federal Highway Administration, Washington, D. C., 1989.

17. Majeed, Abdul "Axle Load Survey" National Transport Research Centre, Planning Commission, Islamabad (NTRC-65), October 1982.

18. Majeed, Abdul "Multi Axle Vehicle Survey" National Transport Research Center, Planning Commission, Islamabad (NTRC-63), October, 1982.

19. B.J Coree and T.D. White. "AASHTO Flexible Pavement Design Method: Fact or Fiction. Transportation Research Record 1286, National Research Council Washington, D.C.1990.

20. J.F. Shook and F.N. Finn. Thickness Design Relationships for Asphalt Pavements. Proc., 1st International Conference on the structural design of Asphalt Pavements, Ann Arbor, Mich., 1962.